2019

Investigation of the Effect of Edge-Oxidized Graphene Oxide (EOGO) on The Properties of Cement Composites

Yousef Alharbi
University of Central Florida, yrharbi@KSU.EDU.SA

INVESTIGATION OF THE EFFECT OF EDGE-OXIDIZED GRAPHENE OXIDE (EOGO) ON THE PROPERTIES OF CEMENT COMPOSITES

by

YOUSEF ALHARBI

B.S. King Saud University, Saudi Arabia, 2007
M.S. King Saud University, Saudi Arabia, 2012

A dissertation submitted in partial fulfillment of the requirements
for the degree of Doctor of Philosophy
in the Department of Civil, Environmental and Construction Engineering
in the College of Engineering and Computer Science
at the University of Central Florida
Orlando, Florida

Spring Term
2019

Major Professor: Boo Hyun Nam

ABSTRACT

The use of edge-oxidized graphene oxide (EOGO), produced by a mechanochemical process that allow to deliver a product suitable for large-scale production at affordable cost, as an additive in cement composites was investigated. Comprehensive experimental tests were conducted to investigate the effect of EOGO on the properties of cement composites. The experimental tests were designed for three subtasks: (1) investigation of the performance of EOGO and its mixing method on the strength, pore structure and microstructure of EOGO-cement composites, (2) evaluation of the rheological and fluidity behavior of EOGO-cement paste and mortar, and (3) investigation of the mechanism of the enhanced workability of EOGO-concrete. EOGO content ranged from 0.01% to 1% and two mix design methods were employed for cement paste and mortar to explore an optimum and feasible mix design of EOGO. Compressive and flexural strength tests were conducted to investigate the mechanical performance of EOGO-cement composites. Total porosity and water sorptivity were performed to investigate the pore structure of EOGO-cement paste and mortar. Furthermore, petrographic analyses were conducted to characterize the microstructure of EOGO-cement composites. Imaged based-mini-slump and flow table tests were performed to measure the fluidity of EOGO-cement paste and mortar. The rheological properties of EOGO-cement paste were measured through viscometer test. The mechanism of the enhanced workability of EOGO-concrete was investigated by performing slump and water absorption of aggregate in cement paste tests. The key findings are (1) the addition of EOGO into cement composites improves the compressive and flexural strength, (2) 0.05% of EOGO is the optimum content to improve the strength and pore structure of EOGO-cement

composites, (3) the addition of EOGO reduces the fluidity and increases the viscosity of EOGO-cement composites, (4) the addition of EOGO improves the workability of concrete, and (5) dry-mix design is feasible and more practical for large-scale production.

ACKNOWLEDGMENTS

I would like to express my sincere gratitude and deepest appreciation to my advisor, Dr. Boo Hyun Nam, for his encouragements, assistance, and support of my Ph.D. study. This research would not have been possible without his guidance. Appreciation is also extended to my dissertation committee, Professor Manoj Chopra, Dr. Ricardo Zaurin, and Dr. Kawai Kwok for their valuable time, insightful comments and encouragement.

I would also like to thank Dr. Jinwoo An and Dr. Byoung Cho for the time and help they provided towards my research and this dissertation. I have a special appreciation for my lab mates, Mohammad Khawaji and Titchenda Chan for their assistance in experimental work. I would also like to thank Mr. Yeong-Lin, who is a lab coordinator, for providing help when I needed.

This page would be not complete without giving my appreciation to my mother, wife, brothers, sisters, and friends for their love, support, and encouragement during my Ph.D. study at UCF.

Last but not least, I would like to acknowledge King Saud University for the financial support throughout my Ph.D. degree.

TABLE OF CONTENTS

LIST OF FIGURES

LIST OF TABLES

CHAPTER 1: INTRODUCTION[1]

1.1 Research Motivation

Recently, developments in the field of nanotechnology have prompted the creation of innovative nanoscale fibers, which has resulted in the inception of multifunctional materials [1]. Moreover, carbon nanomaterials such as graphene, carbon nanofiber (CNF), and carbon nanotubes (CNTs) have been studied and adopted as reinforcing materials in cement-based mixtures. Currently, Graphene oxide (GO), another 2D form of carbon-based nanomaterial, has garnered much interest due to its unique properties that can effectively enhance the properties of cement-based materials. However, GO utilized in previous studies have been made by using common methods like Hummer's method, a chemical process to oxidize graphite, which appears untenable as an additive in concrete due to the scalability and cost. One of the major hindrances encountered by previous studies that prevented of the incorporation of GO into concrete (relatively large scale) is the small-scale production of GO.

Another hindrance to the addition of GO into concrete is the dispersion issue of GO in the mix. With respect to this, graphene oxide utilized in this research was produced with the use of an innovative mechanochemical process. This innovative technology eliminates the costs of hazardous waste disposal and offer a product appropriate for large-scale production at affordable prices. This promising alternative method of producing large-scale production of graphene oxide is a criterion for introducing GO into the concrete industry. Additionally, this technology produces

[1] The partial content of this chapter appeared in:
Alharbi, Y., An, J., Cho, B.H., Khawaji, M., and Nam, B.H.* "Mechanical and Pore Structure Characteristics of Edge-Oxidized Graphene Oxide (EOGO)-Cement Composites: Dry and Wet-Mix Design Methods", Nanomaterials (2018)

edge-oxidized graphene oxide (EOGO) alongside a few layers. The preparation of GO with other common methods (e.g. Hummer's method) produces a full oxidation (bottom, top, and edges) graphene oxide. This particular GO is composed of a strong van der Waals force that requires a sonicater to disperse the GO layers in the water, which make using it as a powder difficult being well dispersed into the cement composites. Nevertheless, the van der Waals force between GO layers can be weakened with the use of the edge of the oxygen-containing functional groups [2,3], and this will assist for a better dispersion of EOGO as dry powder in cement composites compared to GO. In this matter, EOGO, its mixing methods, and the effects of each mix on the properties of the cement composites, including its feasibility as an additive material should be carefully examined.

1.2 Research Objectives

EOGO produced by a mechanochemical process can be done in a large scale with significantly reduced cost, which allows for practical use in infrastructure construction. The critical objectives of current research are to:

- Evaluate the mechanical performance, pore structure of EOGO-cement composite and identify the optimum content of EOGO.
- Explore a feasible and more practical mix design for massive EOGO-cement composites production by comparing two different mix design methods (Dry-mix design and Wet-mix design).
- Evaluate the effect of EOGO on cement hydration and the microstructure of cement composites.

- Investigate the effect of EOGO for both mix design methods on the rheology and fluidity behaviors of cement paste and mortar.
- Investigate the mechanism of the workability of EOGO-concrete.

1.3 Organization of Dissertation

This dissertation consists of six chapters that are organized as follows: Chapter one presents the research motivation and objectives. Chapter two is a literature review of nanomaterials and their effects on cement composites properties. There are specific details dedicated to the properties of graphene oxide, the nanomaterial investigated in this research. Chapter three characterizes the performance of EOGO-cement composites. Extensive tests are conducted to investigate the effect of EOGO on the strengths of cement paste, mortar and concrete as well as the total porosity and durability of cement paste and mortar. In addition, two different mix designs were employed to evaluate the feasibility of using EOGO as an additive material in cement composites. Chapter four presents the rheological properties of cement paste with the addition of EOGO, and the effect of EOGO on the workability of mortar and concrete. In chapter five, a mechanism study on the workability of EOGO-concrete is delineated. Chapter six provides the conclusion and recommendations.

CHAPTER 2: LITERATURE REVIEW[2]

2.1 Introduction

Presently, the popularity of ordinary Portland cement (OPC) has been retained as the chosen construction material in the civil engineering field. The international cement production has exceeded 3.6 billion tons in order to meet the demands of new infrastructure and building construction, particularly in rapidly developing countries like India and China [4]. Furthermore, cement is considered the principal binder that holds the aggregates together for the production of concrete when water is present for hydration. As engineered material, concrete composites are desired for their excellent compressive strength. Nevertheless, the main drawback to the use of concrete is the nature of its brittle material, which is attributed to its poor resistance to crack formation, strain capacities, and low tensile strength. Depending on the mix proportions of cement, water, and aggregates, the concrete's tensile strength is found within 2 to 8 MPa [5]. Numerous efforts have been made to improve the cement-based material performance through the manipulation of the cement composite properties with admixtures [6–8], supplementary cementitious materials [9–12], and fibers [13–15]. Fibers replace large cracks with a dense microcracks system but cannot stop the crack initiation at nanoscale. The advancements of nanotechnology have offered interesting chances to likewise increase the performance bar with the inclusion of nanomaterials in cement. Many recent studies have been conducted on developed nanomaterials like graphene and graphene oxide (GO) sheets, nano-silica (nano-SiO_2), and carbon

[2] The partial content of this chapter also appeared in:
Alharbi, Y., An, J., Cho, B.H., Khawaji, M., and Nam, B.H.* "Mechanical and Pore Structure Characteristics of Edge-Oxidized Graphene Oxide (EOGO)-Cement Composites: Dry and Wet-Mix Design Methods", Nanomaterials (2018)

nanotubes (CNTs). In this chapter, the current research on effects of GO on cement composite properties are reviewed, including hydration, rheology, workability, mechanical, and microstructure properties.

2.2 Characterization of Graphene and GO

2.2.1 Graphene

Graphene is a single atom thick sheet of carbon atoms, which are covalently bonded directly to three other atoms alongside a length of carbon-carbon bond of about 0.142 nm. It forms a hexagonal ring type of structure [16]. On the other hand, graphite is known as a 3-dimensional layered crystal lattice structure that is made by a stack of parallel 2-dimensional (2D) graphene sheets, which is indicated in Figure 2-1. The adjacent graphene sheets present in the graphite are bonded by weak forces of van der Waals with the separation distance of 0.335 nm from one another. The graphene is the fundamental building block of the entire graphitic carbon forms like fullerenes and nanotubes (CNTs) [17] as shown in Figure 2-2 .

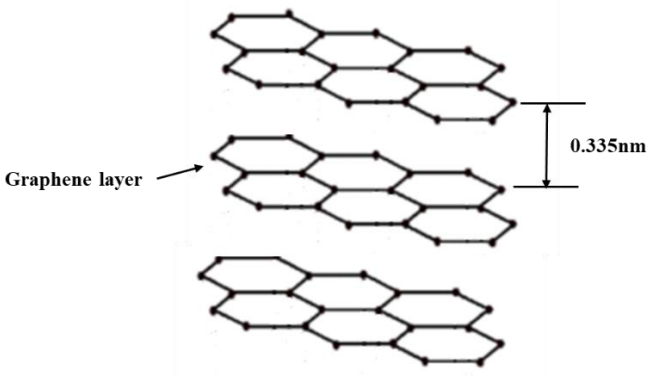

Figure 2-1. Layered structure of graphite showing carbon atoms tightly bonded in hexagonal rings [16]

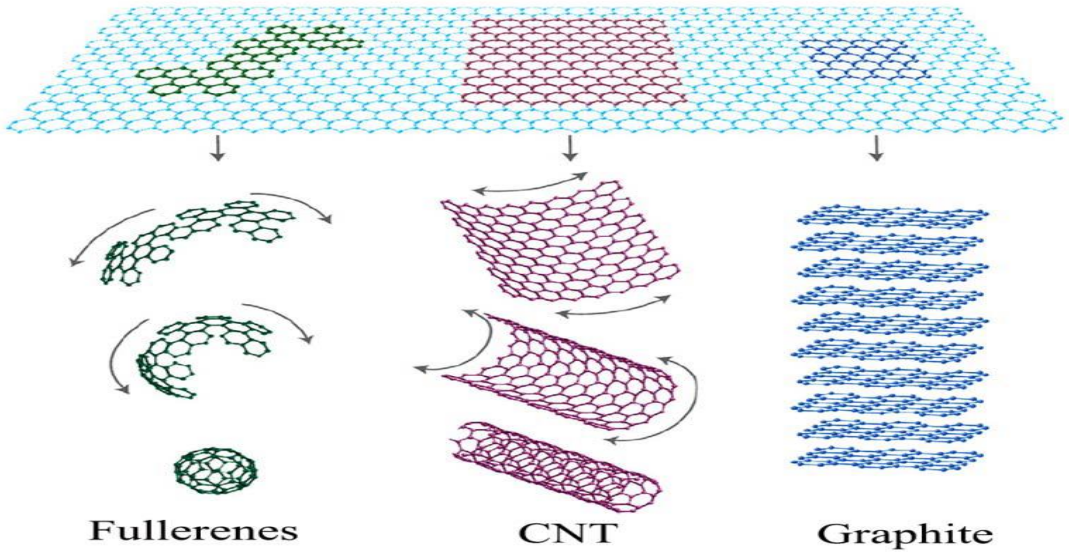

Figure 2-2. Basis of all graphitic forms. Graphene is a 2D building material for other dimensionalities of carbon materials (Reproducing with permission from [18], Springer Nature, 2007)

For decades, scientists have theorized about graphene, but nothing thinner than 50 to 100 layers was produced prior to 2004. Geim et al. [19] were able to get and identify a single layer of graphene. Since the first demonstration of monolayer graphene was reported, there has been tireless effort to achieve high quality, pristine graphene. Much of the reason is its excellent in-plane structural, electrical, mechanical, and thermal properties. Nevertheless, graphite exfoliation to monolayer graphene sheet is considered extremely essential in the accomplishment of these excellent properties. Graphene has very large surface area and is densely packed due to van der Waals interactions. Thus, graphene layers have to be perfectly separated from each other or they tend to reaggregate and restack. Due to this, a major difficulty in synthesis of bulk quantity graphene is aggregation avoidance.

2.2.2 Graphene Oxide (GO)

2.2.2.1 Structure of GO

Graphene oxide (GO) is the highly oxidized derivative graphene that have different oxygen-containing functional groups like hydroxyl (-OH), carbonyl (-C=O), and even carboxyl (-COOH) groups [16]. These groups can be found on both the edge and basal planes of nanosheets, as schematically shown in Figure 2-3.

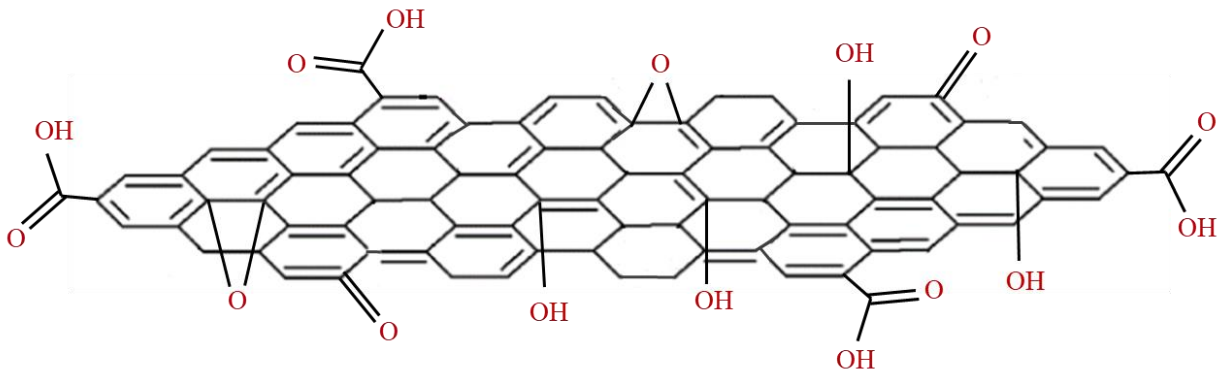

Figure 2-3. Schematic structure of graphene oxide (GO) sheet associated with the functional groups [16].

GO is essentially produced through the chemical oxidation of graphite, with subsequent dispersion and exfoliation in water or in other suitable organic solvents. The good solubility of GO in water makes graphene oxide an interesting material that is capable of being utilized in different devices such as transparent conducting films, flexible displays, and transistor for massive area electronics. The precise atomic structure of GO is still uncertain due to its amorphous characters and the inhomogeneous distribution of oxygen groups. Regardless of this, there have been a few model propositions over years. In the 1939, Hofmann and Holst [20] proposed the first humble model of GO: simple epoxy groups held together on the planar graphene layers. Then Ruess in 1946 [20] proposed a different model than that of Hofmann, one that, incorporates hydroxyl groups

into the ether-oxygen and basal plan functionalities, which are randomly spread out on the carbon skeleton. This particular model provided a change to the structure of the basal plane directly to a sp^3 hybridized system, instead of the sp^2 hybridized Hofmann's model; Ruess still assumed the presence of a repeating unit, allowing for the formation of a regular lattice structure.

Describing the graphite oxide acidic properties, requires a history back to 1957, where Hofmann et al. [20] were able to revisit the previous structure where carbonyl and hydroxyl groups were incorporated on graphene planes. In 1969, Scholz and Boehm [21] were able to propose a fresh structure alongside corrugated carbon backbone, in which were the hydroxyl and carbonyl groups were bonded. At the same time, Nakajima et al. [22,23] proposed a model whereby graphene oxide is composed of two carbon layers linked to each other by sp^3 carbon-carbon bonds, which are perpendicular to the layers where the hydroxyl and carbonyl groups are found in relative amounts.

In 1998, Lert and Klinowski [24] proposed what is now the most well-known model. They included carboxyl groups only on the edges of GO sheet.

2.2.2.2 Synthesis of GO

Graphite oxide was initially synthesized by the British chemist B. C. Brodie in 1859 [25]. He was investigating the graphite structure by the observation of the reactivity of graphite flakes. Out of the different reactions he performed, one of them consisted of the inclusion of potassium chlorate ($KClO_3$) directly to slurry of graphite with respect to a fuming nitric acid (HNO_3). The obtained material consisted of hydrogen, oxygen, and carbon, with C:H:O composition of (80.13:0.58:19.29). Successive oxidative treatments determined an additional increase in the

oxygen content with C:H:O proportion variation to (61.04:1.85:37.11). Oxygen presence made the material dispersible in basic water or pure water, but not in acidic media; this made Brodie identify the material as “a graphic acid.”

Nearly 40 years after the Brodie’s discovery, Staudenmaier in 1898 enhanced the protocol provided by Brodie using a mixture of sulfuric and fuming nitric acid followed by the include of potassium chlorate in many aliquots over the course of the reaction. This small alteration in the procedure brought an overall extent of oxidation (C:O_2:1), which is the same as what was obtained by Brodie with a different oxidation approach. However, Staudenmaier’s protocol was performed in just one reaction.

After another 60 years, Hummers and Hoffman [26] established an alternative process for graphite oxidation that integrates the combination of sodium nitrate ($NaNO_3$) and potassium permanganate ($KMnO_4$) in concentrated sulfuric acid (H_2SO_4). This achieved the same levels of oxidation obtained with the former method.

There are at least three different vital benefits of the Hummer’s method compared to the previous ones: (1) the reaction can be completed in just a few hours; (2) a replacement of $KClO_3$ by $KMnO_4$ improves the safety of the reaction by preventing the explosive production of Chlorine dioxide (ClO_2); (3) The utilization of $NaNO_3$, rather than fuming nitric acid, eliminates the acid fog formation. Nevertheless, it has two drawbacks: the oxidation reaction releases toxic gasses, which are nitrogen dioxide and dinitrogen tetroxide (NO_2 and N_2O_4). In addition, the residual nitrate and sodium (NO_3^- and Na^+) ions are hard to remove from the waste water, which are made during the processes [27]. Modified Hummer’s method follows the same procedures of Hummer’s method without using sodium nitrate ($NaNO_3$) [28].

2.2.2.3 Morphology of GO

GO's morphological features can be observed with the use of different microscopic techniques: Transmission and Scanning Electron Microscopy (TEM and SEM), and Atomic Force Microscopy (AFM). The thickness and number of layers are given by the AFM. As observed by Stankovich et al. [29], an exfoliated sample thickness of GO tends to be uniform and close to 1nm (Figure 2-6).

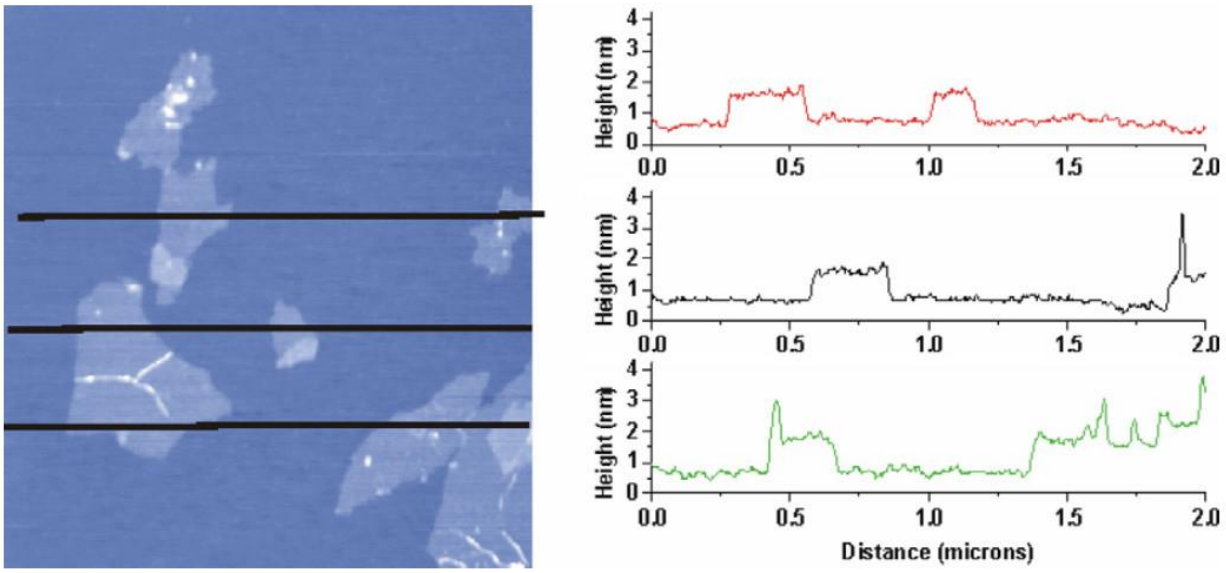

Figure 2-4. AFM image of GO sheets with three height profiles in different locations (Reproducing with permission from [29]. Copyright Elsevier, 2007).

When Shang et al. [30] synthesized graphene oxide, the results showed that GO sheet's average thickness after ultrasonication is roughly 1nm. This result is consistent with the research conducted by Stankovich et al. [29].

Wang et al. [31] utilized the AFM, TEM and elemental analysis for the characterization of synthesized GO (Hummer's method). The results demonstrated that GO is an almost transparent

nanosheet with many wrinkled and folded feature. The AFM results showed irregular shapes with around 1 μm length and around 1 nm thickness. Scanning Electron Microscopy (SEM) is one of the most popular techniques used by authors for the morphological characterization of GO. Shahriary et al. [32] observed a layered structure, formed of ultrathin film that folds in space of the synthesized GO.

2.3 Cement Hydration of GO-Cement Composites

Cement is mainly composed of silicates (tricalcium silicate C_3S and dicalcium silicate C_2S) and aluminates (tricalcium aluminate C_3A and tetracalcium aluminoferrite C_4AF). Table 2-1 shows the main cement constituents prior to hydration [33].

Table 2-1. Principal cement constituents [33].

Constituents	Chemical formula	Notation	Name
Tricalcium silicate	$3CaO \cdot SiO_2$	C_3S	Alite
Dicalcium silicate	$2CaO \cdot SiO_2$	C_2S	Belite
Tricalcium aluminate	$3CaO \cdot Al_2O_3$	C_3A	Celite
Tetracalcium aluminoferrite	$4CaO \cdot Al2O_3 \cdot Fe_2O_3$	C_4AF	-

The aluminates hydrate faster compared to the silicates. Also, the aluminates hydrates are relevant for the setting and hardening process, but they have no impact on the mechanical properties of the cement. The silicate hydration majorly determines the final mechanical properties of the cement but have no effects on the setting process. The aluminates' hydration reaction should be considered. Once the water is added to cement, the hydration of C_3A is immediate; it becomes critically exothermic and generates similar C_4AF hydration crystals. The reaction of water and C_3A

is extremely fast and has to be slowed down by adding gypsum to the mixture. Upon contact with water, calcium ions (Ca^{+}) and sulfate ions (SO_4^{-}) are both released to react directly with the aluminates ion (Al_4O^{-}) to form a trisulfate known as Ettringite ($3CaO \cdot Al_2O_3 \cdot 3CaSO_4 \cdot 32H_2O$) that tend to transform to the monosulfate form [36]. Moreover, the Ettringite is characterized by a needle-like structure, rather than the monosulfate that has a plate morphology. Also, the Ettringite provides a covering for the cement grain that reacts and slows the reaction for some hours. The quantity of gypsum required is based on the content either of silicates or of C_3A; the sulfate does not only delay the aluminates' hydration, but also increases the speed of the silicates' hydration. The C_4AF hydration provides similarly hydrated products, which is Ettringite, but its hydration is not fast as C_3A [34].

At this point, the hydration of silicates should be considered. This reaction prompts two different products: hexagonal crystals of calcium hydroxide, known as Portlandite ($Ca(OH)_2$) and a variety of calcium hydrate product that have the same structure with various composition (various proportion Si/Ca and bonded water) called cement gel or gel C-S-H. Meanwhile, considering a given mass, the C_2S produces a larger quantity of gel C-S-H with respect to the C_3S. The hydration of C_3S generates a larger quantity of Portlandite, but both C_2S and C_3S contribute to the total amount of Portlandite and of C-S-H. The Portlandite crystals tend to be weak and subject to fracturing due to the weaker bonds between the layers of its crystals. Otherwise, the nanostructure of the C-S-H is still a debatable topic because their structure has not fully resolved. The C-S-H structure represents 80% of the final volume and 50% of hardened mass. Thus, it is responsible of the mechanical properties of cement composites.

Anhydrous cement is made up of four different mineral types namely alite (C_3S), belite (C_2S), aluminate (C_3A) and ferrite (C_4AF). When water is added to the cement grains, different chemical reactions take place simultaneously to prompt the rigid cement paste formation. The resulting porous multi-phase matrix is composed of CH with some traces of unhydrated clinker and aluminates integrated into the binding agent, the C-S-H gel. The CH byproduct is responsible for the cement alkalinity. Therefore, additional attention has to be considered towards the dispersal of nanomaterials in a cement medium of high pH value. Additionally, the heterogeneous nature of cement contains mostly calcium ions with some aluminum, potassium, magnesium, sulfur ions, and sodium. The interaction of nanomaterials with these ions must also be taken into account [35].

In general, the adoption of nanomaterials like nanofibers, nanotubes, or nanosilica can help in the acceleration of the hydration degree [36]. GO likewise helps in the acceleration of hydration rate. The non-evaporated water can be measured with the help of TGA with the progression of hydration per time. The intention of the test is to measure the hydration degree by recording the CH content and non-evaporable water within the cement composite. Moreover, GO cement tends to increase the non-evaporable water content by around 9 % and CH by roughly 6 % [37]. The disparity in CH content and water is consistently at a higher proportion compared to the ordinary Portland cement (OPC) for all ages. Therefore, GO increases the degree of crystallinity in polymeric nanocomposite by providing preferential nucleation site at its oxygen functional groups. According to the study conducted by Gong et al. [37], the creation of hydration products was monitored periodically under SEM. They found that the functional groups of GO play an important role as the growth points of hydration products through attraction of C_3A, C_3S, and C_2S.

The cement hydration was examined within the presence of GO by several researchers. Lv et al. [38] proposed a regulatory mechanism of GO on cement hydration products. The GO surface is composed of numerous oxygen functional groups, which majorly consist of O, HO, and COOH. The active functional groups react preferentially with C_3S, C_2S and C_3A and form the growth points of the hydration products, while the Portland cement temporarily retards the hydration reaction. The slowed hydration reaction continues to take place at the growth points on the GO surface. The growth pattern and growth point of the hydration products are all controlled by GO, which is known as a template effect. GO is capable of making numerous neighboring rod-like hydration crystals on the same GO surface develop flower shaped crystals and thick column-like shape. These columnar products are composed of rod-like of ettringite (AFt), monosulfate (AFm), calcium hydroxide (CH) and calcium silicate hydrate gel (CASAH), which grow further from the surface of the GO in similar direction because of increased stress around them, keeping the column shape. The moment the column-shaped crystals are grown into pore, crack or loose structure, there is an isolated growth. They are likewise made into completely-bloomed flower-like crystals, which disperse in cracks and pores as fillers and crack arrestors to prevent the propagation of cracking. When GO content exceeds 0.04%, the growth points become extremely dense to create single flower-like crystals. Thus, the hydration crystals will then take on a polyhedron shape and develop a compact structure. Moreover, the flower-like crystals often generated in the gap and holes of the cement composites create cross-linking structure, which have greatly contributed to improving toughness of cement composites.

Lv et al. [38] also investigated the influence of cement hydration time on the microstructure of cement composites with incorporating 0.03% GO. The results of the SEM showed that GO can

possibly facilitate the formation of flower-like hydration crystals. On the first day, SEM showed irregular and small sphere-shaped particles, similar to budding flowers. Many of small rod-like crystals had developed after three days. There was an observation of the presence of small quantity of incomplete flower-like crystals, which can be possibly made by the rod-like crystals. At seven days, the hydrated crystals began to look like incomplete flowers with “petals.” The flower-like crystals showed a fuller and larger flower-like shape at 28 days. Meanwhile, hydrated crystals become denser at 60 and 90 days and the likelihood of forming linked clusters were observed. These results confirm the regulating effect of GO on the formation of flower-like hydration crystals with their likelihood to develop huge compact cross-linking structure through the flower-like crystals over time.

The influence of GO on cement hydration also studied by [39]. Two contents of GO, which are 0.02% (CG2) and 0.04% (CG4), were utilized for this reason. They carried out a measurement of the hydration heat development of cement paste mixes C (control mix), CG2 and CG4 within 72 hours. The results for all cement pastes resembled that of typical Portland cement paste [40], which consists of five different stages: initial reaction, induction period, acceleration period, deceleration period and decline period. The addition of GO did not eliminate or add peaks, but only altered the peaks intensity. The quantity of GO in CG2 used appeared extremely low to cause any essential change of hydration heat development, as the two curves are closely identical. However, the cement hydration process in CG4 was discovered to be accelerated with GO addition, since higher heat (higher peaks) was recognized. Additionally, the characteristic sulphate depletion peak [40] at about 12 hours, which is associated with renewed formation of ettringite [40] turned out to be highly recognizable compared to the sample C. It is clear that there was no prolonging of

the induction period by the integration of GO, but the heat flow was raised (local minimum), particularly at the final point of the induction period by around 6.8%. Compared to sample C, CG4 reached the main hydration peak about 3.5% sooner and the peak was increased by about 3.8%, which suggested that the integration of GO accelerated the induction and acceleration periods of the cement hydration.

From the results of the hydration heat of this study, the introducing of GO increased the hydration peak and hydration rate in the acceleration period. It is evident that the addition of GO provided more nucleation sites for the growth of hydration products.

2.4 Mechanical Properties of GO-Cement Composites

Currently, GO has attracted great interest because of its unique properties that can effectively improve the properties of cement-based materials. Researchers have found that GO with oxygen-containing functional groups improves the performance of GO-mixed cement composites [12,37,38,41–43]. Lv et al. [41] investigated the influence of GO sheets on formation process and cement hydration crystals shape for their direct effect on the mechanical resistance of cement composites. They observed that incorporation of low dosage of GO (<0.03%) formed flower-like crystals. As amount of GO was increased to above 0.03%, polyhedral or lamellar crystals were formed. Furthermore, they noted that the compressive strength increased 34.3% and 38.1% by adding 0.03% and 0.05%, respectively of cement weight GO to plain cement paste. The corresponding flexural strength showed a respective improvement of 52.4% and 52.3% compared to the plain cement paste.

Wang et al. [42] reported that the incorporation of 0.05 wt.% GO to cement paste increased the 28th-day compressive and flexural strength by 40.4% and 90.5%, respectively. Also, the compressive and flexural strength of cement mortar, when they added the same percentage of GO, increased by 24.4% and 70.5%, correspondingly. An improvement in compressive and flexural strength of 15-33% and 41-59%, respectively over ordinary Portland cement paste was reported for the addition of 0.05 wt.% GO [43]. An investigation of the effect of graphene oxide nanoplates (GONPs) on the properties of cementitious materials was conducted by Tong et al. [12], and they found that GONPs reshaped the cement paste microstructure and showed a better interfacial bond between GONPs and C-S-H gels precipitated around them. The compressive strength of mortar samples improved due to the role of the functional groups of graphene oxide.

Gong et al. investigated the effect of GO on Portland cement paste, and they found that adding 0.03% by cement weight of GO sheets to the plain cement paste can enhance the compressive and tensile strength by more than 40%. However, the reduction of the workability was observed [37]. Lv et al. [38] revealed that the compressive, flexural and tensile strength of cement composites significantly increased by around 40%, 60%, and 79%, respectively when 0.03% by cement weight of GO was added to the cement paste.

Babak et al. [44] revealed that the tensile strength of GO-cement composite increased by 48% compare to control sample because of the non-agglomeration of GO in the matrix and nucleation of C-S-H around GO platelets. The Young's modulus of GOCC ranged between 5-20 GPa depending on the GO content as reported by Horszczaruk et al. [45]. After they compared nanosilica cement composite with GO cement composite, they conclude that the latter has similar effect on the hydration process resulting in an emerging nanomaterial into cement composites.

Pan et al. [46] found that the addition of 0.05 wt. % GO in cement composites can increase the compressive strength up to 15-33% and flexural strength up to 41-59%, respectively. In addition, Elastic modulus increased from 3.48 GPa to 3.70 GPa for cement paste indicating slight increased only probably due to the forming of low number of cracks by the crack arresting of GO. Furthermore, Pan et al. [46] observed, based on SEM image, that compared to other nano-fillers, GO exhibited unique 2D structure which can deflect, tilt or twist around the crack. This structure allows for better mechanical properties of samples. Moreover, the pore volume and pore diameter comparison between the plain cement paste and GO-cement paste found to be quite similar in this aspect.

2.5 Pore Structure of GO-Cement Composites

It is hypothesized that the carbon-based material is able to improve concrete permeability by improving the pore structure, which results in improved resistant to fluid ingress and chemical attacks. There is a direct relationship that exists between concrete durability and the mobility of fluids with concrete [47]. The durability is related to the ease with which liquids and gasses are able to enter the concrete [48,49],what is denied as transport properties. Transport properties highly depend on pore size distribution, total porosity, pore connectivity and its tortuosity [50,51]. Recently, it has been recognized that sorptivity is a significant index of concrete durability [52]. The durability of concrete can be improved if the resistance to water penetration is increased [53]. It is vital to analyze the porosity of nano-reinforced cement because of the close relation to the mechanical properties. Many techniques can be utilized to quantify the porous nature of cement

such as water sorptivity, nanoindentation, and mercury intrusion porosimetry (MIP). Nanomaterials play an instrumental role in refining the pore structure.

GO has been shown to have a profound impact on the pore structure and surface area at the nanoscale. The increased surface area directly corresponds to the development of a highly porous phase. Small pores, measuring between 1 and 10 nm (also called gel pores), are made up of pore system in C-S-H gel. The porosity of GO-cement described in a pore size distribution characterized by using an alternative method, which is MIP [37]. The inclusion of GO is able to successfully refine the microstructure of cement composite by lowering the number of capillary pores (between 10 nm and 10 μm) by 27.7%. This is related to the accelerated hydration owing to the 2D shape of GO.

2.6 Rheological Properties of GO-Cement Composites

In general, the addition of GO in cement composites decreases the workability and increases the viscosity due to the large surface area [30,31,39,46,54,55]. Wang et al. [31] noted that two dosage of GO (0.01 wt.% and 0.03 wt.%) reduced the cement paste fluidity by 13.2% and 32.1% and increased the apparent viscosity and yield stress due to the large surface area and high number of oxygen-containing functional groups of GO that lead to cement particles agglomeration and a flocculation structure formation. Shang et al. [30] reported that adding 0.08% by cement weight of GO to cement composites decreased the fluidity by approximately 57% while the plastic viscosity increased by approximately 32% compared to the plain cement paste. This is due to the agglomeration and flocculation formations. These formations occurred probably because of the electrostatic interactions between GO and cement particles.

Wang et al. [54] studied the effect of a GO additive on the rheological behavior of fresh cement pastes. They observed that the addition of GO generated new flocculation structures and re-agglomerated the cement particles. The greater incorporation of GO content increased the cement particles agglomeration and flocculation structures, sharply increasing the plastic viscosity and yield stress. The traditional mini-slump test, which accompanied the rheological studies, addressed the workability dilemma in depth. The results showed a 50% reduction of cement paste workability, which was confirmed by the viscosity test result [55]. Gong et. al [37] observed that when 0.03% by weight GO was added to cement paste, the fluidity reduced by around 35% compared to the plain sample. Further tests using 0.03% by cement weight of GO in cement paste showed a remarkable decline in the mini-slump diameter by 21% compared to the plain specimen due to GO agglomeration that entrap a high amount of mixing water [39].

Pan et al. [46] demonstrated that the incorporation of 0.05% by weight GO reduced the cement paste workability by around 42% via a mini-slump test. Based on the previous studies, there is a contrast correlation between the cement composites workability and GO concentration. The main cause of this issue may be the large surface area of GO, that requiring water to wet their surface reduces the free water in cement matrices required for lubrication. Also, the large scale agglomerates of nanomaterials reduce the cement composites fluidity [30].

2.7 Workability of Concrete

The quality of concrete structure relies on the quality of every component used in the concrete mixture. Nevertheless, this is not considered the only dominating factor. The quality of the concrete structure is also highly reliant on the workability of the fresh concrete in the course

of transportation, placement, compaction and consolidation. The definition of the term "workability" in ASTM C125 [56] is "A property determining the effort required to manipulate a freshly mixed quantity of concrete with minimum loss of homogeneity." Concrete is a complex composite material. The properties of the concrete when it is still fresh can greatly affect the characteristics of the concrete when set. At the time of casting, the concrete should easily flow into all crevices and corners with little or no segregation. The presence of congested reinforcement or awkward sections makes this process more difficult. As a result, this often usually leads to non-homogenous and hardened honeycombed mass. In today's modern concrete technology, it is even more important to define the flow of concrete when special concretes, such as self-compacting concrete (SCC) or high-performance concrete (HPC), are utilized. Also important is to note when concrete is poured in structures that are highly reinforced. These situations require great control of workability. Thus, one of the basic criteria for a good concrete structure is that the fresh concrete has good workability at the time of casting. Many factors affect the workability of concrete. They include water-cement ratio (w/c), the proportions of the mixture, size of aggregate, the surface texture of aggregate, the shape of aggregate, absorption of aggregate and admixture use. Water-cement ratio greatly affects the workability and it is directly proportional to workability. When the water to cement ratio is increased, the workability of concrete is also increased. In addition, the properties of the aggregate including shape, surface texture, size, and absorption have also significant effect on concrete workability. Aggregates that are large in size need less surface area, resulting in the reduction of the paste content [57]. Aggregates that are flaky-shaped and/or elongated reduce the workability because of poor packing unlike rounded aggregates [48,57]. Smooth surface aggregate provides more workable concrete compared to concrete with rough

texture [58]. The absorption of water by the aggregates causes the loss of the workability of concrete [59,60]. This also decreases the effective water-cement ratio (w/c) [61]. The absorption rate of water by the aggregate at the initial stage is critical in order to predict the workability loss of concrete [62].

The slump test is a commonly used practical test. It gives an insight into the variations in uniformity of a fresh concrete mixture of a given nominal proportion as a result of its simplicity. This test is prescribed by EN 12350-2 in Europe and ASTM C143 in the United States. The apparatus comprises a truncated metal cone that is 300 mm high with a base diameter of 200 mm and a top diameter of 100 mm. To carry out the test, the procedure requires that the cone is filled up in three layers of the same volume. Each layer is rodded 25 times. Then the last layer is struck off and leveled. The cone is then gradually lifted up vertically, allowing the concrete sample to slump down under the influence of gravity.

2.8 Research Gap and Focus of this Research

Previous studies focused on the effect of GO sheets, prepared with common chemical processes (e.g., Hummer's method) to produce GO sheets with full oxidations (edges, top, and bottom). These methods make the price of GO very high (approximately $100/g), which is one of the major challenges in promoting GOs in large-scale constructions. The high price of this GO limits its practical usage within the construction industry. The graphene oxide used in this research is produced by a ball milling process along with common reactants. Graphite powder was subjected to milling with non-toxic oxidizing agents. The result was edge-oxidized graphene oxide (EOGO) with a few layers. The direct milling process could achieve a dramatic reduction in cost in the

manufacture of EOGO by eliminating hazardous waste disposal [63]. Therefore, this innovative mechanochemical process can reduce the price of graphene oxide to under $1.0/g. Consequently, this low-cost alternative nanomaterial can be used in construction fields due to the economic advantages. In addition, EOGO can be used to improve the electrical and thermal conductivity of polymers, coating, and composites [64].

The other challenge of introducing GO into large-scale constructions is the dispersion method of GO. Using a sonication method to disperse GO in water is well known as the ideal method [20,35]. However, this method may not be practical for high quantities of cement paste or concrete. Therefore, in this study, EOGO is dispersed as powder in cement before mixing with water to investigate the feasibility of using EOGO as an additive material. The interaction of cement particles with the conventional GO will be higher than EOGO because the oxygen-containing functional groups in GO are higher compared to those in EOGO. This may cause higher agglomeration of cement particles with GO when compared with EOGO. The van der Waals force between GO layers can be weakened with the use of the edge of the oxygen-containing functional groups [2,3]. This will assist in giving a better dispersion of EOGO as powder in cement composites compared to GO. Therefore, EOGO and its mixing methods should be carefully examined to observe the effects that can be had on cement composite properties along with the feasibility of EOGO as an additive material.

In this research, two mix design methods are used: (1) Dry-mix design, where EOGO and cement powders are mixed before cement paste and mortar formation and (2) Wet-mix design where a sonicator is used for 20 minutes to disperse EOGO into water while using that as the mixing water for cement paste and mortar mixes. To quantify the difference between dry and wet-

mix design methods, this research experimentally investigates the effect of different mixing methods of EOGO in the cement paste and mortar on the mechanical properties, total porosity, and sorptivity. Five percentages of EOGO between 0.01% and 1.0% by cement weight for both mix design methods were used in for this purpose. Furthermore, dry mix design was applied to concrete to investigate mechanical and workability performance of EOGO-concrete. The mechanism of the effect of EOGO on the workability of concrete is also studied in this research.

CHAPTER 3: PERFORMANCE CHARACTERIZATION OF EOGO-CEMENT COMPOSITES[3]

3.1 Introduction

This chapter presents an investigation on the use of EOGO in cement composites including cement paste, mortar, and concrete. Performance characterization of EOGO-cement composites is discussed in detail. EOGO produced from graphite through a mechanochemical process characterized by advanced material conversion methods. The design variables explored in the mixture include EOGO content ranged from 0.01% to 1% by cement weight. The mix design method is classified into two designs: (1) Dry-mix design of EOGO mixed with cement as a dry powder prior to paste formation and (2) Wet-mix design of a sonicated EOGO solution used during paste formation. Comparative effects of the mix design method on compressive and flexural strength of cement paste and mortar were evaluated. Moreover, microstructures and crystalline phase changes of cement paste were also analyzed. The comparative effects extend to evaluate the pore structure include the total porosity and water sorptivity of cement paste and mortar for both mix designs. To investigate the feasibility of using EOGO in concrete industry, EOGO was applied to concrete to investigate strength performance of EOGO-concrete. Based on the mechanical properties of EOGO-cement paste and mortar, EOGO contents used with concrete were 0.01%, 0.05%, and 0.1% by cement weight. In addition, dry-mix design as a practical method was

[3] The content of this chapter appeared and will be appeared in:
Alharbi, Y., An, J., Cho, B.H., Khawaji, M., and Nam, B.H.* "Mechanical and Pore Structure Characteristics of Edge-Oxidized Graphene Oxide (EOGO)-Cement Composites: Dry and Wet-Mix Design Methods", Nanomaterials 2018, 8(9), 718.
An J., Nam B.H.*, Alharbi Y., Khawaji M., and Cho B.H. "Edge-oxidized graphene oxide (EOGO) in Cement Composites: Cement Hydration and Microstructure", Peer-reviewed journal paper.

employed for concrete mixes to prepare specimens for compressive and flexural strength of concrete with EOGO.

3.2 Materials

3.2.1 Edge-oxidized Graphene Oxide (EOGO)

Graphene oxide (GO) used in previous studies have been made using chemical methods (e.g. Hummer's method) [2,3,5–9,11,12], a chemical process of oxidizing graphite, which is untenable as an additive in cement and concrete because of cost and scalability. Traditional methods for producing, such as Hummer's method, depend on strong and somewhat harmful oxidizing agents and acids (H_2O_2, H_2SO_4 and $KMnO_4$) and produces significant quantities of acidic byproduct [1]. Figure 3-1 shows the typical manufacturing process of GO through the chemical process.

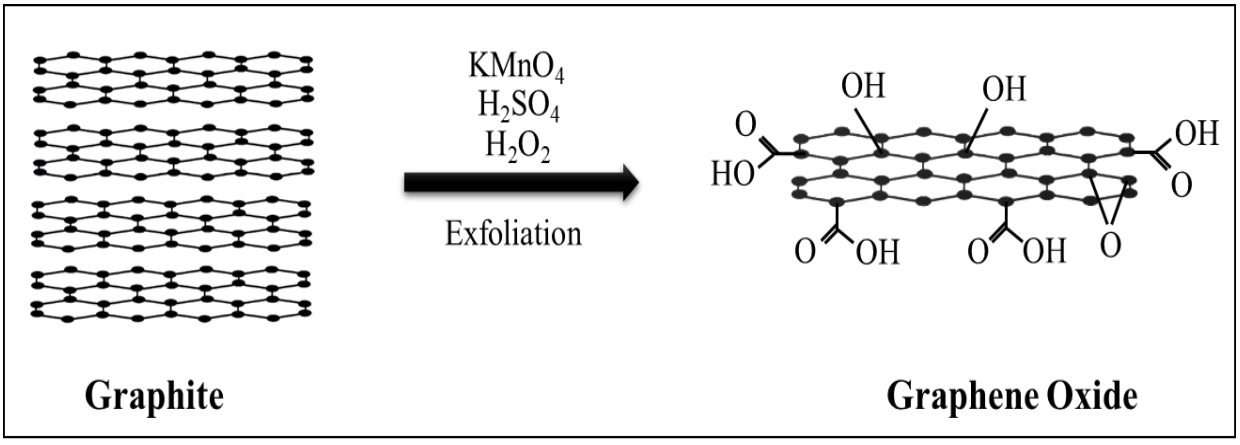

Figure 3-1. Chemical method for producing graphene oxide.

EOGO used in this study were produced using an innovative mechanochemical process which uses milling technology (like those in the mining industry) with common reactants yielding EOGO more cost-effectively and scalability (Figure 3-2). This innovative technology directly mills graphite power with a non-toxic oxidizing agent using conditions that minimize collision forces. It also optimizes shearing forces; thus, graphite powder is simultaneously oxidized and delaminated with a few layers suitable for the manifold purpose. These proprietary achievements eliminate hazardous waste disposal costs and deliver a product suitable for large-scale production at commodity-type prices [16,17]. This promising alternative method to producing EOGO on a large-scale is a requirement for introducing EOGO into the concrete industry. One of the major hindrances encountered by previous researches that prevented the introduction of EOGO into concrete on a relatively large scale is the small production of EOGO. This impediment can be overcome with the manufacturing process of ball-milling EOGO, as shown in Figure 3-2.

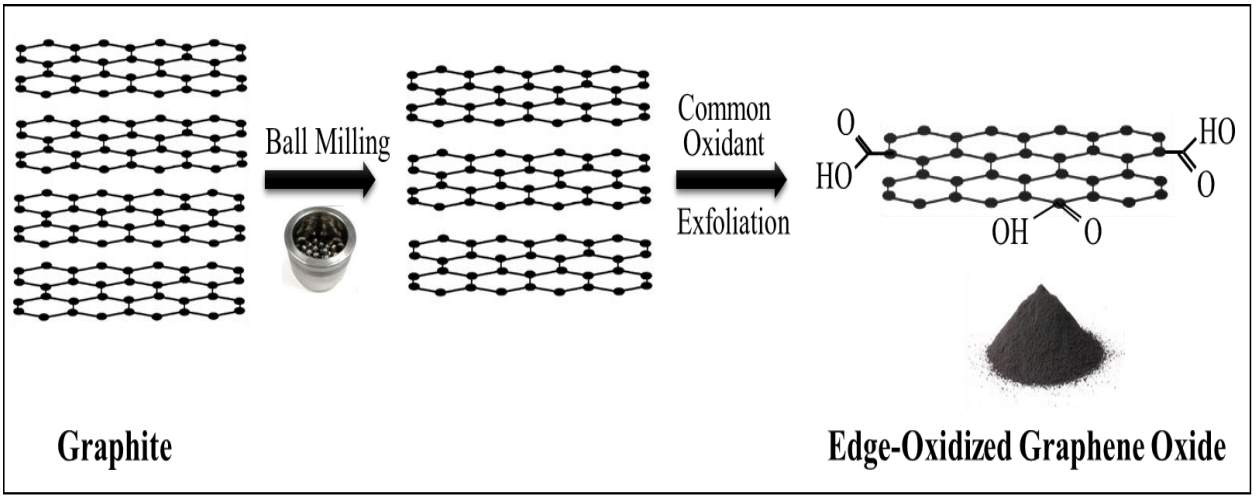

Figure 3-2. Mechanochemical process of producing edge-oxidized graphene oxide (EOGO)

In addition, the GO produced by chemical method and EOGO produced by ball-milling method were characterized by petrographic analysis (Transmission Electron Microscopy (TEM) and Atomic Force Microscopy (AFM)). The results of TEM and AFM for both GO and EOGO are illustrated in Figures 3-3 and 3-4, respectively. Figure 3-3a shows the TEM image of GO and demonstrates that GO is a flat sheet like silk with folds and wrinkles at several places [30]. Figure 3-3b illustrates the TEM image of EOGO and indicates the presence of multi-layers of EOGO. The overlapping areas of EOGO clearly show that EOGO has the multi-layers, and the edge of EOGO is angular and square. This rough surface of EOGO is due to the mechanical process of ball-milling. Figure 3-4a shows the AFM image of GO and illustrates irregular shapes of GO sheets with a dimension of roughly 1 μm and a thickness of approximately 1 nm, indicating that the GO sheets are exfoliated into a monolayer [30]. Figure 3-4b shows the AFM image of EOGO and illustrates that EOGO flakes have irregular shapes with an average dimension of about 400 nm and a thickness of about 2.75 nm. This effectually proves that EOGO has multi-layers.

The EOGO content as a percentage of the cement weight was added into cement paste and mortar. For example, 0.01% of EOGO means 0.01% by cement weight of EOGO. Table 3-1 summarizes the chemical compositions and physical properties of EOGO produced by both ball-milling and chemical methods. The EOGO is hydrophilic, readily suspends in water, and can be functionalized with unique groups.

Table 3-1. Chemical and physical properties of graphene oxide (EOGO and GO) [35,64].

	EOGO (Ball-milling method)	GO (Chemical method)
Carbon (%)	90-95	49-56
Oxygen (%)	5-10	41-50
Surface area (m^2/g)	200-300	700-1500
Density (g/cm^3)	~1.0	~1.8

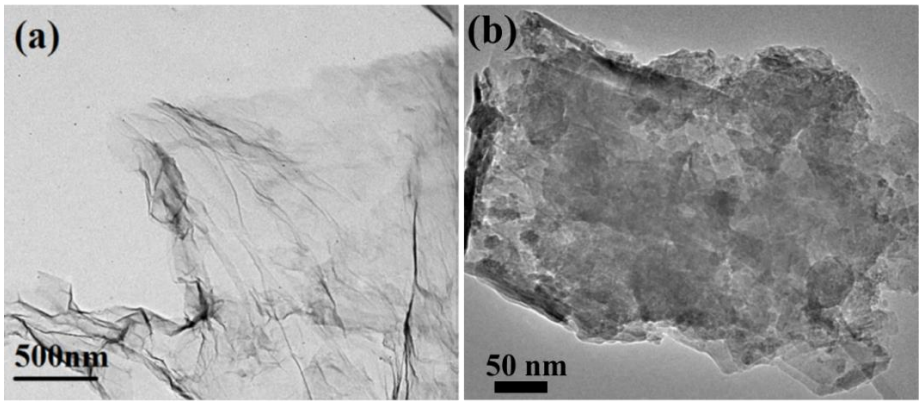

Figure 3-3. The TEM images of (a) GO (Reproducing with permission from [30]. Copyright Elsevier, 2015) and (b) EOGO [64]

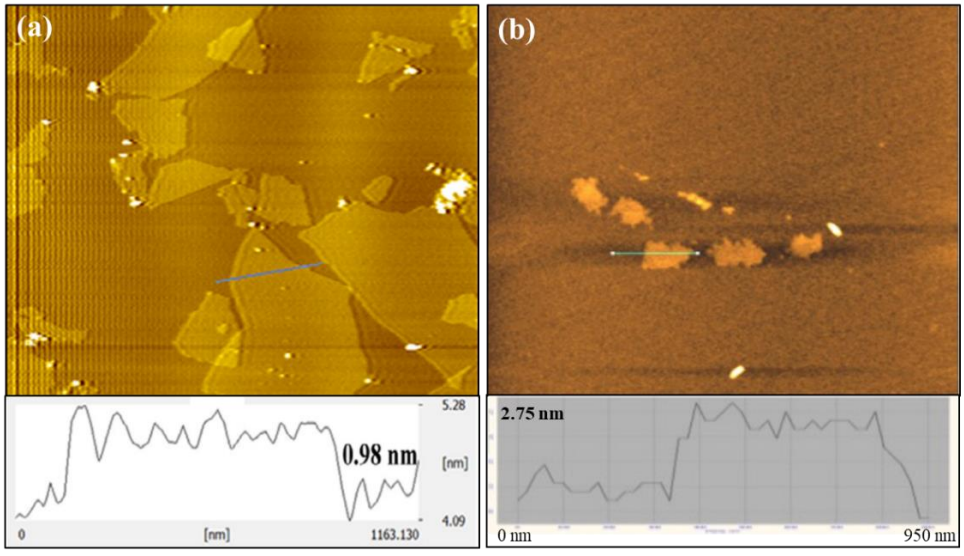

Figure 3-4. The AFM image and height profile of (a) GO (Reproducing with permission from [30]. Copyright Elsevier, 2015) and (b) EOGO [64]

3.2.2 Ordinary Portland Cement (OPC)

Ordinary Portland cement type I according to ASTM C150 [65] (American Society for Testing and Materials) is used as primary binding material in casting of cement composite. The chemical compositions of the cement are shown in Table 3-2.

Table 3-2. Chemical composition of ordinary Portland cement

Component	SiO_2	CaO	Al_2O_3	SO_3	Fe_2O_3	IR	LOI
%	21.49	64.90	4.21	0.7	3.50	1.10	-

3.2.3 Fine and Coarse Aggregates

Florida Department of Transportation (FDOT) certified sand passing the sieve 4.75 mm is obtained from CEMEX and used as a fine aggregate. The gradation curve of the sand met the ASTM requirement (ASTM C33 [22]) as shown in Figure 3-5. Fineness modulus of the fine aggregate is 2.36, which also complies with the American Concrete Institute (ACI) requirement (2.3 to 3.1).

Coarse aggregates obtained from CEMEX with maximum size of 12 mm was used The sieve analysis for the coarse aggregate (Figure 3-6) demonstrated that the particle sizes for the coarse aggregate fell inside the ASTM certified zone (ASTM C 136 [23]).

The specific gravities of fine and coarse aggregates were 2.66 and 2.55, respectively. The absorptions of fine and coarse aggregates were 0.52% and 3.9% by weight of aggregate, respectively.

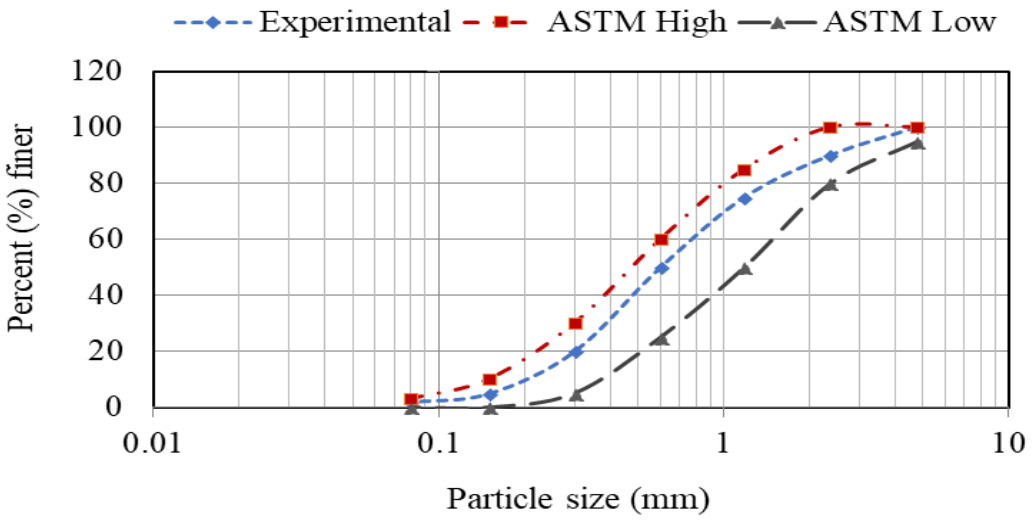

Figure 3-5. Gradation curves for fine aggregate and ASTM C33 [22] grading requirements for fine aggregate.

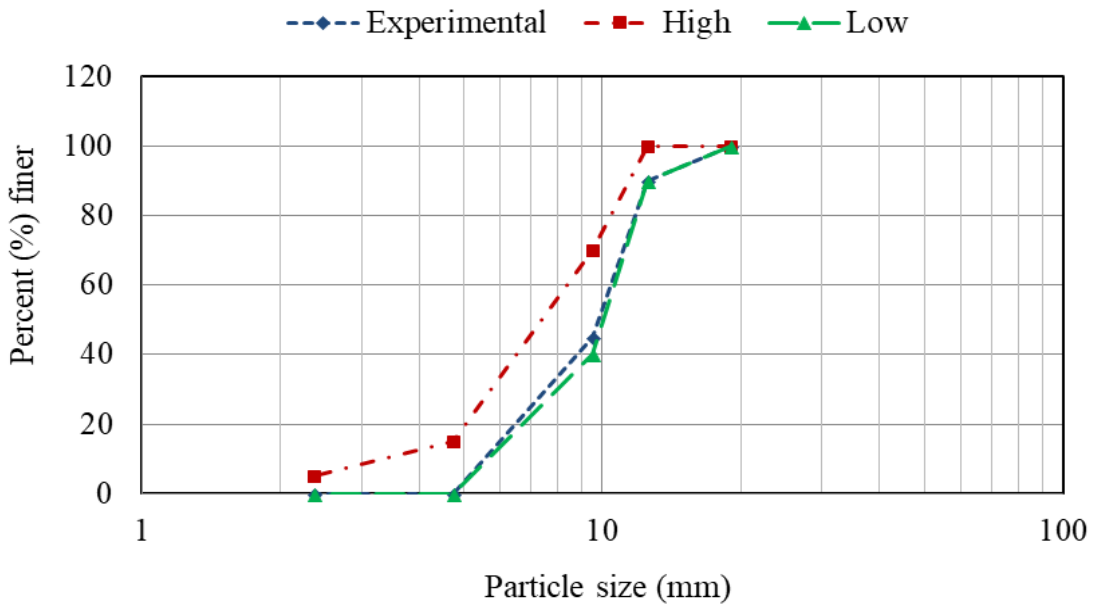

Figure 3-6. Gradation curves for coarse aggregate and ASTM C33 [22]grading requirements for coarse aggregate.

3.3 Mix Design

3.3.1 EOGO-Cement Paste and Mortar

The cement paste and mortar with EOGOs were prepared at different concentrations of EOGO, varying from 0.01% to 1.0% by weight of cement. Two different mix designs, the dry-mix and wet-mix, were explored in order to identify the best performing mix design for both cement paste and mortar. Dry-mix design is prepared by mixing EOGO and cement powders before cement paste and mortar formation. Wet-mix design is prepared by using the EOGO solution as the mixing water with cement paste and mortar mixes.

Figure 3-7 shows dry EOGO powder and EOGO dispersed solution. For dry-mix design, EOGO powder is dispersed by being physically rubbed for a minute to apply shearing force, and then ASTM C305-14 [66] was followed for mixing procedures for both cement paste and mortar. To disperse EOGO in water for the wet-mix design, EOGO powder first is poured into water. A sonicator is utilized for 20 minutes in order to disperse the EOGO into the water. The solution is then used as the mixing water.

The ASTM C305-14 [66] procedure was used for mixing both the cement paste and mortar. The weight ratio of water to cement was kept at 0.5 for cement pastes and 0.45 for mortars. Mix proportions of plain (control) and EOGO-cement pastes and mortars can be found in Table 3-3. The control cement paste and mortar samples denoted as CP for cement paste and CM for mortar.

The EOGO-cement paste specimens are named as GPD for cement paste mixed with the dry-mix design and GPW for cement paste mixed with the wet-mix design. Similarly, The EOGO-mortar specimens are named GMD for the dry-mix design and GMW for the wet-mix design. The number after the abbreviation represents the percentage of EOGO by weight of cement.

Figure 3-7. Edge-oxidized graphene oxide (EOGO): (a) Dry EOGO powder; (b) EOGO solution; and (c) the equipment for ball milling process [64]

Table 3-3. Cement paste and mortar mix proportions.

Specimen ID	w/c ratio	Water (ml)	Cement (gm)	Sand (gm)	EOGO (gm)
CP	0.5	1750	3500	-	-
GPD 0.01	0.5	1750	3500	-	0.35
GPD 0.05	0.5	1750	3500	-	1.75
GPD 0.1	0.5	1750	3500	-	3.5
GPD 0.5	0.5	1750	3500	-	17.5
GPD 1.0	0.5	1750	3500	-	35
GPW 0.01	0.5	1750	3500	-	0.35
GPW0.05	0.5	1750	3500	-	1.75
GPW 0.1	0.5	1750	3500	-	3.5
GPW 0.5	0.5	1750	3500	-	17.5
GPW 1.0	0.5	1750	3500	-	35
CM	0.45	780	1686	4215	-
GMD 0.01	0.45	780	1686	4215	0.1686
GMD 0.05	0.45	780	1686	4215	0.843
GMD 0.1	0.45	780	1686	4215	1.686
GMD 0.5	0.45	780	1686	4215	8.43
GMD 1.0	0.45	780	1686	4215	16.86
GMW 0.01	0.45	780	1686	4215	0.1686
GMW0.05	0.45	780	1686	4215	0.843
GMW 0.1	0.45	780	1686	4215	1.686
GMW 0.5	0.45	780	1686	4215	8.43
GMW 1.0	0.45	780	1686	4215	16.86

3.3.2 EOGO-Concrete

Cement, water, fine, and coarse aggregates were mixed in a conventional rotary drum concrete mixer in accordance with ASTM C192 procedure [67] with different percentages of EOGO (0.01–0.1 wt.%). Detailed mix proportioning of concrete mix can be found from Table 3-4. Unlike EOGO-combined paste and mortar mixes (0.01–1.0 wt.% of EOGO), EOGO was added to concrete mix from 0.01 % to 0.1 wt.% since the optimum content of EOGO was found as 0.05% for the strength improvement of EOGO-combined paste and mortar. Moreover, dry-mix design only was used for the concrete mix. To make EOGO solution for wet-mix, applying sonication is

necessary. Massive production of GO-solution using the ultra-sonicated method would be challenging and costly for practical use. Therefore, wet-mix design may not be feasible for field construction. The specimen ID is referred as C (concrete) and GCD (EOGO-combined concrete with Dry-mix design).

Table 3-4. Mix proportions of EOGO-concrete.

Specimen ID	w/c	Water	Cement	EOGO	Fine agg.	Coarse agg.
	Ratio	(kg/m3)	(kg/m3)	(kg/m3)	(kg/m3)	(kg/m3)
CC	0.5	186	372	-	609	1227
GCD0.01	0.5	186	372	0.372	609	1227
GCD0.05	0.5	186	372	0.186	609	1227
GCD0.1	0.5	186	372	0.372	609	1227

3.4 Experimental Procedure

3.4.1 EOGO-Cement Paste and Mortar

3.4.1.1 Mechanical property tests

Compressive strength tests of EOGO-cement paste and mortar were conducted according to ASTM C109 [68] on cubic specimens (50 mm × 50 mm × 50 mm). A static hydraulic testing system with loading control at a rate of 900 N/sec was used for this test as shown in Figure 3-9a. The loading history indicated by the testing machine was recorded until failure of the samples.The flexural strength was measured by following a procedure as prescribed by ASTM C348 [69]. Three-point loading flexural strength tests were performed on 50 mm × 100 mm × 25 mm prisms. A total of 264 specimens were prepared for cement paste and mortar tests.

3.4.1.2 Porosity test

Effect of the mixing method of EOGO on the total porosity of EOGO-cement pastes and mortars was investigated by conducting the porosity test according to ASTM C1754/C1754M-12 [70] which is a gravimetric method. Two cylinders with 75 mm diameter and 150 mm height were prepared for each cement composite mix. A total of 88 specimens were prepared for this test. The test was performed at 7 and 28 days. At first, the submerged mass of each specimen was measured until the submerged mass became constant. Secondly, the specimens were placed in an oven at a temperature of 38 ± 5 ^{o}C and the mass of the drying specimens were measured every 24 hours until the mass became constant.

3.4.1.3 Water sorptivity test

The water absorption rate of cement composites was determined by conducting water sorptivity test for each cement paste and mortar specimen in accordance to ASTM C1585-13 [71]. Two-disc specimens (100 mm in diameter and 50 mm in height) were prepared for each mix. A total of 44 specimens were prepared for this test, and the test was performed at 28 days. The water absorption rate was measured by exposing the bottom surface of cement paste and mortar specimens to water. The other surfaces were sealed with Latex based water proof paint. As illustrated in Figure 3-8, the water level in the test setup was maintained approximately 2 mm from the bottom of the specimens as specified in the standard method. The weight variation of each specimen was recorded at specific time intervals after the first contact with water. Mainly, this test determines the increase in cement paste or mortar prism masses due to capillary-rise absorption. The mathematical equation to calculate the absorption can be expressed as:

$$I = \frac{m_t}{a*d} \quad (1)$$

Where I = is the absorption (mm), m_t is the change in specimen mass (g) at the time t, a is the exposed area of the specimen (mm^2), and d is the density of the water (g/mm^3).

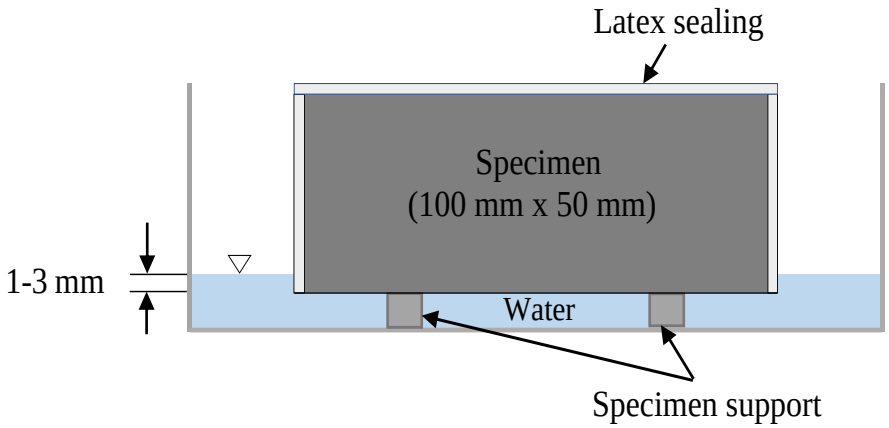

Figure 3-8. Schematic of water sorptivity test setup

3.4.2 EOGO-Concrete

3.4.2.1 Mechanical Property Test

The compressive and flexural strength tests were conducted according to ASTM C39 [72] and ASTM C293 [73], respectively on concrete cylinder with 100 mm diameter and 200 mm height for compressive strength and 75 mm × 260mm × 70 mm prisms for flexural strength tests that were carried out by displacement control at a rate of 0.005 mm/min. The compressive and flexural strength tests setups are shown in Figure 3-9b and c. A total of 48 specimens were prepared for concrete tests. All specimens were cured at 25 ^{o}C and 90% relative humidity and tested at 7 and 28 days. All tests were conducted in triplicate to evaluate the influence of EOGO content on the strengths of cement composites. Then the results were averaged.

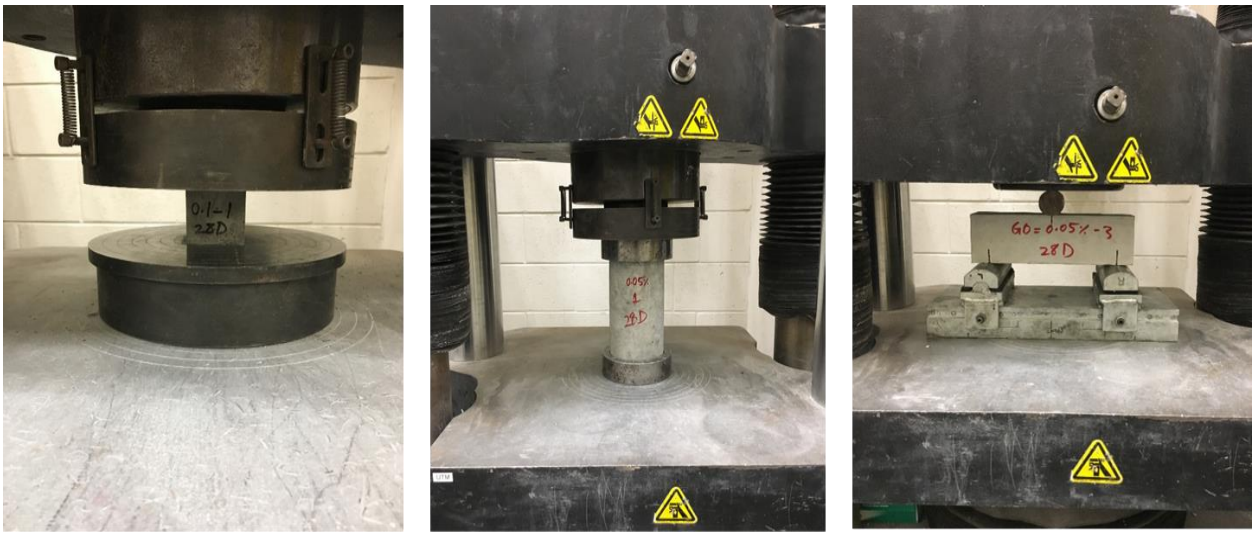

(a) (b) (c)

Figure 3-9. Mechanical properties testing setup: (a) compressive strength for cube specimens, (b) compressive strength for cylinder specimens and (c) flexural strength for beam specimens

3.5 Results

3.5.1 Cement Paste Study

3.5.1.1 Compressive and Flexural Strengths

The results of the compressive and flexural strength tests for cement pastes using dry-mix design method are shown in Figures 3-10 and 3-11. The compressive and flexural strength increased as EOGO content rose until the EOGO reached 0.05%. Then a reduction in the strength with a further increase in EOGO content is observed. The compressive and flexural strength of control specimens (CP) were 23.66 MPa and 4.8 MPa at 7 days, and 31.12 MPa and 5.48 MPa at 28 days, respectively. Figure 3-10 shows that specimens containing 0.05% and 0.1% of EOGO (GPD 0.05 and GPD 0.1) exhibited 14.93% and 13.11% increase in compressive strength at 7 days compared to CP. After 28 days, the compressive strength increased 19.6% and 17% in comparison

with CP. Figure 3-11 shows that the flexural strength of GPD 0.05 and GPD 0.1 increased by 33.95% and 28.18% at 7 days when compared to CP. Also, the flexural strength of GPD 0.05 and GPD 0.1 increased 28.02% and 23.18% at 28 days, respectively compared with that of CP. Therefore, the optimum EOGO content was 0.05% (GPD 0.05). However, the strength of specimens containing 0.1% (GPD 0.1) were slightly lower than those of GPD 0.05. These results indicate that using dry-mix design for cement paste containing EOGO specimens has significant effect on the mechanical properties of those specimens.

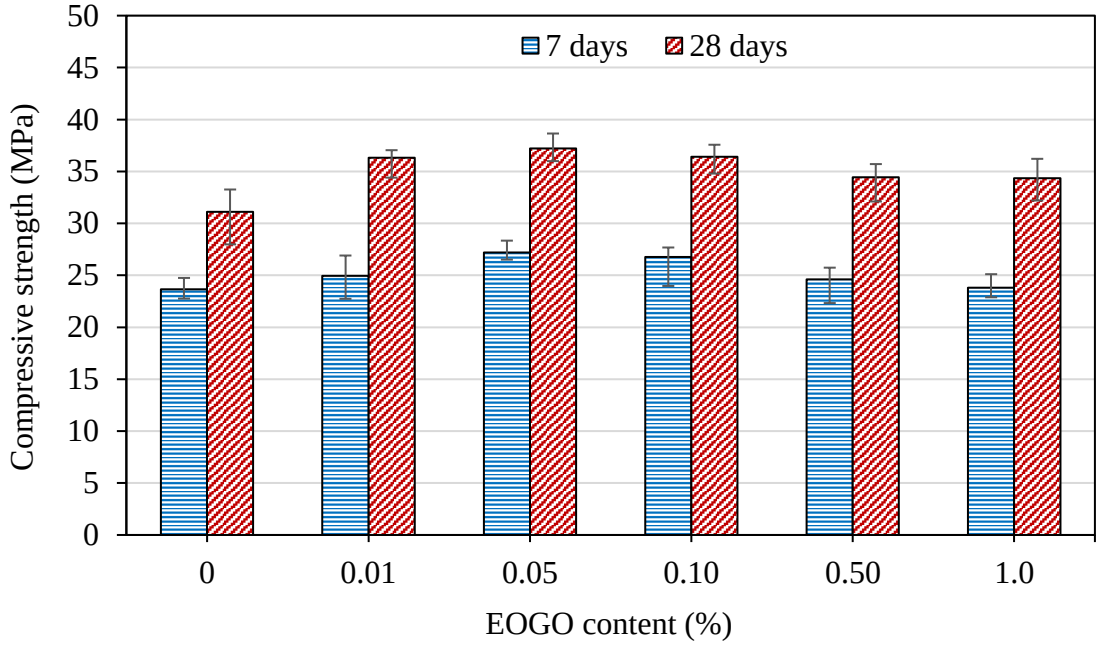

Figure 3-10. Compressive strength of EOGO-cement pastes with dry-mix design.

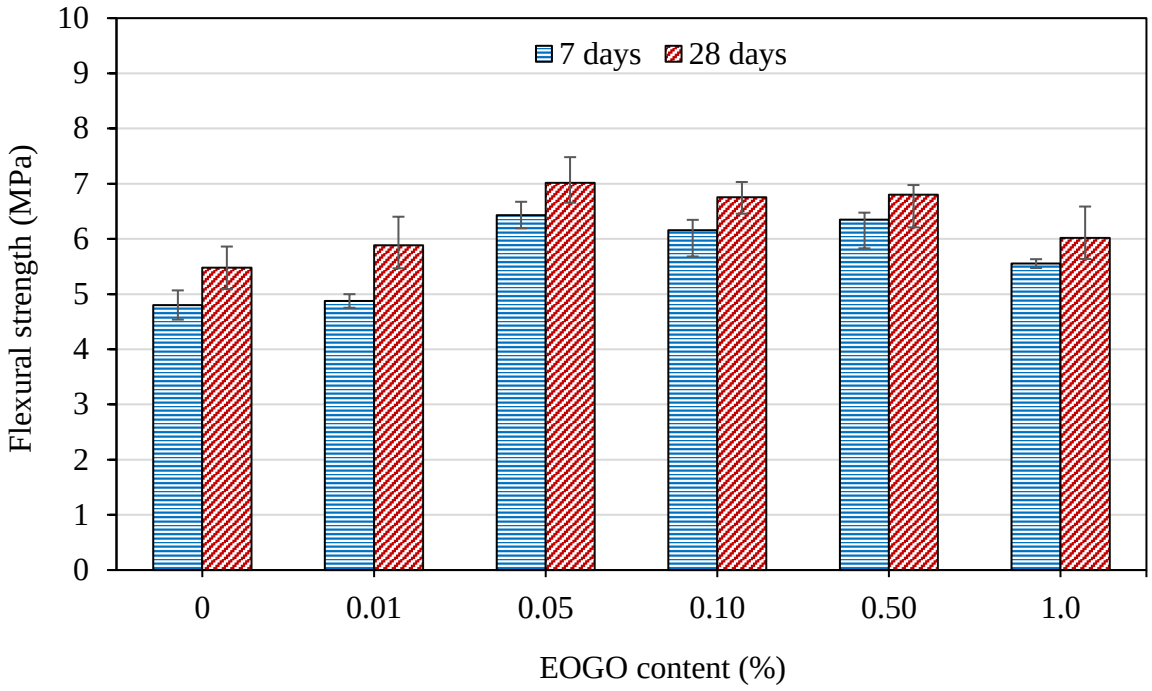

Figure 3-11. Flexural strength of cement pastes with dry-mix design

To compare the effect of different mix design methods, namely the dry and wet-mix design methods, specimens that were mixed by wet-mix design methods (GPW) were tested. The results of the compressive and flexural strength tests of those specimens are shown in Figures 3-12 and 3-13. The compressive and flexural strength of GPW specimens are higher than those of CP and show a similar pattern of strengths improvement compared with GPD specimens.

Figure 3-12 shows that the compressive strength of GPW 0.05 and GPW 0.1 increased by 19.39% and 26.92% at 7 days, respectively. It is also found that compressive strength of GPW 0.05 and GPW 0.1 increased 25.54% and 16.20% at 28 days, respectively compared with that of CP. Moreover, Figure 3-13 shows that the flexural strength after 7 days curing of GPW 0.05 and GPW 0.1 increased by 34.85% and 29.12%. In addition, after 28 days curing, the flexural strength of GPW 0.05 and GPW 0.1 improved 37.34% and 22.25% , respectively compared with that of

CP. These results indicate that GPW 0.05 and GPW 0.1 exhibited a higher improvement of the mechanical properties of GPW specimens among the other percentages.

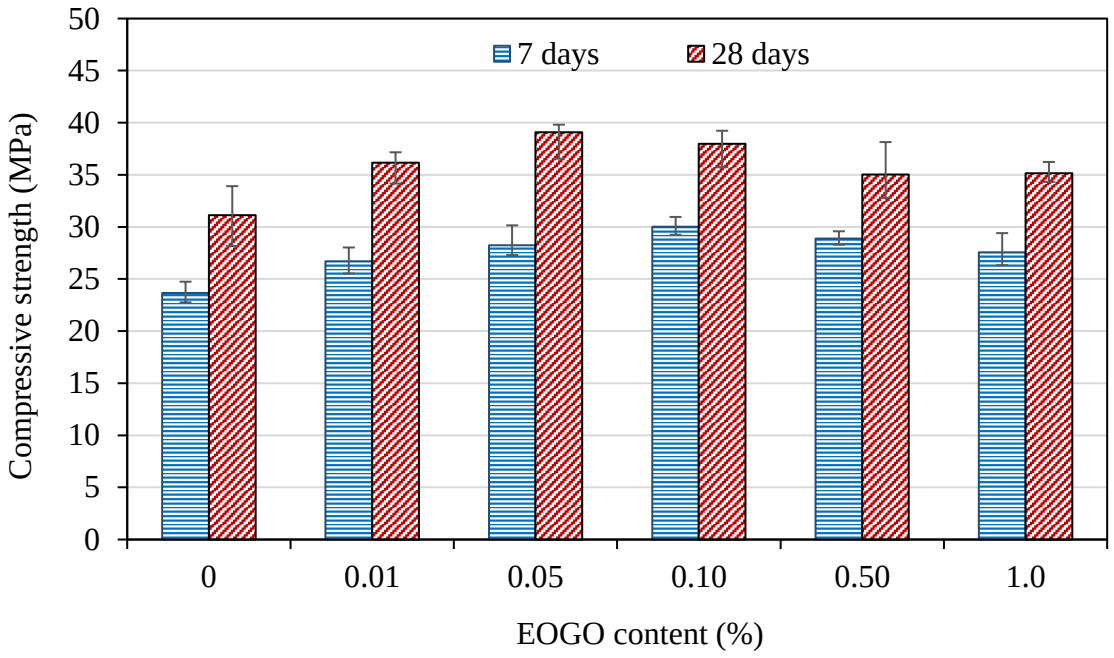

Figure 3-12. Compressive strength of EOGO-cement pastes with wet-mix design

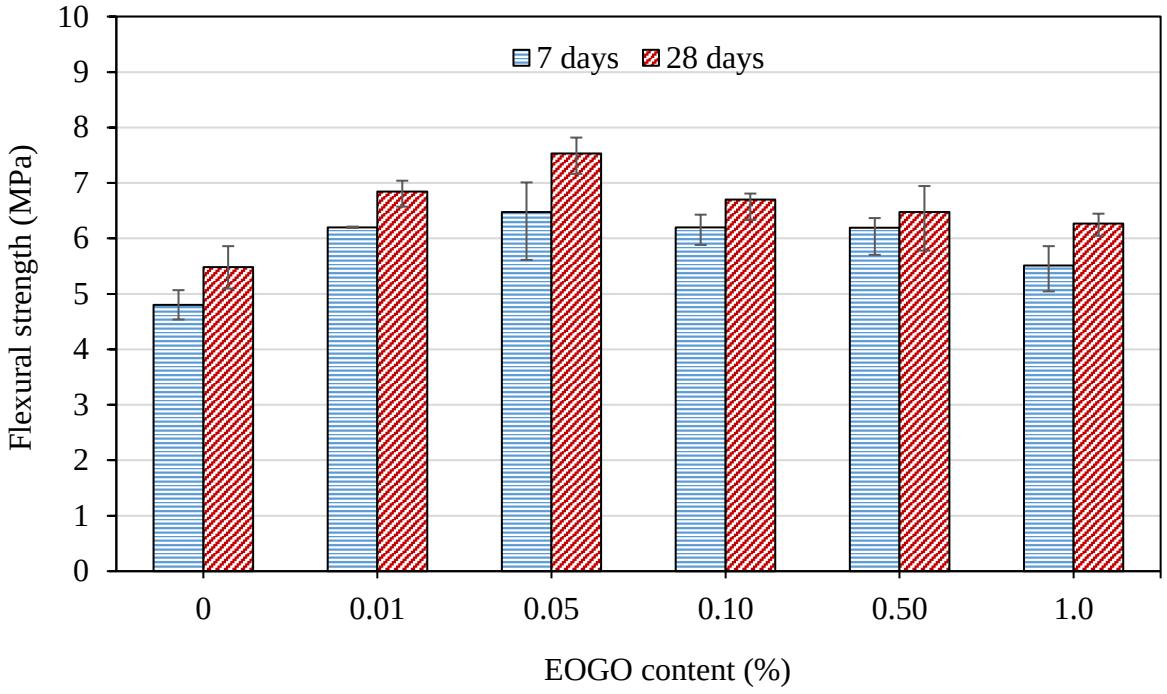

Figure 3-13. Flexural strength of EOGO-cement pastes with wet mix design.

3.5.1.2 Total Porosity

Figure 3-14 shows the relationship between the porosity of the control mix and the mixes with different EOGO contents cured at 7 and 28 days performing dry-mix design method. It is clearly seen that the porosity of GPD samples at 7 days slightly decreased when the EOGO content was 0.05% and more when compared to the control cement paste (CP). The porosity of all GPD specimens cured at 28 days were less than the CP. This indicates that the addition of EOGO using dry-mix design reduces the porosity of EOGO-cement paste specimens. However, the reduction in the porosity of EOGO-cement pastes at 7 and 28 days was not significant. For instance, the greatest reduction of 5% in the porosity was observed on the 28 day of cured specimen when EOGO was 0.1%.

To compare the effects of different mix design methods on the porosity of cement paste, the porosity of GPW samples prepared by using wet-mix design were measured. Figure 3-15 illustrates the effect of the addition of EOGO on the porosity of cement paste cured at 7 and 28 days. It was observed that GPW 0.05 exhibits the highest reduction in the porosity among GPW samples at 7 and 28 days. The porosity of GPW 0.05 cured at 7 and 28 days decreased by around 4.5% and 6%, respectively compared to CP. In addition, it can be seen that the porosity at 7 and 28 days of GPW samples are less than that of GPD samples. For example, the porosity at 28 days of GPW 0.05 is around 6% lower than that of GPD 0.05.

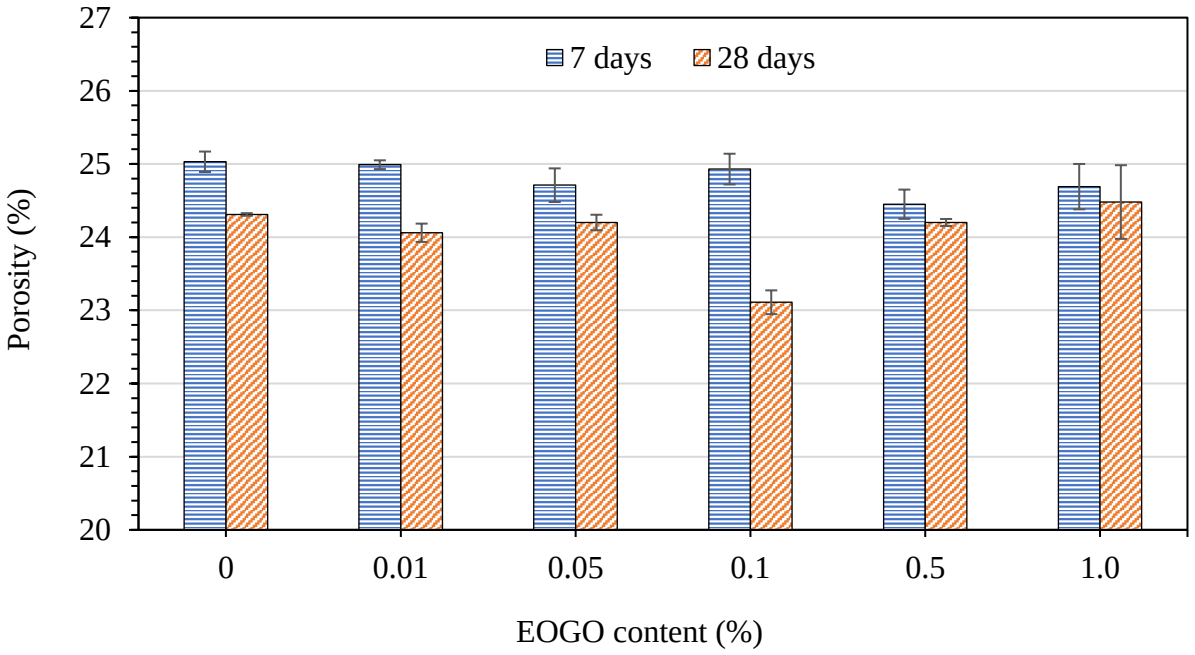

Figure 3-14. Effect of EOGO on the porosity of cement pastes with dry-mix design.

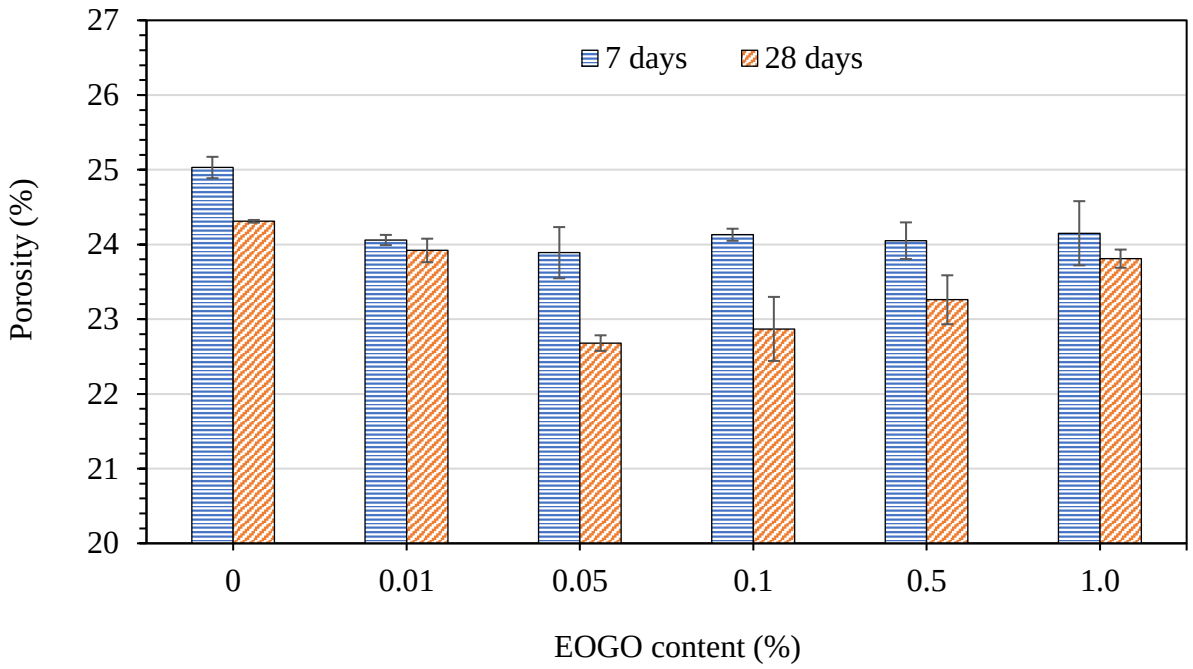

Figure 3-15. Effect of EOGO on the porosity of cement pastes with wet-mix design.

3.5.1.3 Water Sorptivity Test

To investigate the effect of EOGO on a capillary pore system of EOGO-cement composite, the rate of capillary-rise absorption by the hardened EOGO-cement composite specimens were measured by sorptivity test. The capillary pore system of cement composite plays an important role of water penetration through the microstructure of cement composite. There is a strong relationship between the capacity of water to penetrate the microstructure and durability of cement composite. EOGO-composites (GPD and GPW) were chosen for sorptivity test to focus on the effect of mix-designs. Figures 3-16 and 3-17 show the sorptivity results of the dry- and wet-mix designs (GPD and GPW), respectively. The rate of water absorption by GPD and GPW were determined by the mass of a specimen resulting from absorption of water as a function of time.

The increase in mass is due to capillary-rise absorption. In Figure 3-16 and 3-17, the absorption values were plotted against the square root of a as per the ASTM C1585-13 standard.

The unit of the square root of time is used for the x-axis because the absorption which is the capillary suction in cement composite is approximately proportional to the square root of time according to the diffusion theory. The absorption was measured over nine days. The result of sorptivity test can be divided into two phases which are initial and secondary sorptivity. The initial sorptivity is defined as the slopes of the linear regression up to the first six hours. Secondary sorptivity is defined as the slopes of the linear regression from first day to the ninth day. The initial sorptivity slope is generally steeper than the secondary sorptivity slope, indicating a greater rate of absorption during initial sorptivity. In addition, the change in slope of the absorption curve in the late stage, secondary sorptivity signifies the saturation of a specimen. As can be seen in Figure 3-16 and 3-17, the rate of water absorption of EOGO-composites is lower than the control specimen (CP) except GPD1.0. This result of low rate of absorption of EOGO-composites signifies that that EOGO may mean different things. It may be either reduce a continuity of capillary pores or reduce the total amount of pores in cement composite. Or it could mean the reduction of both because of the rate of absorption can be mostly improved by a refinement of capillary pore system. In addition, the strength increment of EOGO-composites might be explained by this absorption refinement of EOGO-composite. Either reductions of a continuity of capillary pores or the total amount of pores in cement composite can improve the strength of cement composite.

It is interesting to note that the lowest rate of absorption is found from GPD0.05 and GPW0.1 for the dry and wet-mix designs. In the case of the wet-mix design, the absorption results of GPW0.05 and GPW0.1 are very similar. The reduction of initial and secondary absorptions for

GPD0.05 are 29% and 48%, respectively. The reduction of initial and secondary absorptions for GPW0.05 are 70% and 57%, respectively. All results of the initial and secondary sorptivity of EOGO-composites are presented in Table 3-5. This improvement in sorptivity with the addition of 0.05% EOGO has a strong correlation with the strength improvement of EOGO-composite. It was found that the optimum EOGO content for the strength improvement is 0.05% of EOGO. Both sorptivity and strength of cement composite can be improved by a refinement of microstructures of cement composite. Through the refinement of microstructures, the capability of water to penetrate the microstructures of cement composite can be diminished, thus the sorptivity of cement composite can be reduced. Moreover, with the refinement of microstructures, the continuity of capillary pores and the total amount of pores could be diminished, thus possible locations of stress concentration can be reduced. The stress concentration typically happens at the continuous capillary pores or a pore itself. Based on the results of strength and sorptivity tests, the addition of 0.05% EOGO refine the microstructures of cement composite well. A more in-depth microstructure analysis of EOGO composite is discussed in the section 3.5.1.4.

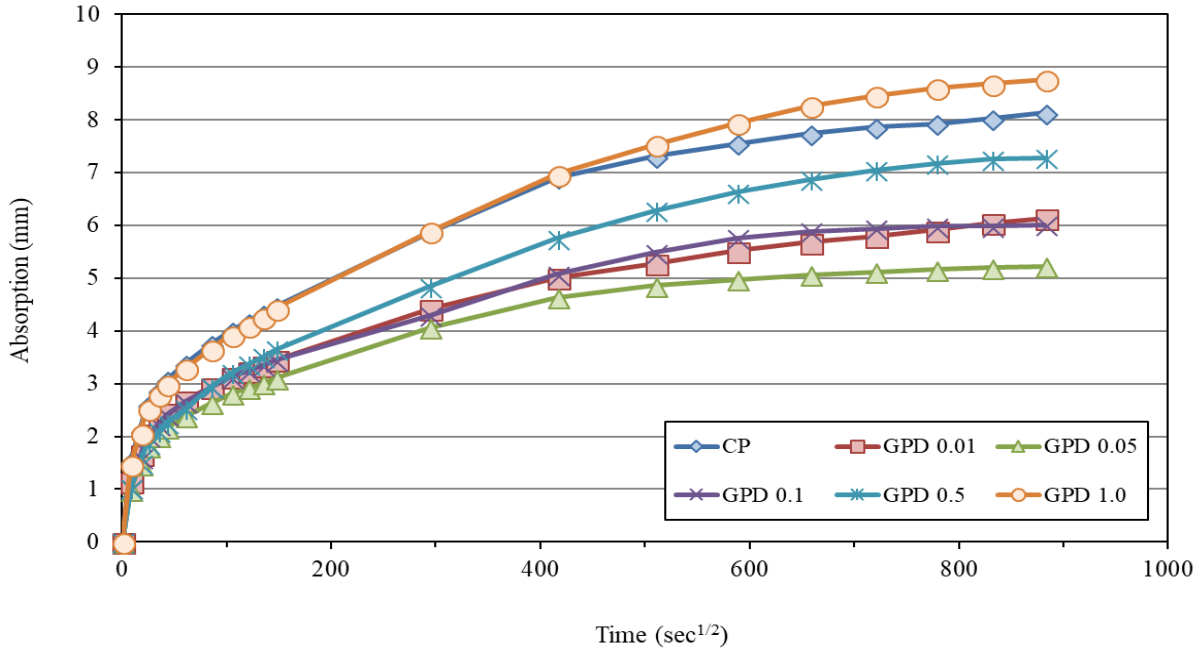

Figure 3-16. Water sorptivity of EOGO-cement pastes with dry-mix design.

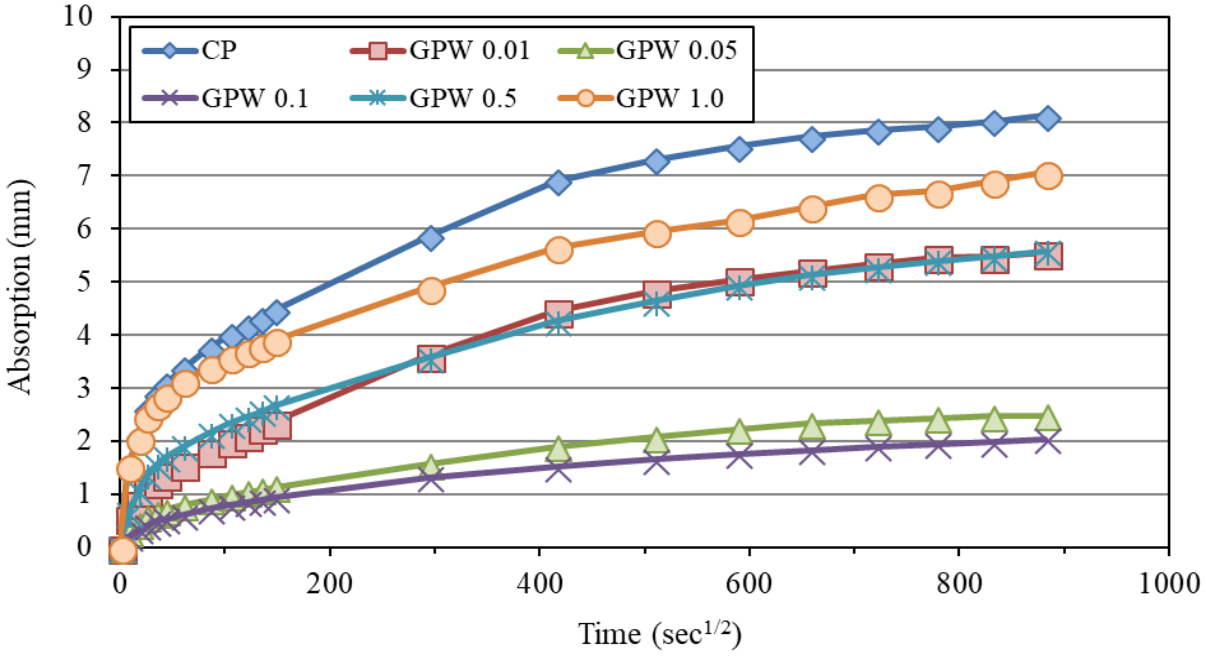

Figure 3-17. Water sorptivity of EOGO-cement pastes with wet-mix design.

Table 3-5. Initial and secondary sorptivity of cement pastes for dry and wet-mix designs*

Samples	Initial sorptivity ($mm/s^{1/2}$)	% reduction compared to plain paste	Secondary sorptivity ($mm/s^{1/2}$)	% difference with plain paste
CP	0.0183	-	0.0035	-
GPD 0.01	0.0147	-19.7	0.0028	-20.0
GPD 0.05	0.0130	-29.0	0.0018	-48.6
GPD 0.1	0.0140	-23.5	0.0027	-22.9
GPD 0.5	0.0170	-7.1	0.0040	+14.3
GPD 1.0	0.0183	0	0.0042	+20.0
GPW 0.01	0.0118	-35.5	0.0030	-14.3
GPW0.05	0.0054	-70.5	0.0015	-57.1
GPW 0.1	0.0048	-73.8	0.0012	-65.7
GPW 0.5	0.0126	-31.1	0.0033	-5.7
GPW 1.0	0.0146	-20.2	0.0034	-2.9

* (-ve means reduction, and +ve means increase compared to CP)

3.5.1.4 Microstructure Analysis

3.5.1.4.1 X-Ray Diffractometer (XRD) Analysis

In order to investigate the phase identification and crystalline phase change of EOGO-cement composites with the change in concentration of EOGO in cement mix, XRD analysis was carried out after different curing times of 7 and 28 days. EOGO-cement composite specimen with dry-mix design (EOGO ranging from 0.01 to 0.1%) was specifically chosen for the XRD analysis based on the strength result. As found in the section 3.5.1, dry-mix design is feasible and practical for cement/concrete industry in comparison with wet-mix design since ultra-sonication can be omitted. The diffraction patterns of EOGO-cement composites were recorded by using Rigaku D/MAX XRD II with CuKa radiation at wavelength of 1.545Å operated at 40 mA and 45 kV. The range of the diffraction angle is from 5 to 60°. Figure 3-18 shows the diffraction patterns of EOGO-cement composites with shorthand notations of crystalline compounds. To verify the phase identification of crystalline compounds, the peak diffraction position of each crystalline compound is presented in Table 3-6.

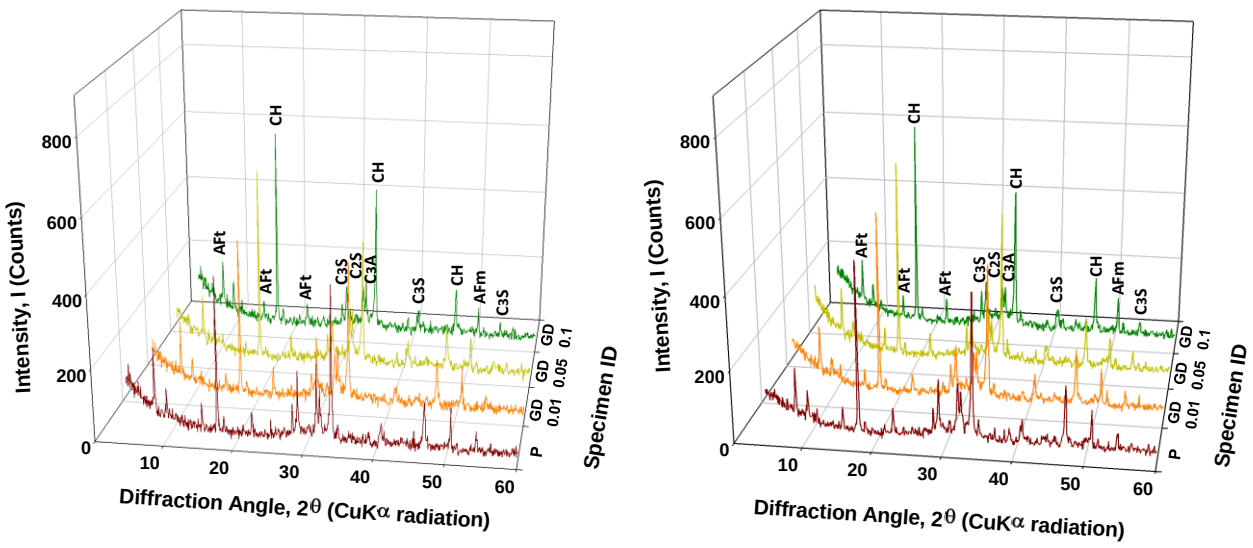

(a) XRD pattern of GPD specimen (Day 7) (b) XRD pattern of GPD specimen (Day 28)

Figure 3-18. The diffraction patterns of EOGO-cement paste cured at (a) 7 days and (b) 28 days

Table 3-6. Phase identification of EOGO-cement composite [74–76].

Compound	Chemical Formula	Shorthand Notation	Crystal Structure	Peak Position 2θ°
Portlandite	$Ca(OH)_2$	CH	Hexagonal	18.10, 34, 47
Alite	$3CaO.SiO_2$	C_3S	Triclinic	29.44, 41, 51.7
Belite	$2CaO.SiO_2$	C_2S	Monoclinic	32.2
Celite	$3CaO.Al_2O_3$	C_3A	Isometric	32.6
Ettringite	$Ca_6Al_2(SO_4)_3(OH)_{12}.26H_2O$	AFt	Hexagonal	9.24, 15.8, 22.9, 50.7

The XRD results in Figure 3-18 shows the presence of major hydration product of cement which are portlandite (CH) and ettringite (AFt). The other major hydration product, calcium silicate hydrate (CSH), is not presented in the XRD result since CSH is amorphous. Figure 3-18

also shows that the major phases of Portland cement such as alite (C_3S), belite (C_2S) and celite (C_3A) are presented in the harden EOGO-cement composites cured at 7 and 28 days.

Peak positions of XRD intensity of control specimen and EOGO-cement composites are similar. However, the magnitude of XRD intensity of specimens are varied. According to Klug, Reynolds and other researchers, the intensity (y-axes of Figure 3-18) of the XRD result offers the information about the relative percentage of a crystalline compound in the specimen. To quantify the crystalline phase change of EOGO-cement composites with the change in concentration of EOGO, the rate of increase/decrease of relative crystalline compounds were calculated using following equation:

$$X(\%) = \frac{I_{EOGO} - I_{Control}}{I_{Control}} \times 100 \quad (2)$$

Where, X (%) is the percentage increase or decrease in crystalline phase change of EOGO-cement composite. I_{EOGO} and $I_{Control}$ are the peak intensities corresponding to crystalline compounds in EOGO-cement composite and control specimen.

Table 3-7 demonstrates the rate of increase and decrease of relative crystalline compounds based on the intensity of XRD result with the proposed equation. It was observed that CH crystal formation was expedited with the addition of EOGO in cement mix. This acceleration of CH crystal formation indicates two possible hypotheses. First, EOGO acts as Nano-seeding material to promote CH crystal formation. Second, EOGO expedites CH crystal formation by delaying and hindering the formation of other hydration products such as CSH and AFt. For the first hypothesis, the acceleration of CH crystal formation due to the presence of EOGO can be supported and

explained with the mix proportion. Since mix proportions of EOGO-cement composites are the same as the control except the amount of EOGO, the total amount of alite and belite are same for all cases. The CH crystal formation increases when alite and belite dissolve and react with water molecules in cement pore solution. The reduction of alite and belite compounds in EOGO-cement composite in comparison with the control can be found in Table 3-7. In other words, the reaction of alite and belite with water was catalysed by EOGO. Unlike the first hypothesis, the second hypothesis is unsuitable according to the strength result. Since CSH is primarily responsible for the strength gain, the total amount of CSH in EOGO-cement composite should be higher than the control specimen based on the strength result. In addition, it is noteworthy that the highest increase rate of CH crystal is found with GPD0.05 at different hydration times (see Table 3-7). This result corresponds to the highest strength result of GPD0.05 among all EOGO-cement composites by dry-mix design.

Another hydration product which was chosen for XRD analysis is ettringite (Aft). The rate of ettringite formation depends on the curing time. On day seven of curing, the rate of ettringite formation decreased in proportion to the addition of EOGO. On the contrary, the rate of ettringite formation at 28 days has increased in proportion to the addition of EOGO. There is no clear mechanism found regarding this phenomenon. However, it can be noted that there is a relationship between celite (C_3A) and ettringite formation. It is known that ettringite forms by the reaction between celite and gypsum. As can be seen in Table 3-7, the rate of ettringite formation decreases with the increment of unhydrated celite (On the 7the day). And, it increases with the reduction of celite (at 28th day). This indirectly points toward the delayed reaction between celite and gypsum at the early stage of hydration with the presence of EOGO.

Table 3-7. Rate of increase/decrease of relative crystalline compound of EOGO-cement composite

Day	Specimen ID	Rate of increase/decrease (%) of relative crystalline compound				
		CH (Portlandite)	C_3S (Alite)	C_2S (Belite)	C_3A (Celite)	Aft (Ettringite)
7	GOD0.01	1.3	-5.7	-34.0	8.9	-10.8
	GOD0.05	31.5	-26.1	-30.0	9.4	-15.6
	GOD0.1	24.2	-30.4	-26.0	10.0	-19.7
28	GOD0.01	9.7	-6.4	-10.8	1.7	4.3
	GOD0.05	27.0	-10.9	-11.7	-3.3	7.1
	GOD0.1	20.8	-4.3	-6.4	-5.0	10.0

3.5.1.4.2 Scanning Electron Microscopy (SEM) and Electron Dispersive Spectroscopy (EDS) Analyses

SEM and EDS analyses helped in investigating microstructures and chemical composition of cement hydration products when EOGO was introduced into cement matrix. EOGO-cement composite specimen with the optimum EOGO content (0.05%) made by the dry-mix design (GPD0.05) was chosen for the microstructural analysis as described in Section 3.5.1.4.1 SEM/EDS analyses of GPD0.05 mixes were carried out with the designated time intervals (15 minutes, 1 hour, 24 hours and 72 hours) to evaluate the microstructure change of cement composite caused by EOGO. To investigate the crystalline structures of each specimen, interested spots of crystalline structures were chosen from the image of SEM and a high-energy beam of X-ray was emitted to those chosen spots. Yellow boxes indicate those chosen spots of crystalline structures for EDS analysis.

Figure 3-19a shows the crystal morphology of GPD0.05 at 15 minutes (5.0 kX magnification). As Figure 3-19a shows, it is difficult to judge the exact crystalline phase based on the morphology since it is the beginning stage of a nucleation. Table 3-8a shows the chemical compositions of yellow boxes (1, 2, and 3) of GPD0.05 at 15 minutes. The results of 1 and 2 areas

show that these spots have the high percentage of carbon and oxygen which indicate the presence of EOGO. Moreover, these spots (1 and 2) have a relatively high percentage of calcium element compared to other elements. It may indicate that the dissolved calcium ions from cement particle initiate a nucleation of crystalline phase on EOGO or at least calcium ions and the functionalized oxygen groups of EOGO react to each other. Unlike yellow boxes of 1 and 2, the crystal morphology and chemical composition of yellow spot of number 3 indicate that it is ettringite. The needle-shape crystal and the presence of calcium, sulfur, and aluminum elements are the evidence of ettringite. Figure 3-19b shows crystal morphology of GPD0.05 at 1 hour (5.0 kX magnification). In comparison with Figure 3-19a, amorphous morphology of C-S-H (boxes 1 and 3) and needle-shaped ettringite (spot 4) can be clearly seen from Figure 3-19b. The result of EDS analysis (Table 3-8b) also supports the findings from SEM image. Crystals in yellow box 2 could be a combination of ettringite and C-S-H. It is noteworthy that carbon element is found in high percentage in CSH in comparison with ettringite. It may indicate either EOGO is embedded in CSH or CSH forms on EOGO. Figure 3-19c presents cement hydration products of GPD0.05 at 24 hours (10.0 kX magnification). Unlike the previous two SEM images (15mins and 1hour) of GPD specimen, Figure 3-19c shows a different pattern of hydration products. Different crystal phases of CSH and Aft are blended as one. Even though microstructures in boxes 1 and 2 look like a bundle of ettringite, EDS data of Table 3-8c indicates that those hydration products are a mixture of CSH and ettringite. In addition, EDS data of three boxes (1, 2 and 3 in Figure 3-19c) shows that EOGOs are spread out in those spots. Figure 3-19d depicts microstructures of GPD0.05 at 172 hours (10.0 kX magnification). SEM image of Figure 3-19d shows different types of hydration products more clearly. Hydration products in boxes 1 and 4 clearly show amorphous morphology of CSH. Also,

the needle-shaped hydration product at spot 3 is ettringite crystal. EDS data of boxes 1, 4 and spot 3 (Table 3-8d) are in good agreement with the morphologies of those hydration products. The hydration product in box 2 looks as if it is an amorphous CSH; however, it is jennite, one of the ordered crystalline CSHs according to the EDS data. EDS data of area 2 (Table 3-8d) shows Ca/Si ratio of 2.5 which directly indicates the presence of jennite in that area. It is noteworthy that carbon elements are mostly found in either amorphous or crystalline CSHs not in other crystalline compounds such as ettringite crystal. This observation may support two possible explanations made in the previous sections. Firstly, amorphous CSH initiates or forms on EOGO due to the presence of the functionalized oxygen groups. Second, EOGO is embedded in CSH to reinforce microstructures. To achieve higher strength, EOGO-cement composite should either have more of CSH or become denser. In other words, the addition of EOGO makes either more of CSH in cement mix or makes the cement composite denser. XRD data indirectly proves more of CSH formation in EOGO-cement composite. Moreover, EDS data indicates that EOGO are well distributed in different locations of CSH.

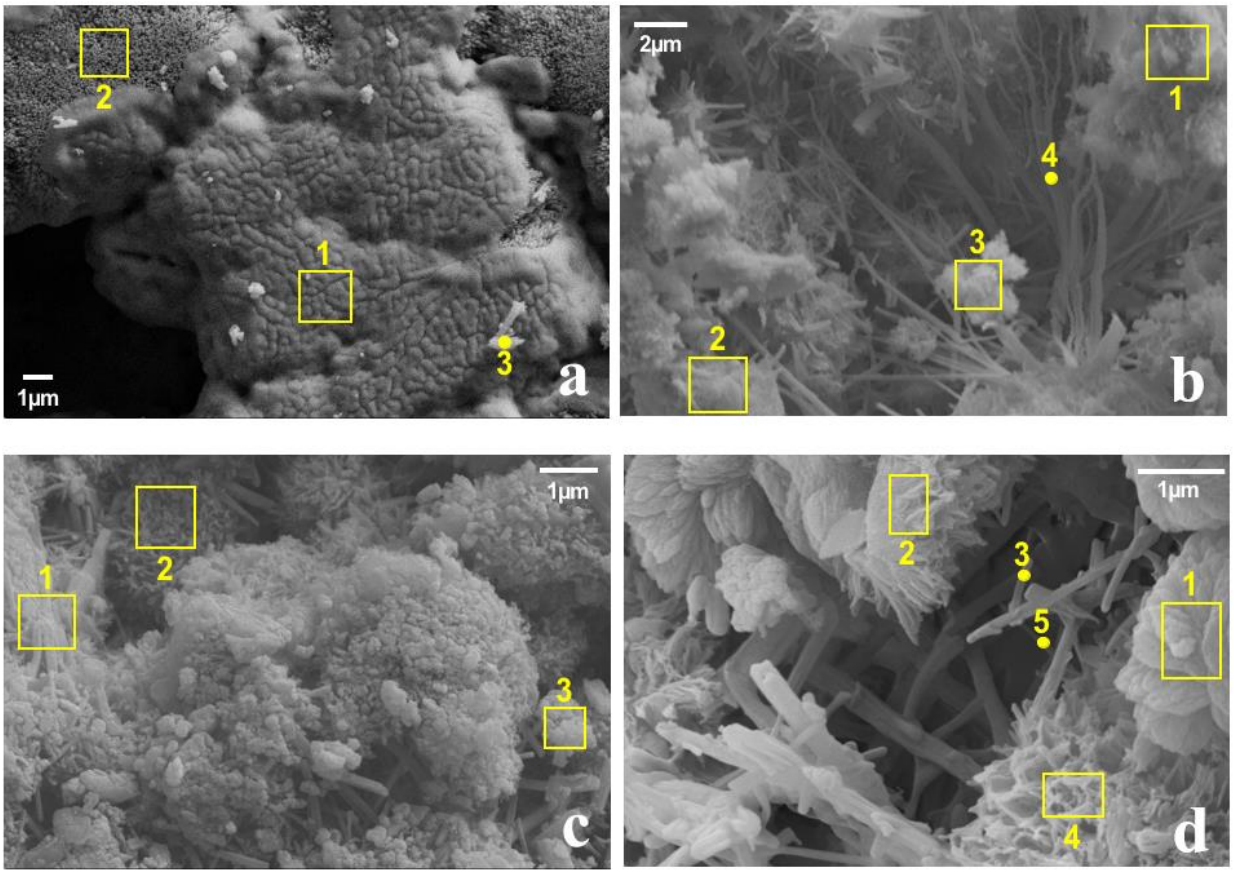

Figure 3-19. SEM images of EOGO-cement composite (0.05% EOGO) specimen at (a) 15 mins, (b) 1hr, (c) 24hrs and (d) 72hrs with different resolutions.

Table 3-8. EDS analysis on EOGO-cement composite (Locations of EDS in Figure 3-19)

Time	Shots	C (%)	O (%)	Al (%)	Si (%)	S (%)	Ca (%)	Total (%)	Probable Compounds
15 mins	1(Area)	62.20	19.35	---	0.09	6.54	11.83		Nucleation + EOGO
(a)	2(Area)	49.02	26.23	---	0.43	1.21	23.12	100	Nucleation + EOGO
	3(Point)	0.61	----	0.46	0.06	27.51	71.37		Ettringite (AFt)
1 hr	1(Area)	14.94	47.28	1.91	8.30	---	27.56		C-S-H + EOGO
(b)	2(Point)	9.27	55.56	3.97	3.75	3.59	23.86	100	AFt + C-S-H + EOGO
	3(Area)	16.73	54.56	1.94	5.31	---	21.46		C-S-H + EOGO
	4(Point)	6.12	42.54	3.59	6.51	6.66	34.58		AFt+ EOGO
24 hrs	1(Area)	25.32	52.15	3.48	2.28	1.89	14.87		C-S-H + AFt+ EOGO
(c)	2(Area)	21.29	48.32	2.83	5.33	2.34	19.91	100	C-S-H + AFt + EOGO
	3(Point)	34.75	45.76	1.00	3.98	1.42	13.10		C-S-H + AFt + EOGO
72hrs	1(Area)	13.29	30.91	---	4.03	---	51.79		C-S-H + EOGO
(d)	2(Point)	17.10	41.53	2.40	11.69	---	27.30		Jennite + EOGO
	3(Point)	---	13.70	2.58	9.23	5.47	69.01	100	AFt
	4(Area)	19.28	41.68	---	10.72	---	28.34		C-S-H + EOGO
	5(Point)	---	7.29	1.58	12.91	2.35	75.87		AFt

Based on the investigations of the analyses of XRD and SEM/EDS, a potential reaction mechanism between EOGOs and cement hydration products can be proposed as shown in Figure 3-20. EOGO with the functional oxygen groups such as -OH and -COOH may act as a Nano-seeding material to promote the nucleation of C-S-H and other cement hydration products. This would make EOGO-cement composite denser. As a result, strength of cement composite was enhanced with the increase of hydration products, especially CSH in cement composite. In addition, sorptivity of cement composite was improved with the reduction of a continuity of capillary pores and the total amount of pores in cement composite. Figure 3-20 is a schematic diagram to explain the proposed role of EOGO in cement composite. The black dot and gray dot in Figure 3-20 indicate cement particle and EOGO, respectively. The expansion of the dots represents the crystal growth from cement particle and EOGO. Figure 3-20a shows the

crystallization of hydration products in cement pore solution at 3-day (left) and 28-day (right) with the absence of EOGO. Figure 3-20b shows the crystallization of hydration products in cement pore solution with the presence of EOGO (gray dots) at 3-day (left) and 28-day (right). By adding EOGOs which could be initiating points of the crystallization of dissolved ionic components from cement particles in cement pore solution, EOGO-cement composite can be denser, and the capillary pore system can be refined.

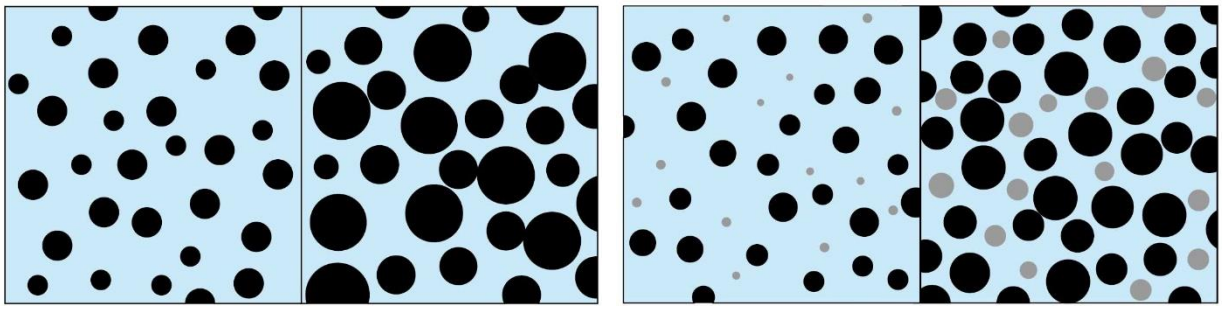

(a) (b)

Figure 3-20. Schematic diagram of crystal growth at 3 and 28 days of (a) control mix and (b) EOGO-cement composite

3.5.2 Cement Mortar Study

3.5.2.1 Compressive and Flexural Strengths

The results of the compressive and flexural strength tests for the mortar samples prepared by dry-mix design are illustrated in Figures 3-21 and 3-22. The compressive strength of specimens without EOGO (CM) and EOGO-mortar specimens (GMD) are shown in Figure 3-21. The compressive strengths of CM were 29.9 MPa at 7 days and 36.8 MPa at 28 days. All GMD specimens showed higher compressive strengths compared with CM. Specimens with EOGO

contents of 0.05% (GMD 0.05) and 0.1% (GMD 0.1) exhibited the greatest compressive strength among the other specimens. The compressive strength of GMD 0.05 and GMD 0.1 were 35.1 MPa and 34.3 MPa at 7 days, representing approximately 17% and 15% increases compared with CM. The compressive strength of GMD 0.05 and GMD 0.1 were 43.7 MPa and 42.5 MPa at 28 days, representing approximately 19% and 16% increases compared with CM. Figure 3-22 shows the flexural strength of EOGO-mortar with different EOGO contents. The flexural strengths of CM were 5.1 MPa at 7 days and 6.5 MPa at 28 days. The flexural strength of GMD 0.05 and GMD 0.1 were 6.5 MPa and 6.2 MPa at 7 days, representing 17% and 15% increases compared with CM while the flexural strengths of those specimens were 7.5 MPa and 7.4 MPa after 28 days of curing, representing 16 and 14% compared with CM. The results indicate a remarkable increase in the mechanical properties of EOGO-mortars when 0.05% and 0.1% of EOGO were incorporated using dry-mix design.

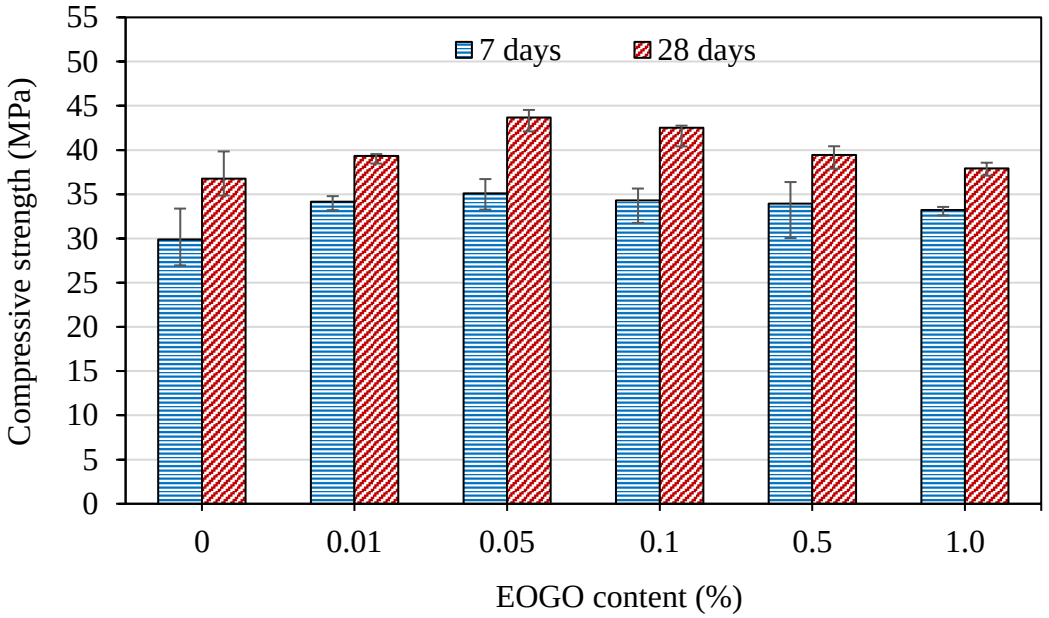

Figure 3-21. Compressive strength of EOGO-mortars with dry-mix design

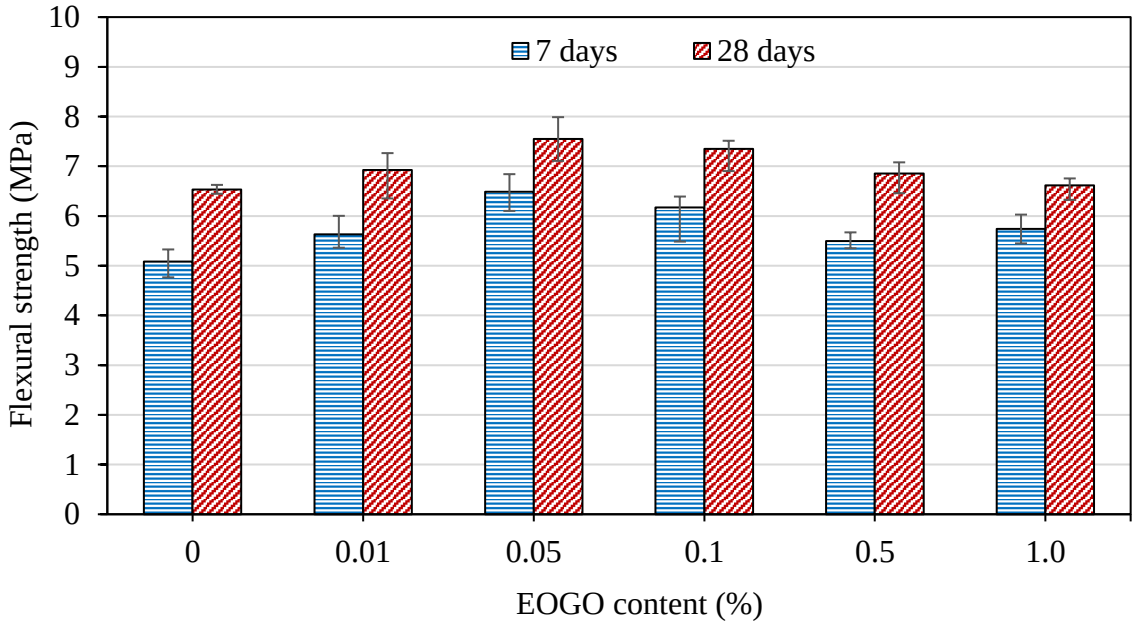

Figure 3-22. Flexural strength of EOGO-mortars with dry-mix design

To compare the effect of the mix design on the mechanical properties of mortars containing EOGO, strength tests were conducted on wet-mix mortars. Figures 3-23 and 3-24 show the compressive and flexural strengths of the EOGO-mortar specimens. Figure 3-23 illustrates that the compressive strength of all GMW samples are higher than the CM specimens at both curing times. It can be seen that GMW 0.05 and GMW 0.1 had the highest compressive strength compared with the other specimens, similar to dry-mix design. The compressive strength at 7 days of GMW 0.05 and GMW 0.1 were 35.6 MPa and 37.9 MPa, respectively, which increased 19% and 27% compared with CM. The compressive strength at 28 days of GMW 0.05 and GMW 0.1 were 44.1 MPa and 45.8 MPa, respectively, which increased 20% and 25% compared with CM. Figure 3-24 shows that the flexural strength of GMW 0.05 and GMW 0.1 were 6.7 MPa and 6.4 MPa, respectively at 7 days, which are 31% and 26% higher than that of CM. Flexural strength after 28

days curing of GMW 0.05 and GMW 0.1 were 7.6 MPa and 7.4 MPa, respectively, which are 17% and 14% higher that of CM.

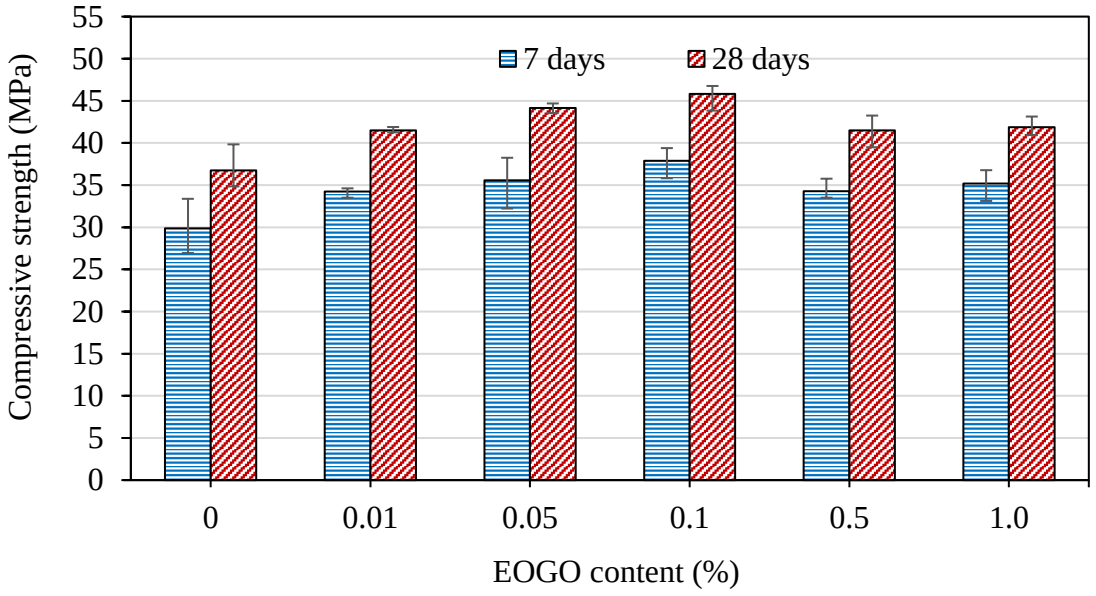

Figure 3-23. Compressive strength of EOGO-mortars with wet-mix design

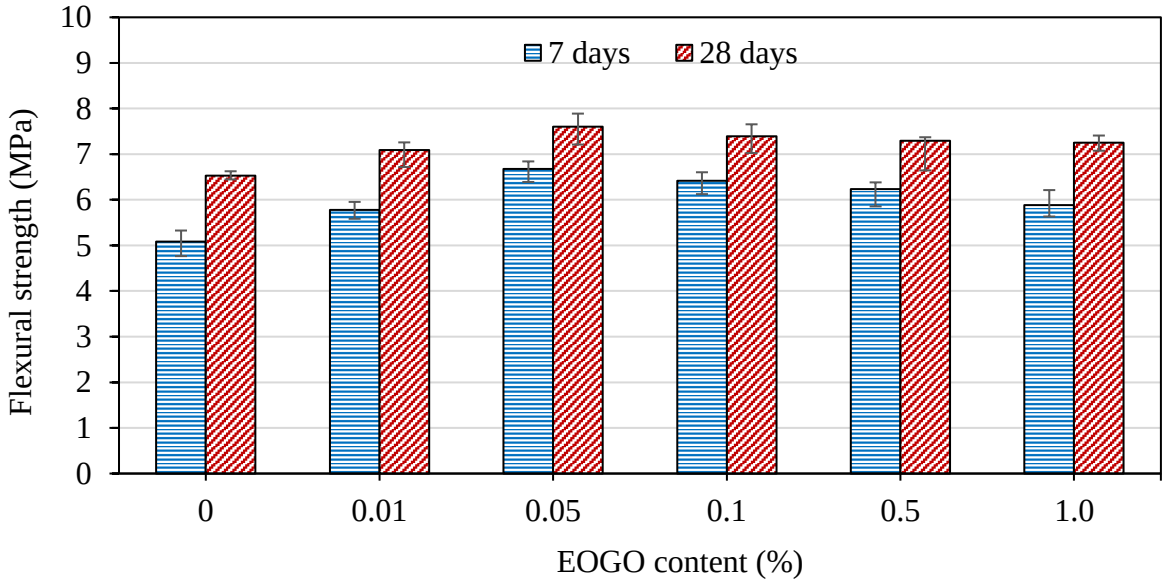

Figure 3-24. Flexural strength of EOGO-mortars with wet-mix design.

In comparison of dry and wet-mix designs, the wet-mix method is shown to exhibit slightly higher compressive and flexural strengths at 28 days over all percentages of EOGO for cement paste. For example, the compressive and flexural strength at 28 days of GPW 0.05 are around 5% and 7%, respectively higher than GPD 0.05. The strengths of GMW specimens were somewhat like those of GMD specimens when EOGO contents were 0.1% and lower. However, when EOGO content in mortars was 0.5% and higher, the compressive and flexural strengths of GMW specimens were higher than those of GMD. For instance, the compressive and flexural strength at 28 days of GMW 1.0 are 10.5% and 10.6% higher than those of GMD 1.0. This is due to that the large content of EOGO with wet-mix design (GMW 1.0) has a better exfoliation and dispersion compared to GMD 1.0 with dry-mix design. Consequently, GMW 1.0 has a better effect on the mechanical properties of EOGO-mortars than GMD 1.0.

3.5.2.2 Total Porosity

Porosity for both dry and wet-mix design methods were measured in order to observe the effect of different percentages of EOGO on the total porosity of cement mortar. Figure 3-25 shows the effect of the addition of different contents of EOGO on the porosity of mortar mixes cured at 7 and 28 days using dry-mix design. The results indicate that the total porosity of GMD specimens decreased compared to the control mortar (CM) specimen. It was observed that the porosity decreases when the EOGO content increases up to 0.1%, then it begins to increase when 0.5% and more of EOGO is added. The porosity at 28 days of GMD 0.05 and GMD 0.1 has the most reduction in strength among all GMD samples which they decreased by 6.6% and 7.1% compared

to CM. This result demonstrates that using dry-mix design can affect the total porosity of EOGO-cement mortars by adding moderate percentages of EOGO (0.05% and 0.1%).

Then the porosity cured at 7 and 28 days of GMW mixes that were prepared by using wet-mix design were measured. Figure 3-26 shows the effect of various of EOGO percentages on the porosity of cement mortars using wet-mix design method. The results show that all GMW samples have a lower result than the CM. The general trend is similar to that of dry-mix design. GMW 0.05 and GMW 0.1 have the most reduction in the porosity for both curing times. The porosity at 28 days of GMW 0.05 and GMW 0.1 decreased by approximately 7.9% and 8.2% compared to the CM.

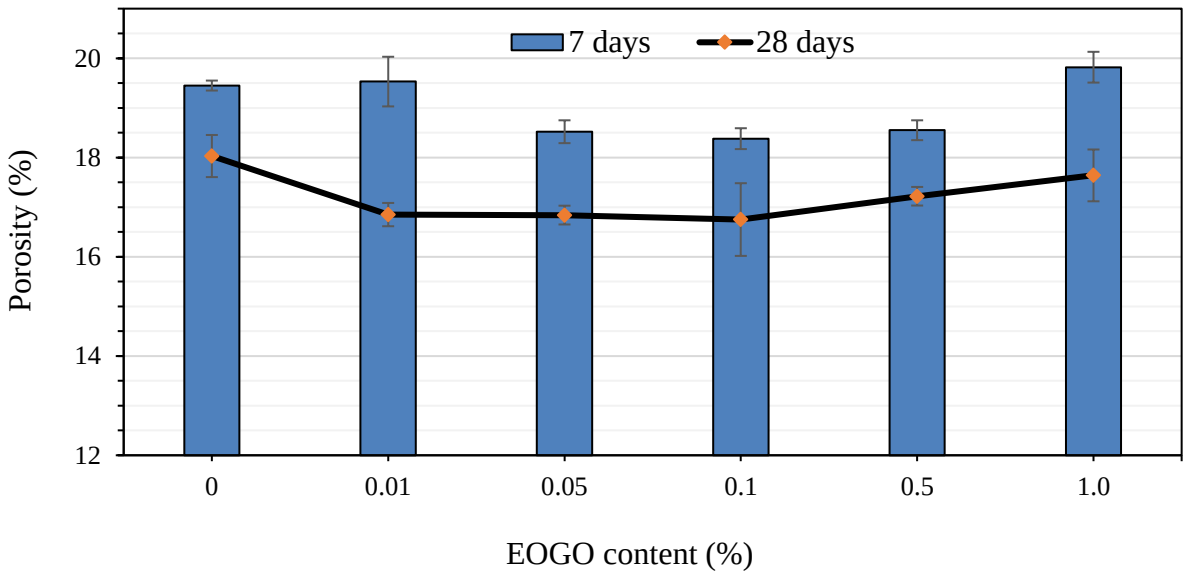

Figure 3-25. Effect of EOGO on the porosity of mortars with dry-mix design.

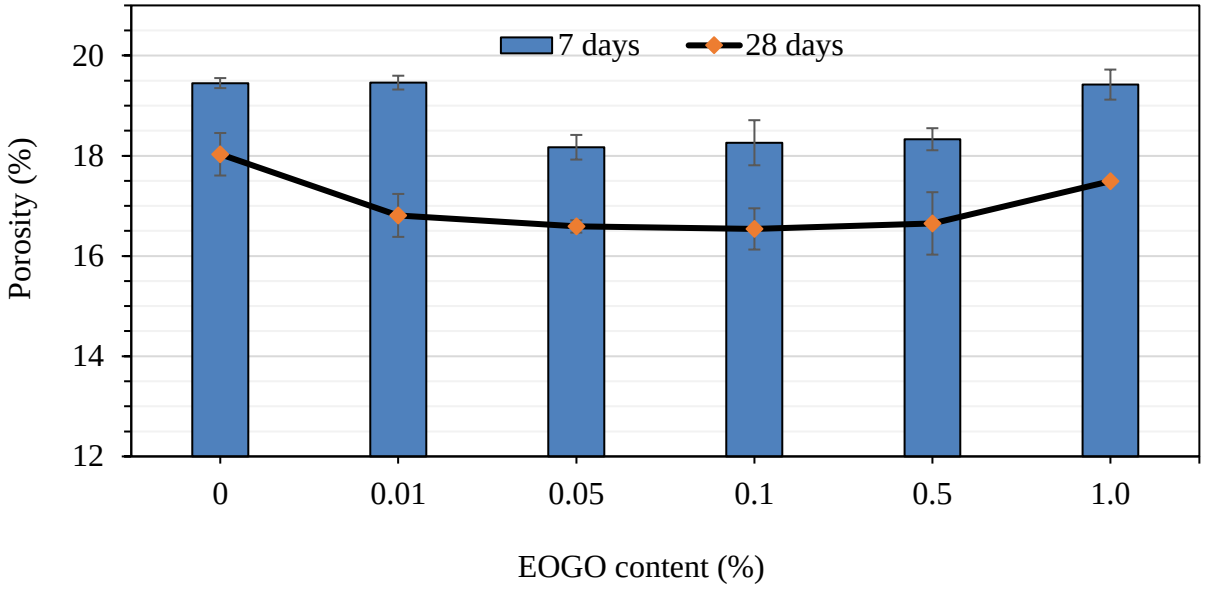

Figure 3-26. Effect of EOGO on the porosity of mortars with wet-mix design.

3.5.2.3 Water Sorptivity

Water sorptivity test with different concentration of EOGO was conducted for both dry and wet-mix design methods in order to investigate water absorption rate of cement mortar. Figures 3-27 and 3-28 show the cumulative absorption of different EOGO-mortar mixes using dry and wet-mix design. Figure 3-27 shows that the addition of EOGO to mortar using dry-mix design reduces the water absorption of EOGO-mortar specimens.

The results are summarized in Table 3-9. It is seen that the GMD 0.05 and GMD 0.1exhibit the lowest initial and secondary sorptivity. The same trend was found for dry-mix design of EOGO-cement paste specimens. The initial sorptivity of GMD 0.05 and GMD 0.1% reduced by 27.3% and 48%, respectively, while the secondary sorptivity of the same samples reduced by 40% and 27.3%, respectively, compared to the control sample (CM). This pattern is consistent with the porosity test at 28 days of mortars with dry-mix design method. The results indicate a less effective

of the addition of EOGO in cement mortar mixes using dry-mix design when the EOGO percentage is 0.5% or more.

The water sorptivity test also was performed on EOGO-mortar specimens using wet-mix design to compare the effect of the mixing method of EOGO in cement mortars on the water absorption of those specimens. Figure 3-28 illustrates the plot of water absorption against the square root of time of EOGO-mortar specimens that mixed by using wet-mix design method. It is apparent that the water absorption decreases with the addition of EOGO in cement mortars. GMW 0.05 and GMW 0.1 samples show a significant reduction in the initial and secondary sorptivity. The initial sorptivity of GMW 0.05 and GMW 0.1% reduced by 48.9% and 37.3%, respectively, while the secondary sorptivity of the same samples reduced by 55.6% and 40%, respectively compared to CM.

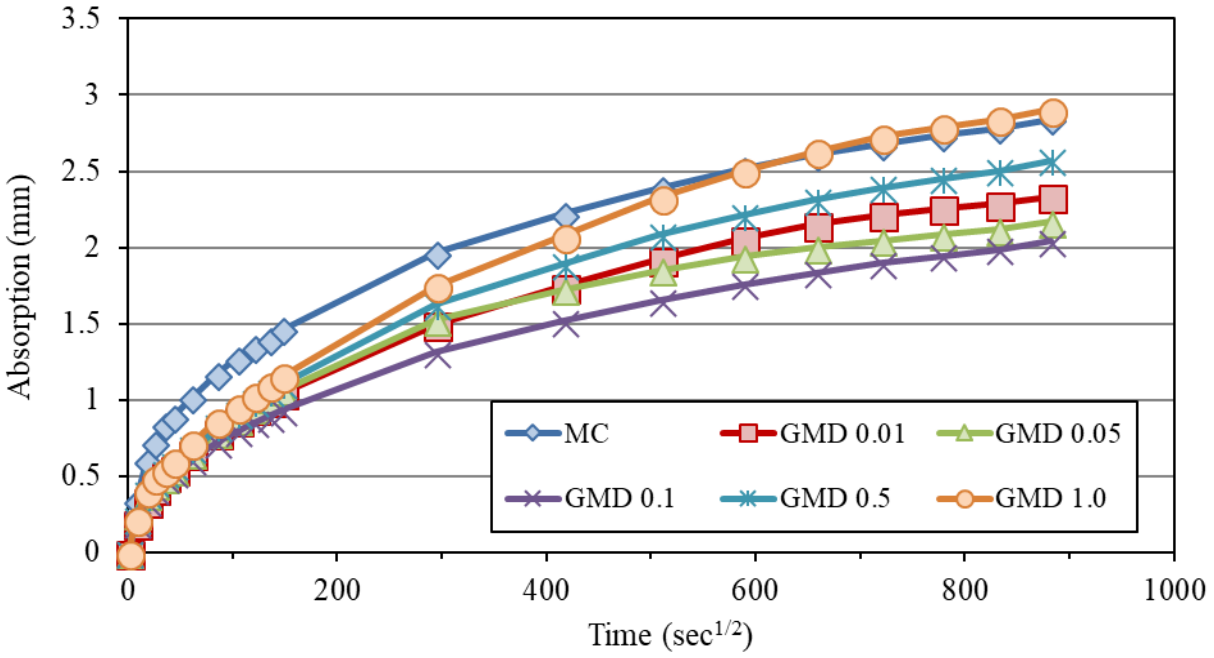

Figure 3-27. Water sorptivity of EOGO-mortars with dry-mix design.

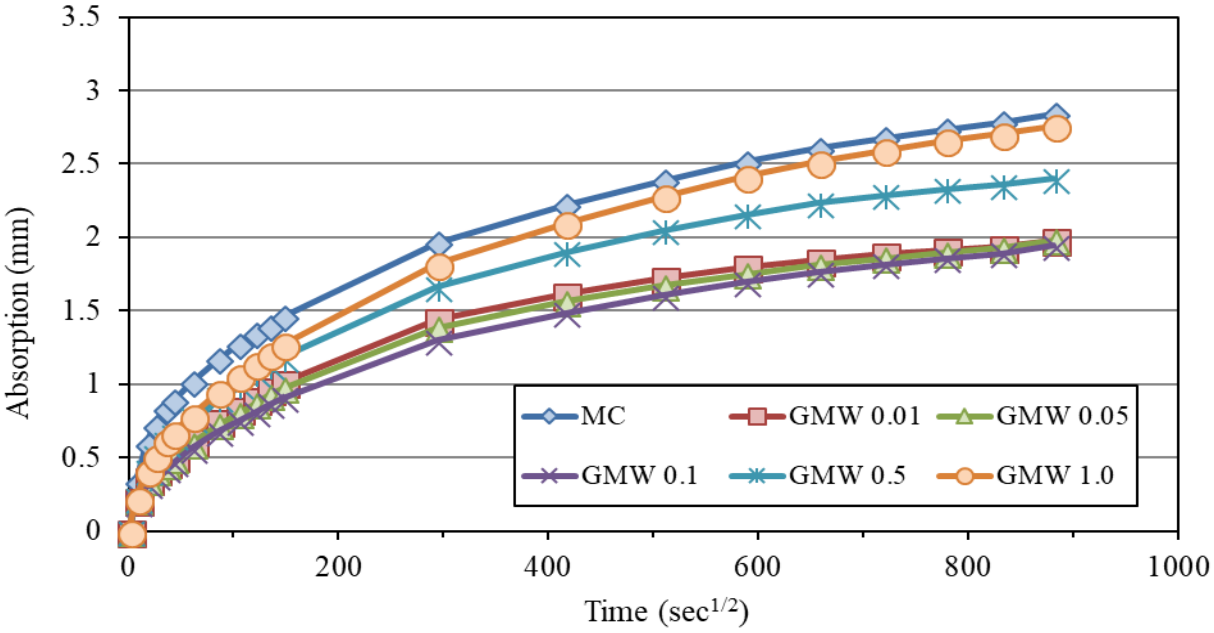

Figure 3-28. Water sorptivity of EOGO-mortars with wet-mix design.

Table 3-9. Initial and secondary sorptivity of mortars for dry and wet-mix designs*.

Samples	Initial sorptivity ($mm/s^{1/2}$)	% reduction compared to plain mortar	Secondary sorptivity ($mm/s^{1/2}$)	% difference with plain mortar
CM	0.007	-	0.0014	-
GMD0.01	0.0057	-22.8	0.0013	-7.7
GMD0.05	0.0055	-27.3	0.001	-40.0
GMD 0.1	0.0047	-48.9	0.0011	-27.3
GMD 0.5	0.0058	-20.7	0.0016	+12.5
GMD 1.0	0.0061	-14.8	0.0019	+26.3
GMW0.01	0.0054	-29.6	0.0011	-27.3
GMW0.05	0.0047	-48.9	0.0009	-55.6
GMW 0.1	0.0051	-37.3	0.001	-40.0
GMW 0.5	0.0062	-12.9	0.0012	-16.7
GMW 1.0	0.0069	-1.4	0.0016	+12.5

* (-ve means reduction, and +ve means increase compared to CM)

It is interesting to note that when EOGO contents were 0.5% and 1.0% (GMW 0.5 and GMW 1.0), there was insignificant effect on the water absorption rate compared to the other percentages of EOGO. This result was observed with both dry and wet-mix design methods for cement paste and with dry-mix design for mortar. In addition, the results of water sorptivity of GMW specimens were slightly lower than those of GMD specimens. For instance, the secondary sorptivity of GMW 0.05 and GMW 0.1 are 10% and 9% lower than GMD 0.05 and GMD 0.1 specimens. This indicates that wet-mix design has a slightly better influence on water sorptivity of EOGO-mortar mixes than dry-mix design.

3.5.3 Concrete Study

3.5.3.1 Compressive and Flexural Strength

To investigate the feasibility of the use of EOGO in the concrete industry with no regard for the sonication, dry EOGO powder was incorporated into concrete mix. The effect of EOGO on the strength of hardened concrete was investigated. The specimen identifications with GCD

indicate that EOGO-combined concrete specimens were made with Dry-mix design. Figure 3-29 and 3-30 show the results of compressive and flexural strength tests of GCD specimens. As expected, the results indicate that the compressive and flexural strengths of GCD specimens are higher than the control concrete (CC) specimens at 7 and 28 days. This result confirms that the addition of EOGO in cement composite can lead to the improvement in strength. Also as importantly, 0.05% EOGO addition results in 16% strength increment compared to the control CC specimen. From the strength test results of EOGO-combined paste and mortar, 0.05% EOGO addition was found as the optimum EOGO amount. And, this optimum EOGO amount was the reason for the range of EOGO content (0.01%–0.1%) for CC specimen. Similarly seen in EOGO-cement paste and mortar was that 0.05 wt.% of EOGO led to the highest flexural strength increment of GCD specimen. This phenomenon might be due to more cement hydration products and two-dimensional interlocking between hydration products. In addition, the ability of EOGO to reduce the nano and micro-cracks propagation can explain the strength improvement of EOGO-concrete.

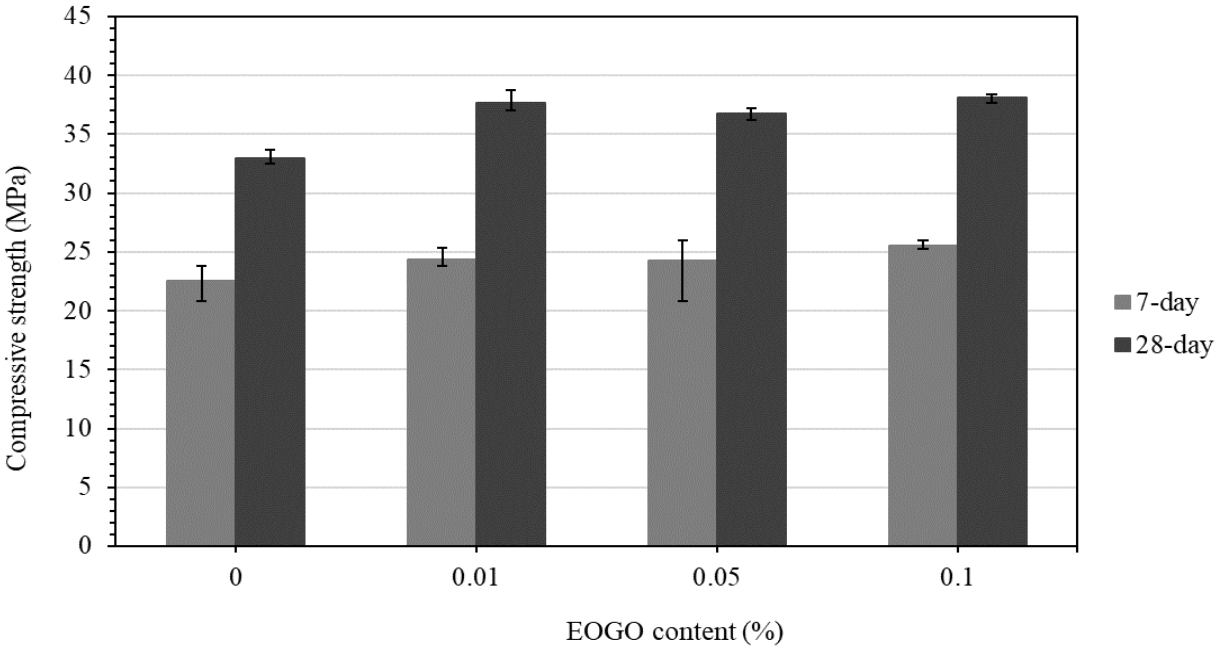

Figure 3-29. Compressive strength results of EOGO-concrete with dry-mix design.

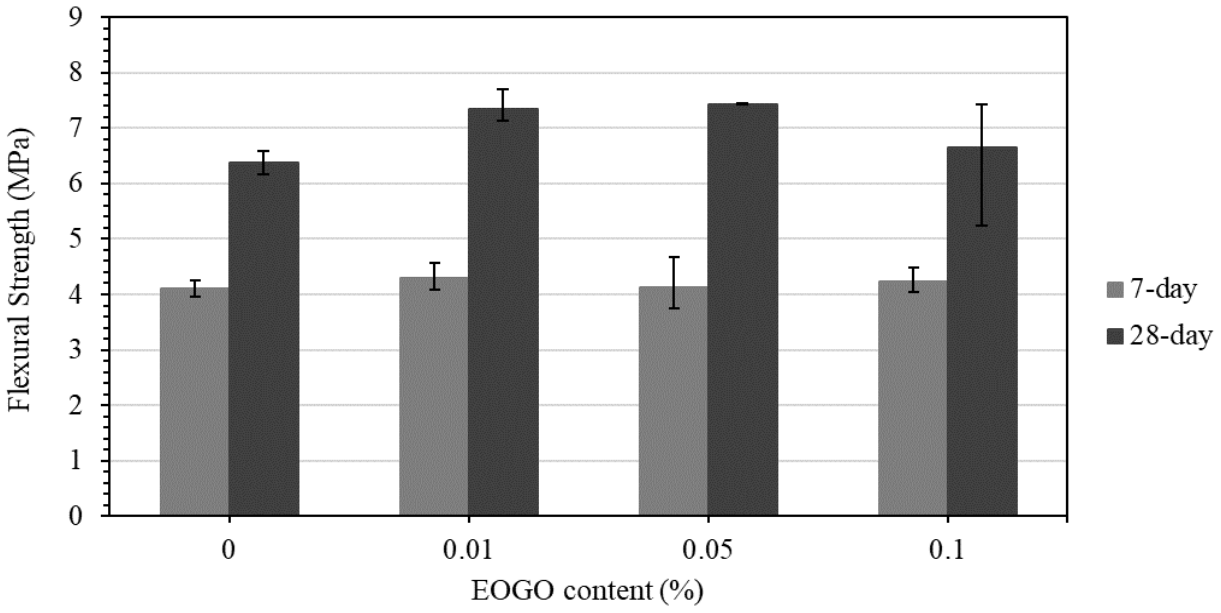

Figure 3-30. Flexural strength results of EOGO-concrete with dry-mix design.

3.6 Discussion

The results of the mechanical properties of EOGO-cement composites show significant improvements compared to cement composites without EOGO as presented in sections 3.5.1.1 and 3.5.2.1. This was the case for both dry and wet-mix design methods. These improvements can be attributed to the following rationale. First, EOGO as a two-dimensional nanomaterial can effectively hinder the propagation of nano-cracks. It is believed that the extremely small size of graphene oxide can resist crack initiation at very early stages, which are measured by nano-cracks and bridge cracks in the cement matrix [77,78]. Second, the EOGO functionality has an impact on the crystal seed growth of the calcium silica hydrate (C-S-H) gels [38,79–82]. Oxygen groups alongside the edges of the EOGO may react with dissolved ions of cement grains, and thus promote the cement hydration reaction to produce more cement hydration products such as C-S-H and calcium hydroxide ($Ca(OH)_2$) compared to the control mix. Third, EOGO as a nano-scale material can fill the nano- and micro-pores of the cement matrix. This phenomenon is called either nano- or micro-filler effect [39,78,83]. The mechanical properties of EOGO-cement composites exhibited the greatest improvements when EOGO content was 0.05%. Previous studies conclude that small amount of graphene oxide provide significant improvements in the mechanical properties of cement composites [30,38,84–87]. For both cement paste and mortar, it is noted that the trend of the compressive and flexural strength decreased after the optimum content of EOGO (0.05%). The main reason is that increasing EOGO content causes agglomeration of EOGO flakes. This agglomeration form large voids in cement matrix and stresses cannot be transferred across the bundles. If the EOGO bundles remain intact, they are not within the nanoscale range. As a result, they gather between hydration products and create zones of weakness instead of filling the

nanosized void in the cement matrix [44]. In addition, for both mix designs, the significant improvement in mechanical properties with incorporating 0.05% of EOGO can be referred to the significant reduction in capillary pores when the same percentages added to cement paste and mortar. Moreover, the mechanical properties of cement composites show good improvement when 0.1% of EOGO was incorporated to the mixes.

The test results have shown that effects of EOGO in terms of strength improvements on cement paste and mortar are less than the use of conventional GO nanosheet, which is produced by chemical process such as Hummer's method. Previous studies for effects of GO nanosheets on cement paste and mortar have reported significant improvement of compressive and flexural strength up to 40% and 60%, respectively [38,41–43,47,88]. Therefore, the difference of the strength increments is due to the different degree of hydration by different amounts of functional oxygen groups and different layer characteristics in between EOGO and GO. EOGO has relatively lower percentages of oxygen and more layers in comparison with GO [45].

The total porosity of cement composites containing EOGO for both dry and wet-mix design methods cured at 28 days are lower than those cured at 7 days. The increase of curing time provides more sufficient environment for cement hydration, reducing the total porosity of cement based materials [89,90]. A slight reduction in the total porosity of cement composites specimens was noticed after the incorporation of EOGO for both mix designs compared to the control samples as presented in sections 3.5.1.2 and 3.5.2.2. A similar result has been reported in cement composites incorporating graphene oxide [37,39]. The possible mechanism is that the EOGO as a nano-scale material can fill the nano and micro-pores of the cement matrix. Additionally, the addition of the 2D shape of graphene oxide accelerates the hydration of cement composites, refining the

microstructure by reducing the total porosity [35]. Interestingly, increasing the EOGO content to 0.5% or more has a lower effect in reducing the porosity of cement composites for both mix designs. This could be because of poor dispersion and workability that exacerbate large pores [39].

The results of the water sorptivity tests for both dry and wet-mix design show the significant effect of EOGO on the water sorptivity of cement composites as presented in sections 3.5.1.3 and 3.5.2.3. Water absorption rate is mostly influenced by the capillary pores. The capillary pore size can be classified as: large capillaries or macropores (50-10,000 nm), large mesopores (10-50 nm), and small mesopores (2.5-10 nm) [33,39]. According to Li et al. [39], the addition of graphene oxide has no significant effect on pores larger than 50 μm, but it significantly reduces the large capillary pores (50-10,000 nm) and can refine the pore structure. The significant reduction in large capillary pores was detected based on the results of the water sorptivity test. Also observed was the low rate of absorption of EOGO-composites. The results indicate that the addition of EOGO may reduce either a continuity of capillary pores or the total amount of pores in cement composite. It may also be both because the rate of absorption can be mostly improved by a refinement of capillary pore system. In addition, the strength increment of EOGO-composites might be explained by this absorption refinement of EOGO-composite. Either reductions of a continuity of capillary pores or reducing the total amount of pores in cement composite can improve the strength of cement composite. The results also show that further addition of EOGO beyond 0.1% did not further reduce the water absorption rate. This phenomenon indicate an introduction of larger pores due to the poor workability of cement composites with 0.5% and more of EOGO [39]. In addition, incorporating 0.5% or more of EOGO would cause agglomeration of EOGO due to the poor dispersion that can form large voids within cement composites, into porous

clusters. This led to more pathways for water to be sucked by the specimens. This improvement in sorptivity with the addition of 0.05% EOGO has a strong correlation with the strength improvement of EOGO-composite. It was found that the optimum EOGO content for the strength improvement is 0.05% of EOGO. Both sorptivity and strength of cement composite can be improved by a refinement of microstructures of cement composite. Through the refinement of microstructures, the capability of water to penetrate the microstructures of cement composite can be diminished. Thus, the sorptivity of cement composite can be reduced. Furthermore, with the refinement of microstructures, the continuity of capillary pores and the total amount of pores could be diminished. Consequently, possible locations of stress concentration can be reduced. The stress concentration typically happens at the continuous capillary pores or a pore itself. Based on the results of strength and sorptivity tests, the addition of 0.05% EOGO refines the microstructures of cement composite well.

In comparison of dry and wet-mix designs, the results show that wet-mix design has better effect on compressive and flexural strengths, total porosity, and water absorption rate of cement composites than dry-mix design. This is attributed to the better exfoliation and dispersion of EOGO in the cement matrix with wet-mix design. The well dispersion of EOGO in cement matrix may increase the filling and interlocking effect of EOGO, inducing a structure with fewer pores. Moreover, the well-dispersed EOGOs in water with wet-mix design have a larger surface area than dry powder of EOGOs in dry-mix design because of the lower agglomeration. The larger surface area of EOGOs absorbs more free water in the mixes and has more oxygen-containing functional groups, which equates to more nucleation sites. These groups can react as a binder between

graphene oxide nanoflakes and cement paste to obtain greater uniformity of the cement matrix [45,91,92], leading to lower capillary pores and higher strengths.

However, the compressive and flexural strengths gained by the dry-mix design method are sufficiently high as structural materials. In addition, using dry-mix design showed significant improvements in reducing capillary pores of cement composites. The use of edge of the oxygen-containing functional groups is able to make the van der Waals force between EOGO layers weaker. This results in good dispersion of the dry powder of EOGO in cement matrix [2,3]. Therefore, the study results support that the dry-mix design is economical, feasible, and practical for EOGO-cement composites and it can be implemented in concrete industry.

3.7 Summary and Conclusion

This chapter investigated the use of EOGO in cement composites includeing cement paste, mortar, and concrete. A series of laboratory tests were conducted to evaluate the mechanical performance, total porosity, and water sorptivity of EOGO-cement composites. To identify the optimum content of EOGO as well as feasible mix design, different variables were considered in the mix design including EOGO content, mix method while using extensive experimental tests. In addition, microstructural and crystallography analyses (SEM/EDS and XRD) were performed to investigate the mechanism of EOGO in strength, microstructures and crystalline phase change of cement composites. The following conclusions were made on the research findings:

- Mechanical properties of EOGO-cement composites have been improved compared to the control specimen. According to compressive and flexural strength tests, in most cases, the strength of EOGO-cement composites is higher than the control specimens.

- Based on the mechanical test results of EOGO-cement composites, the optimum content of EOGO to achieve the highest strength is 0.05% with respect to the weight of Portland cement in the cement mix.
- For both dry and wet-mix designs, the addition of EOGO has a minor effect on the total porosity of cement composites. For sorptivity test, most of EOGO-cement composites showed significantly improvement. This indicates a reduction of a continuity of capillary pores and the total amount of pores due to the promoted nucleation of hydration products and filling effect, leading to an improvement in the durability of the cement composites.
- The petrographic quantitative analysis of XRD data indicates that EOGO may act as Nano-seeding material in cement pore solution to promote CSH and other hydration products. Petrographic analyses (SEM/EDS) are in good agreement with XRD analysis. EOGOs are mostly found in the presence of CSH, confirming EOGO having a potential role as nano-seeding material in the cement composite.
- There is no significant difference between dry and wet-mix design in strength increase rate. For the mass production of EOGO-cement composite, dry-mix design is feasible and more practical for cement/concrete industry compared to wet-mix design. Unlike dry-mix design, wet-mix design requires applying ultra-sonication to EOGO-water solution prior to paste formation.

CHAPTER 4: RHEOLOGICAL AND WORKABILITY BEHAVIOR OF EOGO-CEMENT COMPOSITES[4]

4.1 Introduction

This chapter mainly investigates rheological behaviors and properties of EOGO-cement composites. In general, the addition of GO produced by common methods in cement composites decreases the workability and negatively affect the rheological properties due to the large surface area [30,31,39,46,54,55]. These studies reported that the loss fluidity of cement paste and mortar relates proportionally to the amount of GO mixed with cement paste and mortar. For example, Pan et al. [46] demonstrated that the incorporation of 0.05% of GO by cement weight reduced the cement paste fluidity by around 42% via a mini-slump test. Shang et al. [30] reported that adding 0.08% by cement weight of GO to cement composites decreased the fluidity by approximately 57% while the plastic viscosity increased by approximately 32% compared to the plain cement paste (due to the agglomeration and flocculation formations). The effect of EOGO as a new nanomaterial on the workability and rheological properties of cement composites was experimentally investigated. Moreover, two mix design methods, dry and wet-mix, were investigated and their performances were compared. Mini-slump test with image processing was conducted to measure the flowability of EOGO-cement paste using the two different mix designs and different amounts of EOGO ranging from 0.01% to 1.0%. The rheological parameters, apparent viscosity, and shear stress of EOGO-cement paste were also investigated through conducting viscometer tests. To investigate the effect of EOGO and its mixing methods on the

[4] The content of this chapter will appear as a peer-reviewed journal paper, authored by the author of dissertation.

workability of mortar, the flow table test was performed by using the same image processing procedure conducted with cement paste. For concrete, dry-mix design with different EOGO amounts ranging from 0.01% to 0.1% were used to investigate the effect of EOGO on the workability of concrete. The slump test as a common method was used for this purpose.

4.2 Materials

4.2.1 Edge-Oxidized Graphene Oxide (EOGO)

Edge-oxidized graphene oxide (EOGO) as described in section 3.2.1 is used in this study as an additive nanomaterial in two conditions, which are dry powder and solution.

4.2.2 Ordinary Portland Cement

Ordinary Portland cement type I according to ASTM C150 [65] is used in casting of cement composites. The chemical compositions of the cement are presented in section 3.2.2.

4.2.3 Aggregates

Fine and coarse aggregates used for investigating the effect of EOGO on the rheological and workability behavior of cement composites are presented in section 3.2.3.

4.3 Experimental Procedure

4.3.1 Mini-Slump Test

A mini-slump test was conducted to evaluate the effect of EOGO on the fluidity of cement pastes. In this study, image processing was employed to accurately measure the flow (or spreading) area of cement paste. Immediately after mixing, the mixtures were poured into a mini-slump cone with 100 mm bottom diameter, 70 mm top diameter, and 50 mm height. Figure 4-1 shows a schematic diagram of the test setup to measure the final spreading area of the cement pastes. A flow table that meets ASTM C230/C230M-14 specifications [93] was mounted on a black poster board. A high-resolution digital camera was installed on the top part records images of the spreading areas of mixtures, and image processing was then applied to determine the spreading areas of the mixtures. This 2-D image processing technique quantifies the spreading areas based on the pixel count.

The color image of the paste on a gold background was converted to a 256-level gray scale image, with black corresponding to 0 and white corresponding to 255. The image was then converted to a binary image using the threshold option. All pixels with a gray level of 128 and higher were converted to white and those with a value of 127 and lower were converted to black [94]. The binary image was inverted and saved as a bitmap file. The bitmap file was processed using MATLAB where the MATLAB code counts the area of pixels based on the difference between the color of the table (1 = white) and the specimen (0 = black). In order to validate the employed method, the surface area of a known area, which is a black rubber circle (Area = 193.6 cm^2), was measured by image processing (Area = 196.26 cm^2), and then was compared with the calculated surface area. The result showed that the difference was around 1.37%.

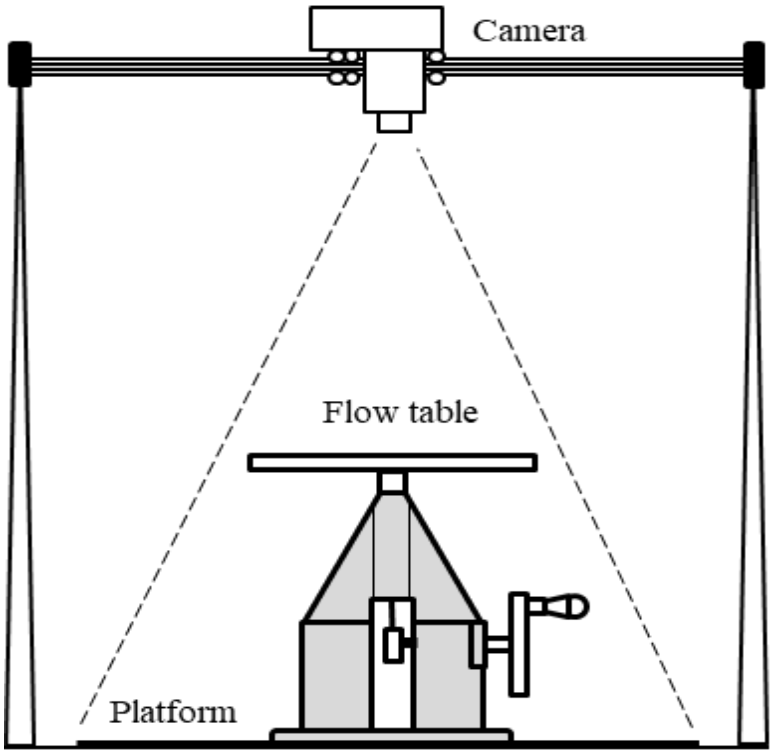

Figure 4-1. Schematic of flow table/mini-slump test setup

4.3.2 Viscometer Test

The rheological parameters of the cement pastes were measured using BROOKFIELD DV-II+Pro Viscometer as shown in Figure 4-2. A 600-ml low form Griffin beaker and spindle SC4-27 were used. After mixing, the cement paste specimens were poured into the 600-ml beaker to perform the rheological measurements. The speed was raised from 20 to 150 rpm with seven speed intervals. The rheological parameters, apparent viscosity, and shear stress were measured during the test. Plastic viscosity (η_P) and the yield stress (τ_0) can be found from the slope and intercept of the linear Bingham model between the shear stress and shear rate [30]. The mathematical form of the Bingham equation model is:

$$\tau = \tau_0 + \eta_p \gamma \quad (3)$$

Where τ is the shear stress (Pa), τ_0 is the yield stress (Pa), η_p is the plastic viscosity (Pa.s), and γ is the shear rate (Sec^{-1}).

Figure 4-2. Viscometer device used to measure the viscosity of cement pastes

4.3.3 Flow Table Test

The flow table test was employed to evaluate the influence of EOGO on the workability of mortar. ASTM C1437-15 [95] was adopted for the test procedures. The mortar mixtures were poured into a cone with 100 mm bottom diameter, 70 mm top diameter, and 50 mm height. The cone was set on the flow table that meets ASTM requirements [93] . The same apparatus that used for the mini-slump test was used to carry out this test. The same image processing technique where

the coded MATLAB program counts the pixels was also applied to calculate the spreading area with each blow (25 blows according to [95]).

4.4 Results and Discussion

4.4.1 Effect of EOGO on the Fresh Cement Paste

4.4.1.1 Fluidity

Figures 4-3 and 4-4 show the image processing results of the flow of cement paste specimen prepared by the dry and wet mix design methods, respectively. It is observed that the flow areas are decreased when the EOGO content increases for both mix design methods. In addition, the reduction in the fluidity is significant when 0.5% and 1.0% of EOGO are added for both mix designs. Figure 4-5 shows the relationship between the flow (or spreading) area and the EOGO content in the mixes for both dry and wet mix design methods. The flow areas reduce with increasing the EOGO content. This result indicates that the addition of EOGO reduces the fluidity of cement paste, which is consistent with past research in literature [30,31,39,46,54,55].

The flow area of the control sample was around 350 cm^2. The flow areas of GPD 0.01, GPD 0.05, and GPD 0.1 reduced to 339.89 cm^2, 318.64 cm^2, 311.64 cm^2, respectively. Similarly, the flow areas of GPW 0.01, GPW 0.05, and GPW 0.1 decreased to 338.74 cm^2, 312.77 cm^2, and 302.58 cm^2, respectively. Adding 0.5% and 1.0% of EOGO to the cement matrix in dry and wet-mix cases exhibited the highest reduction in fluidity of samples. The flow area of GPD 0.5 and GPD 1.0 reduced to approximately 256 cm^2 and 230 cm^2, respectively, and the flow area of GPW 0.5 and GPW 1.0 reduced to around 244 cm^2 and 217 cm^2 respectively. Figure 4-5 shows when the EOGO content was 0.1% and lower, the influence of EOGO addition was not significant;

however, EOGO addition higher than 0.5% showed significant reduction in the cement paste fluidity. This observation is shown in both dry and wet-mix designs. Table 4-1 presents the reduction percentages of GPD and GPW samples with all EOGO contents. It is clear that adding 0.5% and 1.0% of EOGO to cement matrix can noticeably reduce the fluidity. The reduction percentages of the flow areas of GPD 0.5 and GPD 1.0 were approximately 43% and 51%, respectively, compared to the control sample. The flow areas of GPW 0.5, and GPW 1.0 decreased by around 45%, and 60%, respectively, compared to the control sample.

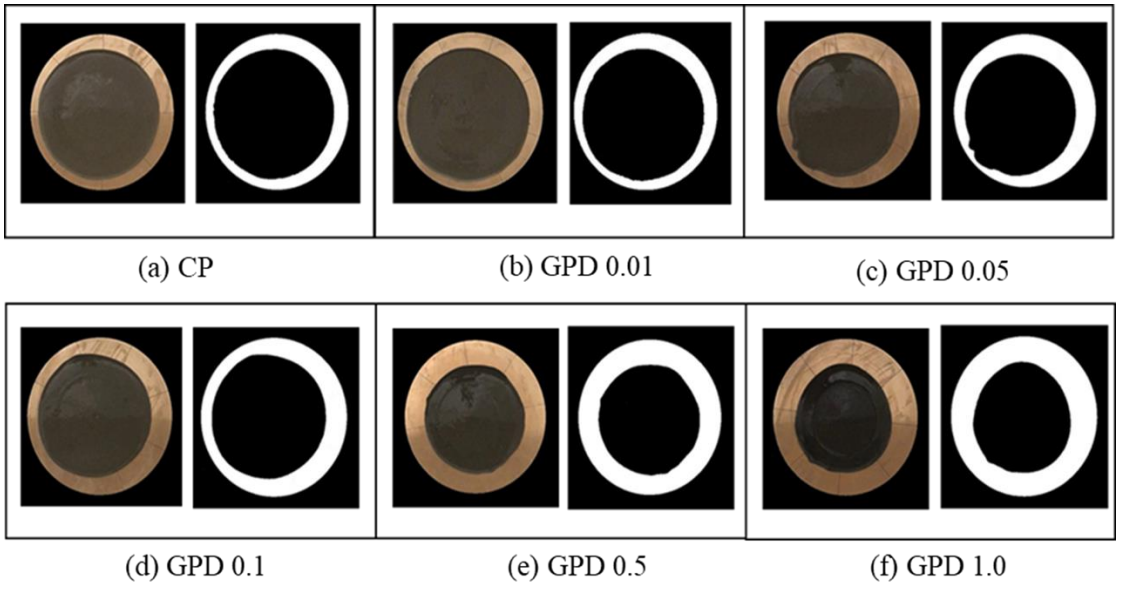

Figure 4-3. Original and processed images for cement pastes (Dry-mix design)

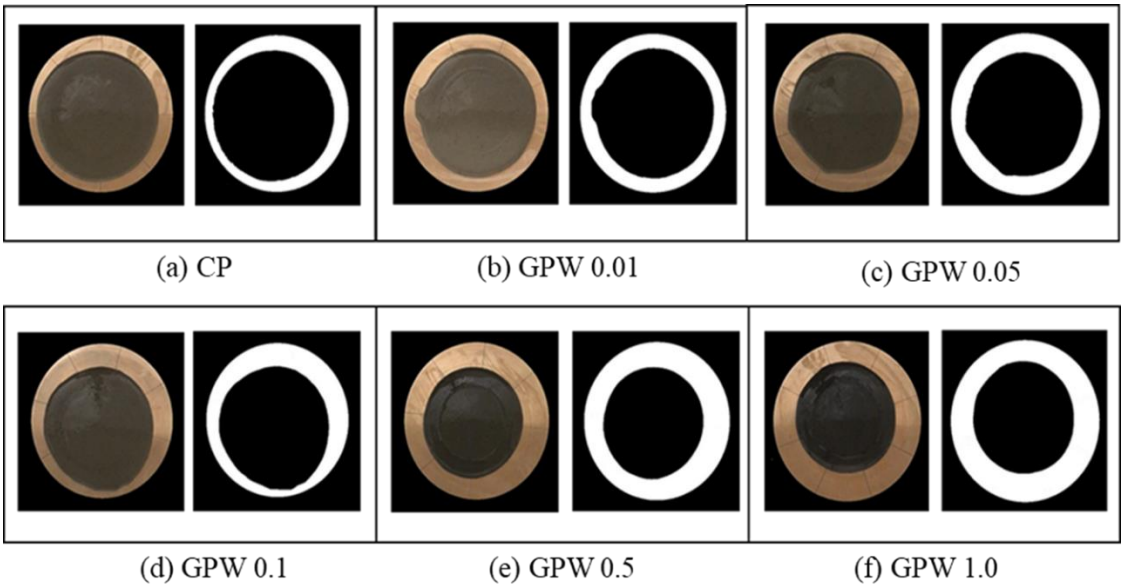

Figure 4-4. Original and processed images for cement pastes (Wet-mix design)

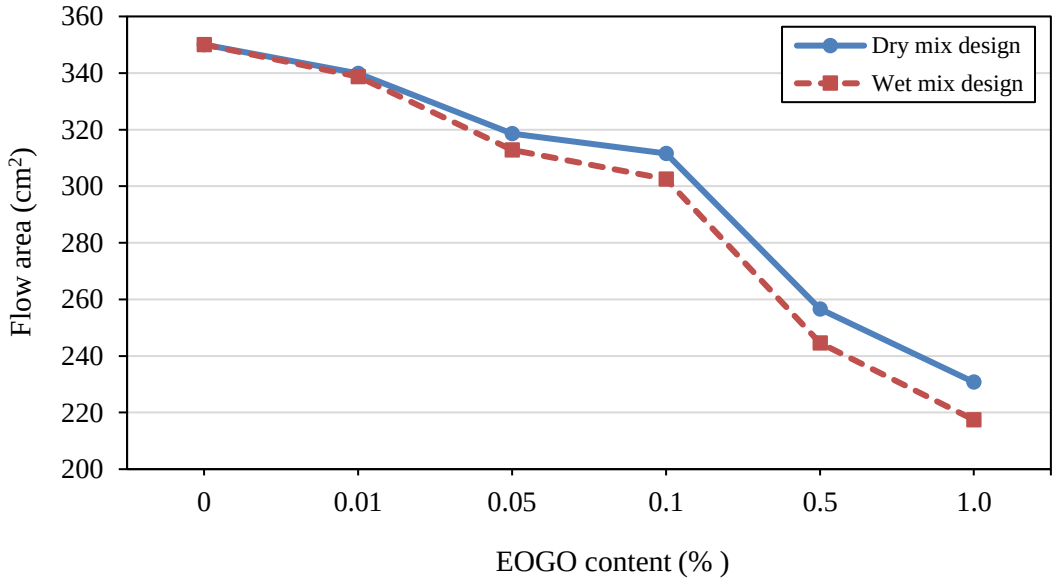

Figure 4-5. Comparison between the effect of the mixing method of EOGO on the fluidity of cement pastes

Table 4-1. Results of the mini-slump test of cement pastes.

Specimen ID	Flow area (cm^2)	Reduction percentage (%)
CP	350.06	0
GPD 0.01	339.89	3.34
GPD 0.05	318.64	9.86
GPD 0.1	311.62	12.34
GPD 0.5	256.64	43.12
GPD 1.0	230.75	51.71
GPW 0.01	338.74	4.35
GPW0.05	312.77	11.92
GPW 0.1	302.58	15.69
GPW 0.5	244.59	45.82
GPW 1.0	217.43	61.0

Table 4-1 shows a difference between the flow areas of GPD and GPW. GPW samples exhibit more reduction in the cement pastes fluidity than GPD. The possible reason is that the surface area of EOGOs increases after they are sonicated as a part of the wet-mix design compared to that in dry-mix design. This increase in surface area increases water absorption. Hence, the free water in cement paste decreases, decreasing the particle space and leading to an immediate increase in the friction between particles. However, the difference between GPD and GPW fluidities was not statistically significant. For instance, the difference of the flow area of GPD 0.05 and GPW 0.05 is 2%. The highest difference observed of 6% was between GPD 1.0 and GPW 1.0. This indicates that using dry-mix design is also effective although EOGO is well dispersed with wet-mix design.

4.4.1.2 The Rheological Properties

Figures 4-6 and 4-7 illustrate the curves of shear rate with apparent viscosity under different EOGO contents for dry and wet-mix designs. Figure 4-6 shows that the apparent viscosity

decreases dramatically with the increase in shear rate. Eventually it is stabilized with dry-mix designs. Meanwhile, at the same shear rate, the apparent viscosity increased with the increase of EOGO content in the mix. When the EOGO content was 0.01% (GPD 0.01), the apparent viscosity of the cement paste was close to the control specimen (CP), where the maximum increase percentage compared to the control sample is 2.7%. The highest percentage increase of the apparent viscosity of GPD 0.05, GPD 0.1, GPD 0.5, and GPD 1.0 are approximately 9.3%, 14.5%, 30.7%, and 51%, respectively when compared to the control sample. Figure 4-7 shows the same trend as Figure 4-6, where the apparent viscosity-shear rate curves shift upward with the increase of EOGO content with the wet-mix design. For any given content of EOGO, at high and low shear rate, the increase in EOGO content increases the apparent viscosity. The highest percentage increase from the control sample of the apparent viscosity of GPW 0.01, GPW 0.05, GPW 0.1, GPW 0.5, and GPW 1.0 are 7%, 13.3%, 21.5%, 35.4%, and 59.2%, respectively. The results indicate that the plastic viscosity of cement pastes with wet-mix design is higher than that with dry-mix design.

Figures 4-8 and 4-9 show the variation of shear stress with shear rate for dry and wet-mix designs with various EOGO contents. At the same shear rate, the shear stress increases as EOGO content increases for both mixing methods. As can be seen in Figures 4-8 and 4-9, the variation of shear stress with shear rate for both mix designs exhibit similar ascending trends. This indicates that the two mixing methods for incorporating EOGO in fresh cement pastes evaluated in this study have a remarkable effect on the shear stress under different shear rates. Furthermore, the shear stress in cement paste with dry-mix design is less than that in cement paste with wet-mix

design at the same shear rate. This indicates that dry-mix design may cause the shear stress in the cement paste to decrease.

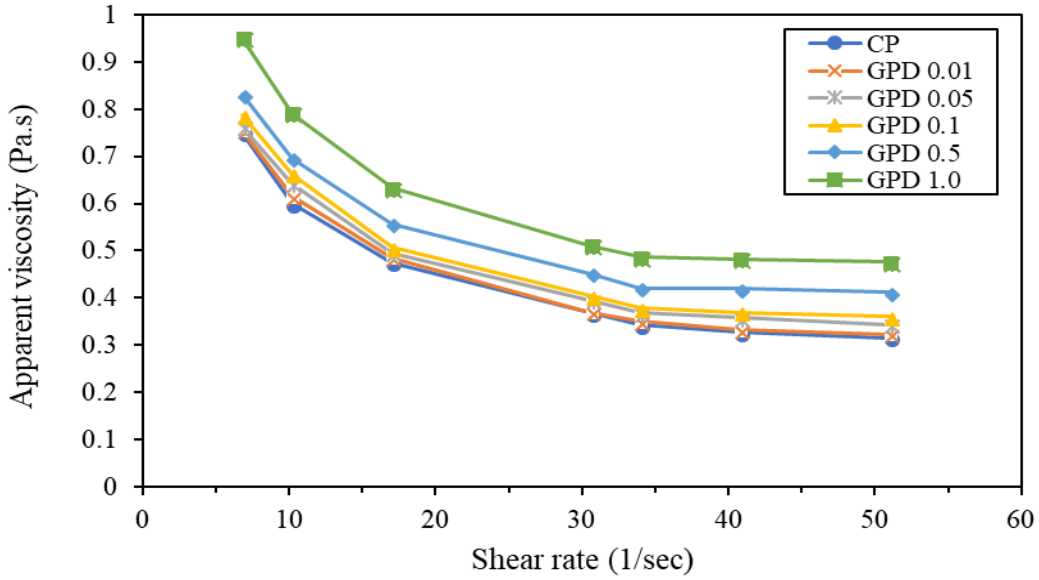

Figure 4-6. Effect of EOGO contents on the apparent viscosity of cement paste (Dry-mix design).

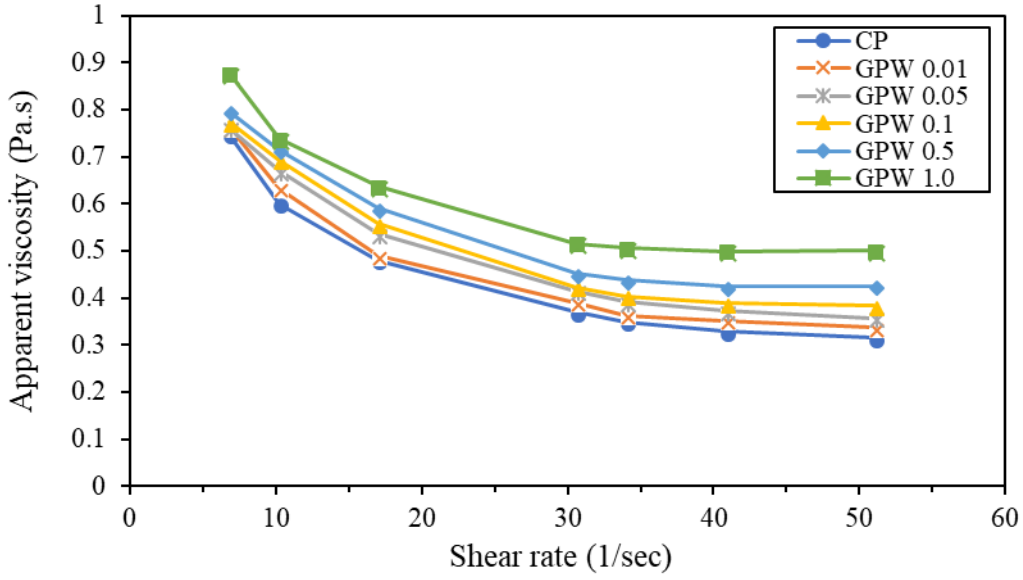

Figure 4-7. Effect of EOGO contents on the apparent viscosity of cement paste (Wet-mix design)

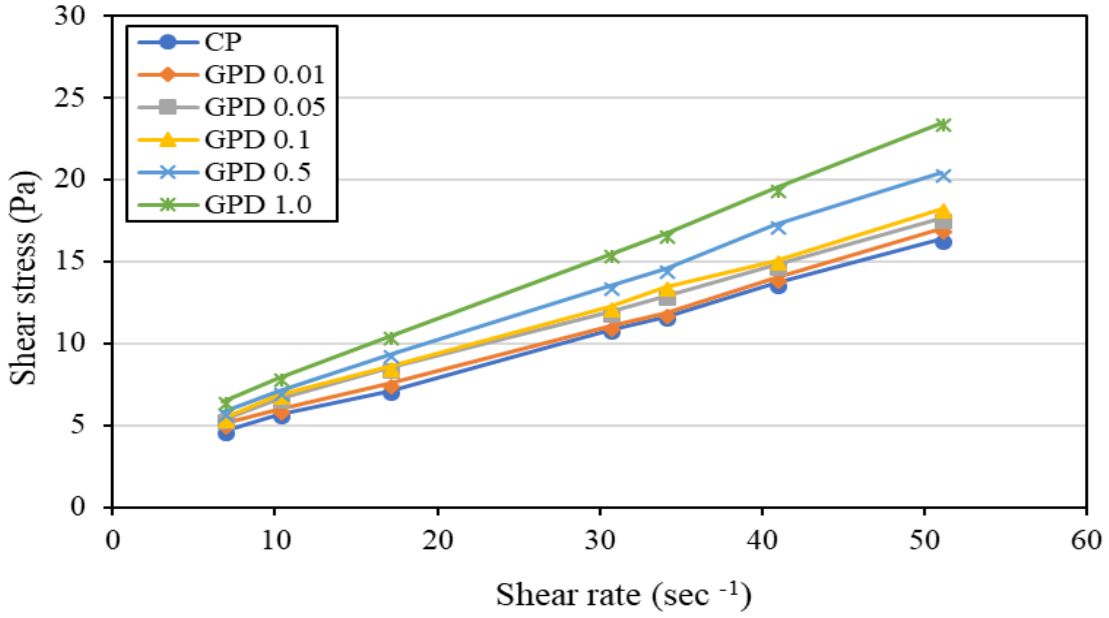

Figure 4-8. Effect of EOGO content on the shear stress of cement paste (Dry-mix design)

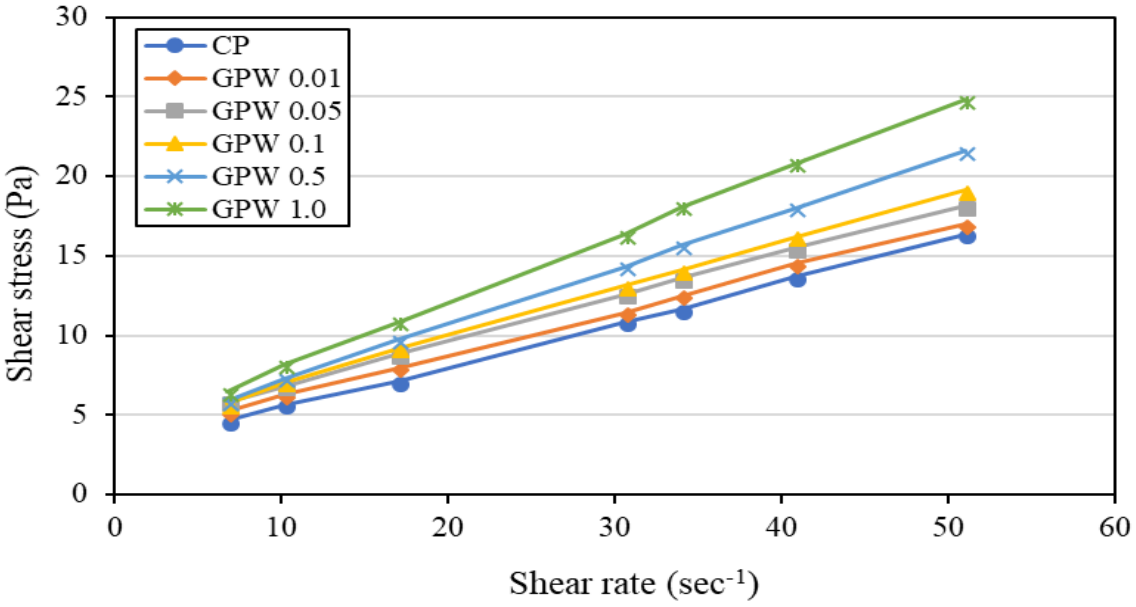

Figure 4-9. Effect of EOGO content on the shear stress of cement paste (Wet-mix design)

The plastic viscosity values of cement pastes are calculated based on the Bingham's model. Figure 4-10 shows a comparison between dry and wet-mix designs based on the effect of EOGO content on the plastic viscosity of cement pastes. The results show that the plastic viscosity increases with higher addition of EOGO for both mix designs. When 1.0% of EOGO is added to the cement paste with dry-mix design, the plastic viscosity of the control cement paste increased from 0.2643 to 0.3809 in Pa·s, which is around 44% higher than that of the control sample. For wet-mix design method with the same 1.0% of EOGO, the plastic viscosity of the control cement paste increased from 0.2643 Pa·s to 0.4143 Pa·s, which is about 57% higher. The results show that wet-mix design has a greater effect on the plastic viscosity than dry-mix design of the cement paste. In addition, the results show that the difference between the plastic viscosity of cement pastes with wet-mix design and dry-mix design increases when the addition of EOGO increases. For example, the plastic viscosity of GPW 0.05 and GPW 1.0 are higher than GPD 0.05 and GPD 1.0 by approximately 2.7% and 8.7%, respectively. The possible reason is that the surface area of EOGO decreases when it used as a dry addition in cement matrix (GPD). The decreased surface area accordingly reduces the absorption of water. This increases the free water in the matrix, contributing more spacing between cement particles and reducing the friction between these particles. As a result, the fluidity is increased, and the viscosity is decreased compared to GPW. In addition, the degree of flocculation is small in GPD, and the force of connection between structures is weak. In contrast, the EOGO in GPW promotes flocculated structures, leading to more formation of structure in the cement paste matrix. It also increases the viscosity that requires high shear stress to break up the cement paste [31]. The large amount of free water entrapped by the flocculated

structures causes the lack of the free water that increases the friction resistance of the cement paste and EOGO particles [30].

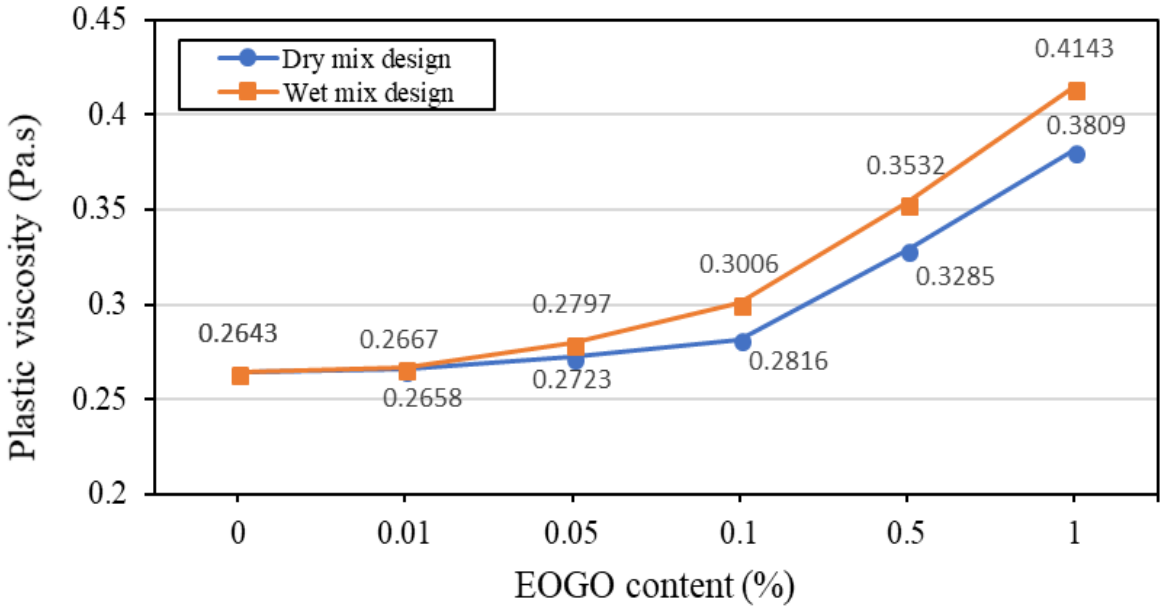

Figure 4-10. Effect of EOGO content on the plastic viscosity of cement paste with dry and wet-mix design methods

In the actual concrete engineering, the rheological properties of cement paste are not widely used, mostly because the correlation between the fluidity and rheological parameters is not fully understood [96]. In this study, the relationship between plastic viscosity and fluidity of cement paste was estimated by mathematical fitting as presented in Figures 4-11 and 4-12. Figure 4-11 shows the relation between the plastic viscosity and fluidity of cement paste with dry mix design. The correlation coefficient of the linear fitted equation is 0.936. Figure 4-12 shows the relation between the plastic viscosity and fluidity of cement paste with wet mix design. The correlation

coefficient of the linear fitted equation is 0.953. This indicates an improved correlation between the plastic viscosity and the fluidity for both mix design. As a result, the plastic viscosity measurements can be used to predict the actual workability [31]. The mini-slump test results were confirmed by the viscosity test results. The both tests showed the same trend and the results were consistent. For both tests, the GPW samples showed lower fluidity and higher apparent viscosity compared to GPD samples. The difference of the plastic viscosity and the fluidity between GPD and GPW samples was around 10%. It can be concluded that even though well dispersion of EOGO in GPW specimens is superior to the dry powder of EOGO in GPD specimens, using EOGO in dry condition affect fluidity and the viscosity of the cement paste.

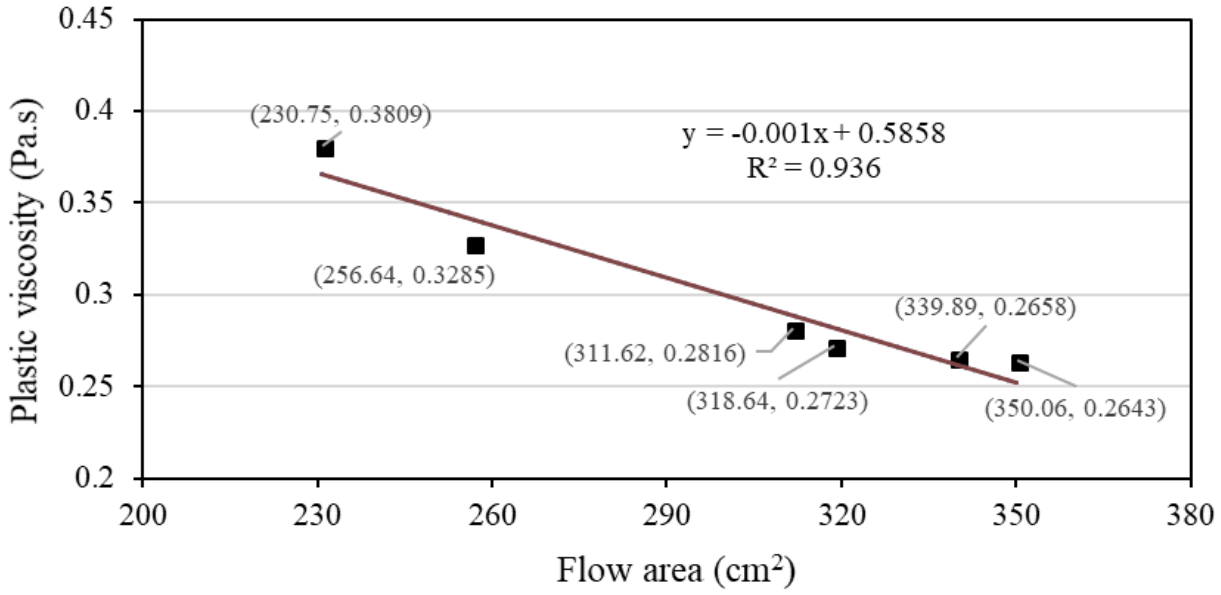

Figure 4-11. Correlation between the plastic viscosity and the fluidity of cement paste (Dry-mix design)

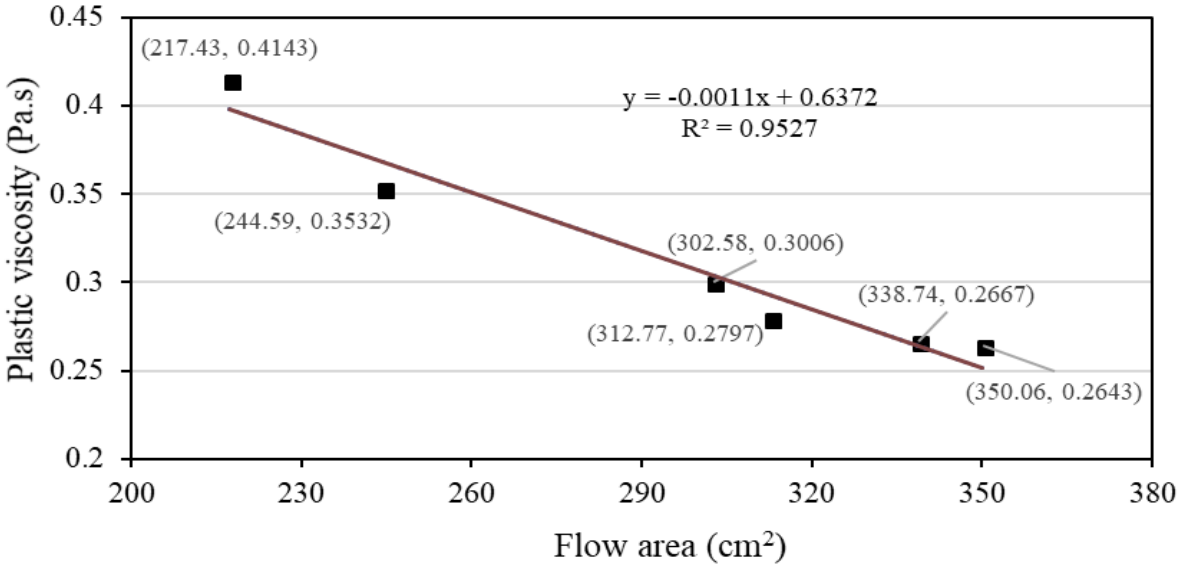

Figure 4-12. Correlation between the plastic viscosity and the fluidity of cement paste (Wet-mix design)

4.4.2 Effect of EOGO on the Fresh Cement Mortar

Figures 4-13 and 4-14 show the original and the image processing of the final spreading areas of each EOGO content in mortars with dry and wet-mix design. Figures 4-13 and 4-14 show that the spread mortar of the control sample is contracted with the increase of EOGO content of dry mix design. This can be clearly seen in the spread of the control sample in comparison with GMD 0.5 and GMD 1.0.

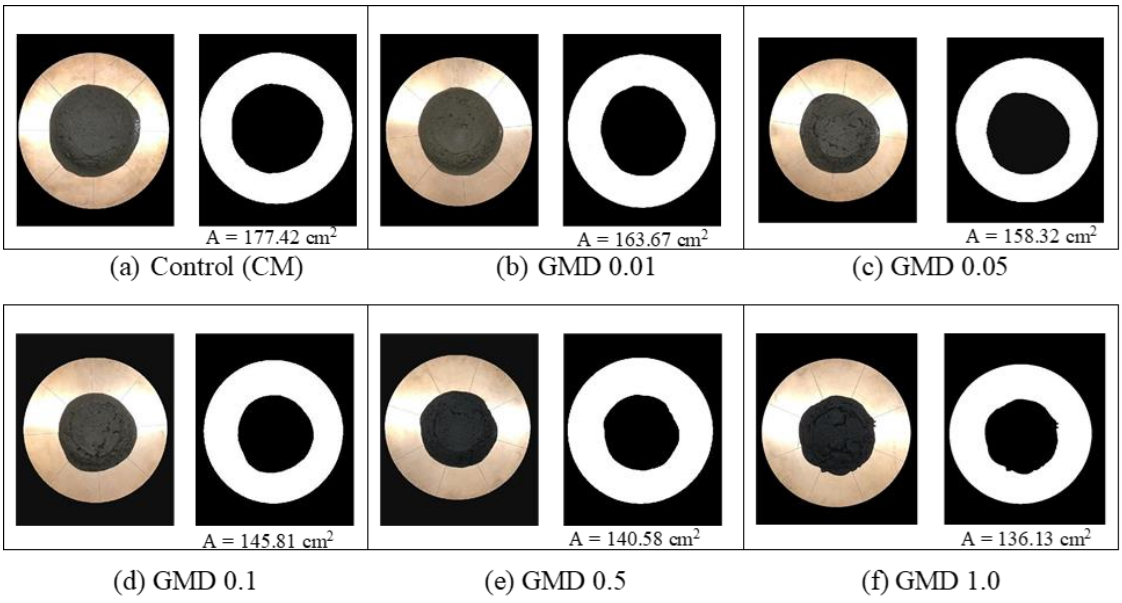

Figure 4-13. Original and processed images for mortars with dry-mix design

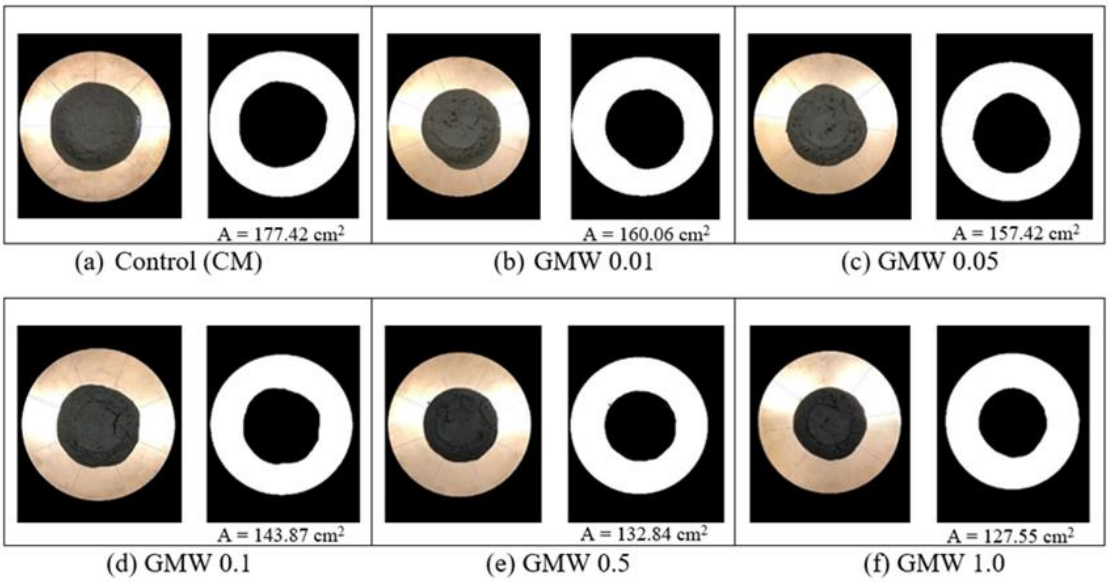

Figure 4-14. Original and processed images for mortars with wet-mix design

Figure 4-15 shows the spreading areas of 25 blows of the dry-mix design of mortars CM, GMD 0.01, GMD 0.05, GMD 0.1, GMD 0.5, and GMD 1.0. The spreading area increases as the number of blows increases. Conversely, spreading area decreases as the EOGO content increases.

Figure 4-16 shows the spreading areas of mortars with the number of blows of wet-mix design GMW 0.01, GMW 0.05, GMW 0.1, GMW 0.5, GMW 1.0, and the control sample CM. Similar to dry-mix, the spreading area increases with the increase of the number of blows. The relation between the spreading area and the number of blows shifts down with the increase of the EOGO content.

Figure 4-17 and Table 4-2 show the final spreading area of mortars after 25 blows with different EOGO contents for both dry and wet-mix designs. The final spreading area of the control mortar decreased as the addition of the EOGO increased. This result indicates that incorporation of EOGO reduces the workability of mortars. It can be seen that the reduction in the workability

of mortars was significant when EOGO content was 0.1% and higher for both mix designs. The spreading area of the control mortar is 177.42 cm^2. This value is reduced to 145.81 cm^2, 140.58 cm^2, and 136.13 cm^2 for GMD 0.1, GMD 0.5, and GMD 1.0, respectively, which are 21.67%, 26.2%, and 30.33% less than the spreading area of the control sample. For wet- mix design, the spreading area of the control mortar is reduced to 143.87 cm^2, 132.84 cm^2, and 127.55 cm^2 for GMW 0.1, GMW 0.5, and GMW 1.0, respectively, which are 23.32%, 33.56%, and 39.10% less than the spreading area of the control sample. The large surface area and agglomeration effects, which are both caused by the reduction of the cement paste fluidity, can explain the reduction of the mortar workability with the addition of EOGO.

It can be observed from Figure 4-17 that the spreading areas of wet-mix design samples is lower than those of dry-mix design. The well-dispersion of EOGO in water may increase the surface area of EOGO when compared to using EOGO as a dry powder, absorbing more free water in the mix and leading to more reduction in the workability. The difference between the spreading areas of dry-mix design and wet-mix design were less than 5% when EOGO content were 0.01%, 0.05% and 0.1%. When EOGO content were increased to 0.5% and 1.0%, this difference in spreading area also increased to be around 7% and 10%, respectively. The same trend was found for the effect of EOGO and mixing methods on the fluidity of the cement paste. This finding indicates that using EOGO is effective since it plays the same role as GO in the reduction of the workability of cement composites. Furthermore, using EOGO with a dry-mix design is a competitive option.

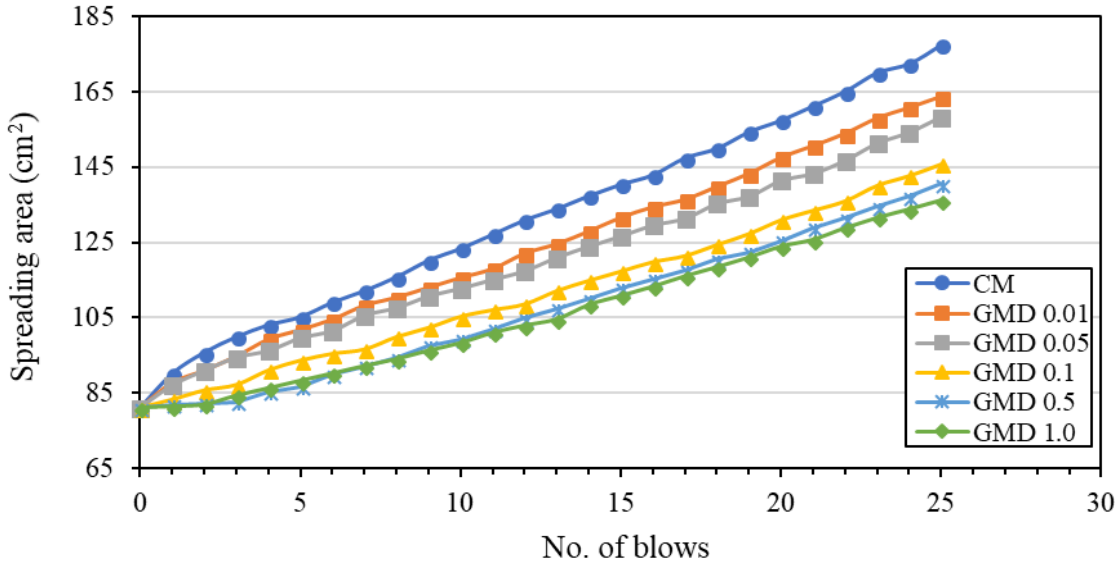

Figure 4-15. Effect of EOGO content on the mortars workability (Dry-mix design)

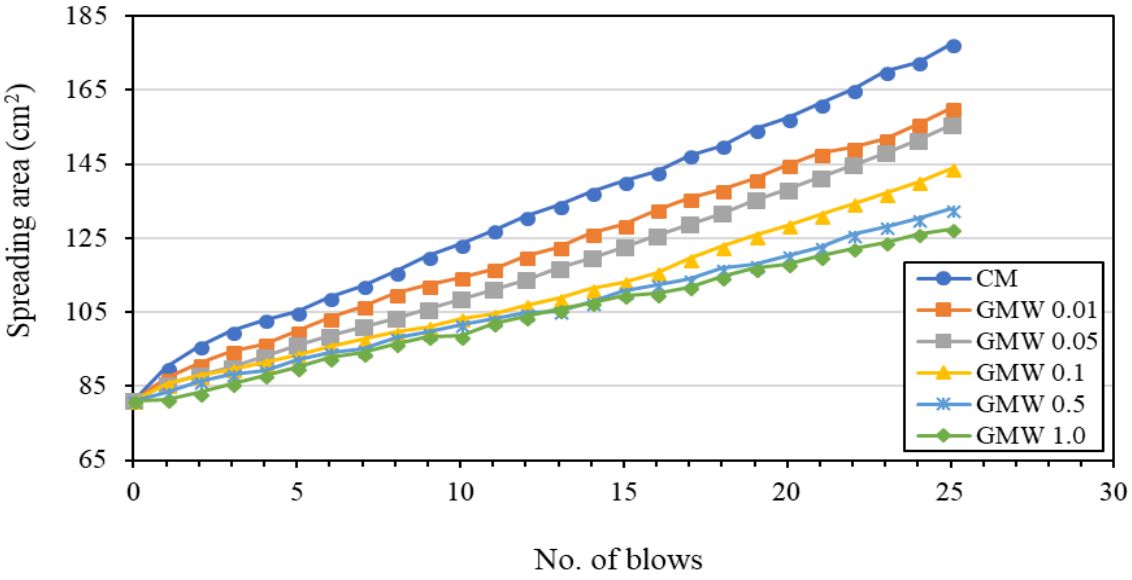

Figure 4-16. Effect of EOGO content on the mortars workability (Wet-mix design)

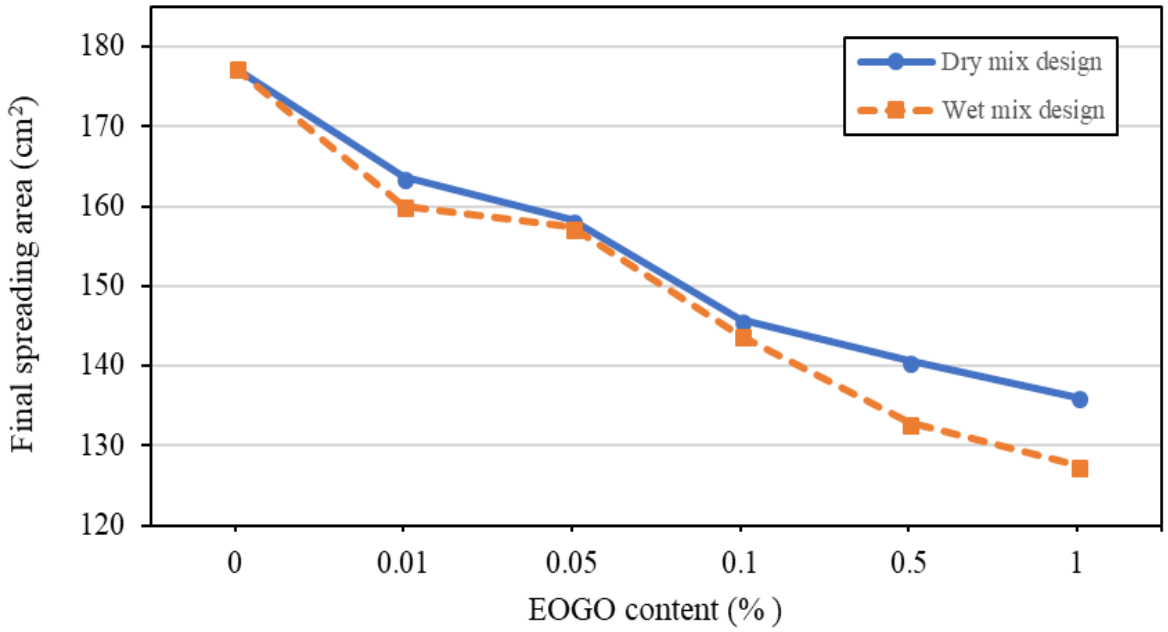

Figure 4-17. Comparison between the effect of the mixing method of EOGO on the workability of mortars

Table 4-2. The flow table test results of mortar (at the final blow)

Specimen ID	Flow area (cm^2)	Reduction percentage (%)
CP	177.42	0
GMD 0.01	163.67	8.40
GMD 0.05	158.32	12.06
GMD 0.1	145.81	21.67
GMD 0.5	140.58	26.21
GMD 1.0	136.13	30.33
GMW 0.01	160.06	10.86
GMW0.05	157.42	12.70
GMW 0.1	143.87	23.32
GMW 0.5	132.84	33.56
GMW 1.0	127.55	39.10

4.4.3 Effect of EOGO on the Fresh Concrete

Different concrete mixes were made with different percentages of EOGO, which are 0.01%, 0.05%, and 0.1% by the weight of cement using dry-mix design. The variation of slump with the EOGO contents for all mixes are illustrated in Figure 4-18. The results show that the slump values of all EOGO-concrete mixes (GCD) are higher than that of the control sample (C). In addition, the figure shows that the slump of GCD mixes increases with the increase of EOGO content. This means that the concrete workability can be improved by low or moderate (0.01% to 0.1%) addition of EOGO. The results signify that the increase in the slump was not significant when EOGO content increased from 0.05% to 0.1%. This indicates that further increase of EOGO beyond 0.1% may reduce the slump, thus, reducing the concrete workability. The reason may be that EOGO reduces the free water absorbed by dry aggregate, leading to an increase the effective ratio of water to cement in the mixes. Chapter 5 discusses this in detail.

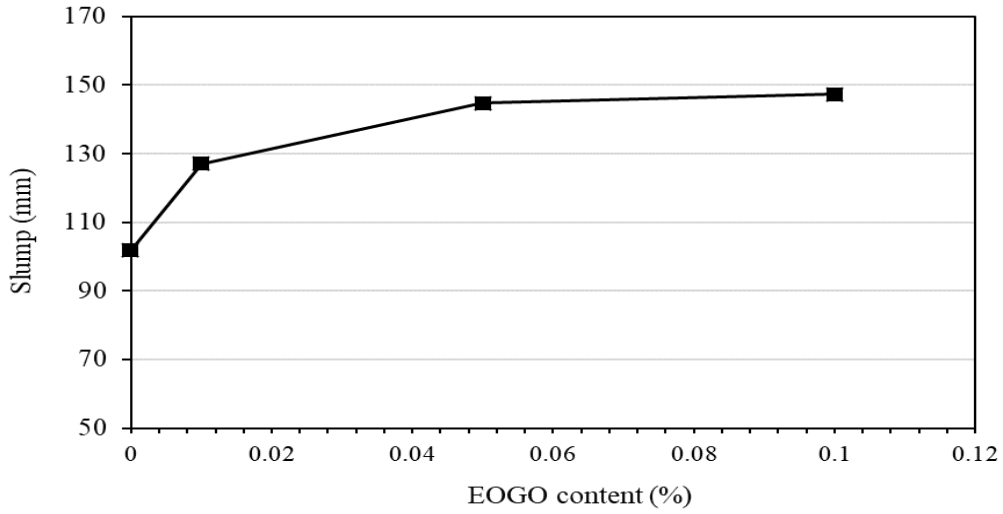

Figure 4-18. Slump test results of EOGO-concrete with dry mix design.

4.5 Summary and Conclusion

EOGOs as an additive in cement composites result in reduced fluidity and workability, which is a similar trend in other studies investigating GO-cement composites. One of the mechanisms can be physical distribution of nanoparticles as an additive, which can cause higher viscosity in fresh cement composites. Another mechanism can be the large surface area of graphene oxide and the presence of oxygen containing functional groups on the surface, leading to an absorption of a large amount of free water during the early aging stages. Previous studies have shown that the effect of cement paste and mortar workability of GO nanosheets is much higher than EOGO. For example, this investigation showed that the workability of the cement paste with wet-mix design decreased by 12% when incorporating 0.05% of EOGO compared to the control sample. On the other hand, Pan et al. [46] noted that the reduction in the workability of cement paste was around 42% when adding 0.05% of GO to the plain cement paste. There are a few reasons for this. First, the amount of oxygen functional group in EOGO (5-10%) is less than that in the chemically manufactured conventional GO (40-50%). The number of oxygen functional group plays a crucial role in initiating faster hydration process, determining hydration crystal shape and enhancing performance of cementitious composites [15]. Of interest is the low to moderate addition of EOGO in concrete improved its workability, when it is generally known that EOGO reduces the workability of other types of cement composites such as cement paste and mortar. The following conclusions have been made based on the research findings:

- For both dry and wet-mix designs, the use of EOGO reduces the fluidity and workability of cement paste and mortar. The viscosity increases as the addition of EOGO increases. This result may be attributed to the large surface area of EOGO, leading to more absorption

of the free water in the mixes, and the fast re-agglomeration of cement particles due to the oxygen-containing functional groups in EOGO.

- The rheological properties of cement paste, and the workability of mortars are more affected by the mixes containing well-dispersed EOGO (wet mix design) than those containing dry powder EOGO (dry mix design). This phenomenon can be rationalized in that the wet-mix design requires more water.
- The slump test results show that the addition of EOGO improves the workability of concrete with dry-mix design. This improvement can be attributed to low absorption of the free water by coarse aggregates when EOGOs are added to concrete mixes.
- The results reveal that the dry-mix design method also has an influence on the workability of cement composites. This indicates that dry-mix design is feasible and might be an economical and practical alternative method for EOGO-cement composites for large-scale production.

CHAPTER 5: MECHANISM STUDY ON THE WORKABILITY OF EOGO-CONCRETE[5]

5.1 Introduction

In this chapter, the workability of concrete in the presence of EOGO is studied to investigate the mechanism behind the workability improvement of concrete when EOGO is added. It is hypothesized that EOGOs are interacted with the surface of coarse aggregate. Aggregate absorption controls the level of the interaction between EOGOs and aggregate. This interaction causes a reduction in the water absorbed by the dry coarse aggregate, leading to increase the effective w/c in the mixes. To study this hypothesis, different types of coarse aggregates with different absorption capacity were used for this purpose. Coarse aggregate types include limestone, granite, glass balls, and lightweight aggregates. These aggregates were used in oven dry conditions to assess the effect of EOGO on the slump measurements of concrete mixes. Lightweight aggregates (LWAs) also were used in saturated surface dry (SSD) condition for comparison purposes. Based on the results found in section 4.4.3, there is a small difference between the effects of EOGO content (0.05% and 0.1%) on the workability of concrete. Consequently, the amount of EOGO used in this investigation was kept at 0.05% by cement weight for economy perspective. Two mixes were made for each type of aggregates. One of those mixes for control concrete and the another for EOGO-concrete. To eliminate the variables affecting the workability of concrete, size of aggregates, EOGO content, and w/c ratio were kept same for all mixes. In addition, two types of tests were performed in this investigation, slump test and water absorption of aggregate

[5] The content of this chapter will appear as a peer-reviewed journal paper, authored by the author of dissertation.

in presence of cement paste test in order to evaluate the suggested hypothesis. Figure 5-1 illustrates the flow chart that describes the process followed for this study.

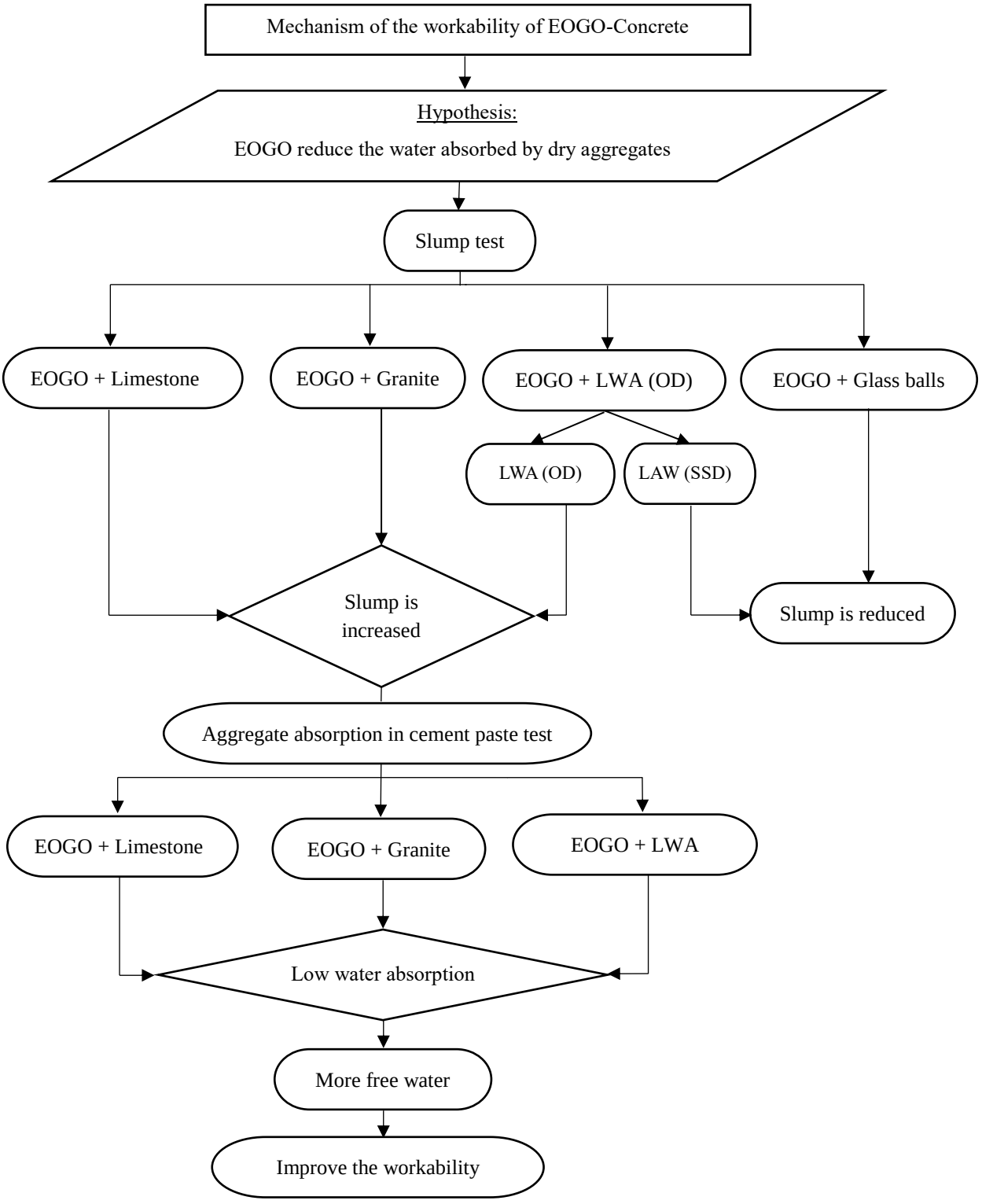

Figure 5-1. The overview of the existing study

5.2 Materials

5.2.1 EOGO

EOGO as dry powder is used for this investigation, and its properties were described in section 3.2.1.

5.2.2 Ordinary Portland Cement

Ordinary Portland Cement Type I, presented in section 3.2.2, is used with all concrete mixtures. Chemical composition of the Ordinary Portland Cement is shown in Table 3-2.

5.2.3 Aggregates

5.2.3.1 Fine Aggregate

Standard sand as fine aggregate was used for the concrete mixtures. The gradation of fine aggregate is presented in Figure3-5.

5.2.3.2 Coarse Aggregates

Four types of coarse aggregates were used to investigate the effect of EOGO on concrete workability. The aggregate selection was based on their absorption capacity. These aggregate types are glass balls (No absorption), granite (Low absorption), limestone (Medium absorption), and lightweight aggregate (High absorption). lightweight aggregate (LWA) used in this research was expanded clay. A single size of all aggregate types (1/2" or 12.5mm) was used as shown in Figure 5-2 to eliminate the aggregate gradation effect on the workability of concrete. The properties of these aggregates are listed in Table 5-1.

(a) Limestone aggregate

(b) Granite aggregate

(c) Glass balls aggregate

(d) Lightweight aggregate (LWA)

Figure 5-2. Various types of coarse aggregates used in this investigation.

Table 5-1. Characteristic properties of coarse aggregates.

Properties	Limestone	Granite	Glass balls	LWA
Bulk Specific Gravity (OD)	2.55	2.69	2.51	0.76
Dry Rodded Unit Weight (kg/m^3)	1577.7	1596.8	1541.3	435.1
Water Absorption (%)	3.96	0.62	0	23.68
Particle Shape	Subangular	Subangular	Rounded	Rounded
Grain size (mm)	12.5	12.5	12.5	12.5

5.3 Mix Design

A total of 12 mixes were considered in this research. All concrete mixes had the same volumetric proportion of fine and coarse aggregates. Coarse (limestone and granite) and fine aggregates were used in oven dry (OD) condition while LWAs were used in two different conditions, which are OD and saturated surface dry (SSD). In oven dry condition, the aggregates were oven-dried at 105 ^{o}C for 24 hours before mixing for oven dry (OD) mixes, which are 10 mixes. In addition, LWAs were soaked in water for 24 hours for SSD mixes, which are two mixes. After 24 hours, the excess water was removed, and the aggregates were used in SSD condition. The water to cement (w/c) ratio was 0.5 for all cases. For EOGO-concrete mixes, EOGO (0.05%) was manually mixed with the cement as a dry powder prior to adding the water for concrete mixture.

All of the mix designs are summarized in Table 5-2. In this table, control concrete and concrete with EOGO made with limestone aggregate are denoted as LCC and LGC, respectively. GCC and GGC are referred to control concrete and concrete with EOGO made with granite aggregate. Concrete mixed with glass ball is denoted as GBCC for control concrete and GBGC is concrete with EOGO. For lightweight concrete, LWCC is control concrete mixed with lightweight aggregate and LWGC is EOGO-concrete mixed with lightweight aggregate.

Table 5-2. Mix design of all concrete mixtures.

Concrete type	Total water (kg/m^3)	Cement (kg/m^3)	EOGO (g/m^3)	Fine aggregate (kg/m^3)	Coarse aggregate			
					Limestone (kg/m^3)	Granite (kg/m^3)	Glass balls (kg/m^3)	LWA (kg/m^3)
LCC	242	408	-	789	848	-	-	-
LGC	242	408	204	789	848	-	-	-
GCC	213	408	-	806	-	848	-	-
GGC	213	408	204	806	-	848	-	-
GBCC	193	378	-	866	-	-	819	-
GBGC	193	378	189	866	-	-	819	-
LWCC	250	378	-	891	-	-	-	241
LWGC	250	378	189	891	-	-	-	241

5.4 Experimental Tests

5.4.1 Slump Test

The workability of concrete was measured by using a slump cone that has 100 mm diameter at the top, 200 mm diameter at the bottom, and is 300 mm in height. The slump test of EOGO-concrete was performed immediately according to ASTM C 134 [97] for all concrete mixes made with the four types of aggregates. Six consecutive readings of slump test for one mix ID were taken within 30 minutes in order to minimize testing errors, and the records were averaged as a slump value of the mixture.

5.4.2 Aggregates Absorption Test

5.4.2.1 Test Method

A test method was developed by Bello et al.[98] was adopted to assess the water absorption in cement paste of coarse aggregates. This method was performed to investigate the effect of EOGO on the absorption of aggregates in fresh concrete. The relationship between the mass of wet aggregates particles extracted from cement paste (A_1) and dry aggregates after oven-dried (A_2) can

be utilized to obtain the quantity of absorbed water by coarse aggregates in cement paste. All the cement paste/aggregate mixes had the same volumetric proportion. The mix proportions used are shown in Table 5-3. The cement and water were hand mixed for a minute for control and EOGO-cement paste. Then the coarse aggregates were added to the cement paste mixture in a bowl and hand mixed for another minute. After that, coarse aggregate particles were extracted from the paste after 15 minutes by sieving with 4.75 mm sieve and then weighed as wet condition. These particles were oven-dried to constant weight at 105 ^{o}C and the particles weight measured as dry condition.

Table 5-3. Mix proportions of coarse aggregates/cement paste mixes.

Mix ID	Total water (g)	Cement (g)	EOGO (g)	Coarse aggregate		
				Limestone (g)	Granite (g)	LWA (g)
LCP	152	264	-	528	-	-
LGP	152	264	0.132	528	-	-
GCP	136	264	-	-	629	-
GGP	136	264	0.132	-	629	-
LWCP	169	264	-	-	-	155
LWGP	169	264	0.132	-	-	155

5.4.2.2 Test Procedure

First, aggregates included limestone, granite, and lightweight aggregates mentioned in section 3.5.1.2.2 were prepared. The aggregates were sieved, and only the aggregates retained on the 12.5 mm sieve were used to eliminate the size or gradation effect in this investigation. The aggregates were oven-dried at 105 ^{o}C for 24 hours and allowed to cool at room temperature. After cooling, the designed weight was measured (A_0) before testing.

Second, the cement paste was mixed by hand for a minute. For EOGO-paste, 0.05% by cement weight of EOGO was manually mixed with the cement before adding the mixing water.

The water to cement ratio (w/c) was kept at 0.5 for all mixes. After that, coarse aggregates were mixed in a bowel with the cement paste for a minute. Summarily, the bowl was covered with plastic wrap in order to avoid water loss. The samples were kept at a room temperature and relative humidity of 50% for 15 minutes before sieving.

Third, the cement paste and aggregate mixtures were mixed again before the aggregates were mechanically separated from cement paste by sieving, and the mixtures were poured in a 4.75 mm sieve with the bottom pan. These sieves were placed on a sieve shaker and sieved for three minutes to extract the aggregate particles and to collect the excess cement paste.

Finally, the aggregates particles surrounded by fresh cement paste were weighed in wet condition (A_1). These particles were oven-dried at 105 ^{o}C to constant weight within 48 hours. After that, the weight of dried particles was measured (A_2) after cooling at room temperature. Figure 5-3 illustrates the different conditions of materials during the test procedure. The water absorption in fresh cement paste for various types of coarse aggregates can be obtained at different time intervals as [98]:

$$W(t) = \left[[c(A_1 - A_2) - w(A_2 - A_0)]/[A_0(c + A_0 - A_2)]\right] * 100 \quad (4)$$

Where $W(t)$ is the percent of water absorption of coarse aggregates in cement paste at time *t*, c is the cement content in grams, A_0 is the dry aggregate weight before mixing, A_1 is the weight in grams of coarse aggregate particles surrounded by fresh cement paste at wet condition, and A_2 is the weight in grams of coarse aggregate particles after being oven dried.

(a) Paste and aggregate mix before sieving

(b) Collected paste after sieving

(c) Aggregate at wet condition after sieving

(d) Aggregates at dry condition

Figure 5-3. The phases of the test procedure.

5.5 Results and Discussion

5.5.1 Slump

Workability of concrete is normally measured using slump test. Figure 5-4 shows the slump measurements carried out six repeated times after mixing of concrete with different types of aggregate. These aggregates were sieved and only the aggregates retained on sieve 12.5 mm were used. In addition, these aggregates were oven dried for 24 hours before being used for the concrete

mixes. The glass balls were not dried as they have zero water absorption. Figure 5-4 (a) illustrates that adding 0.05% of EOGO to concrete mixed with limestone aggregate can increase the slump of concrete mix compared with control sample. Same trend was observed when concrete mixed with granite and LWA aggregates as shown in Figure 5-4 (b) and (d). However, concrete mixed with glass balls shows lower or no effect on concrete slump in the presence of EOGO when compared with control concrete as shown in Figure 5-4 (c). The concrete slump of some reading of each mix is shown Figure 5-5.

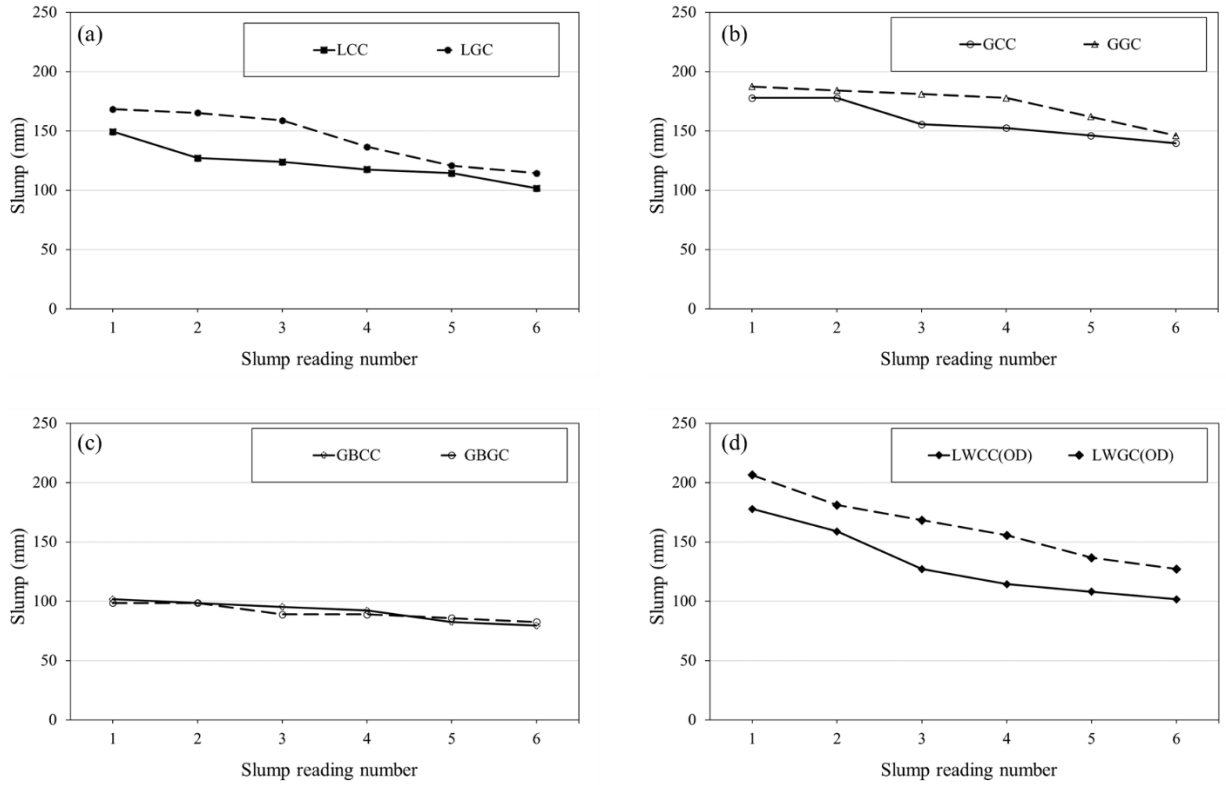

Figure 5-4. Repeatability of slump measurements of concrete made with different types of aggregate: (a) Limestone, (b) Granite, (c) Glass balls, and (d) LWA.

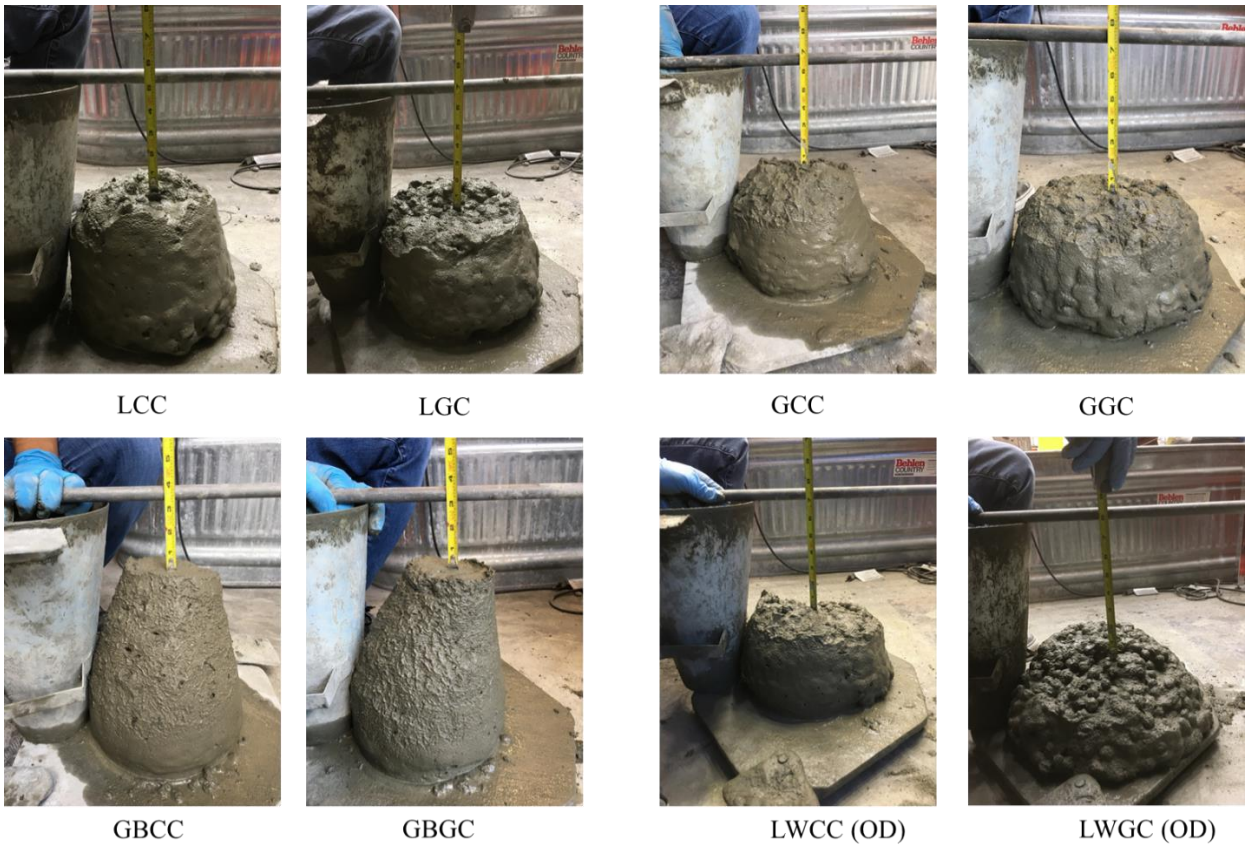

Figure 5-5. Some concrete slump pictures for different mixes.

The average values of the six readings are presented in Figure 5-6. The results of slump show that the slump was increased when EOGO was added to concrete mixes except for concrete mixed with glass balls. The slump of concrete mixed with limestone aggregate and 0.05% of EOGO (LGC) is increased by about 17% compared to the control sample (LCC). The slump of concrete also was increased by around 9% when EOGOs were added to concrete mixed with granite aggregate (GGC) compared with control one (GCC). The increase in the slump of concrete mixed with LWA and EOGOs (LWGC) compared to the control sample (LWCC) reached to 23%. This is the highest improvement in the workability of concrete among the other concrete mixes with limestone and granite aggregate. In contrast, the slump was decreased with adding EOGOs

to concrete mixed with glass balls (GBGC) by around 2% compared with control concrete (GBCC).

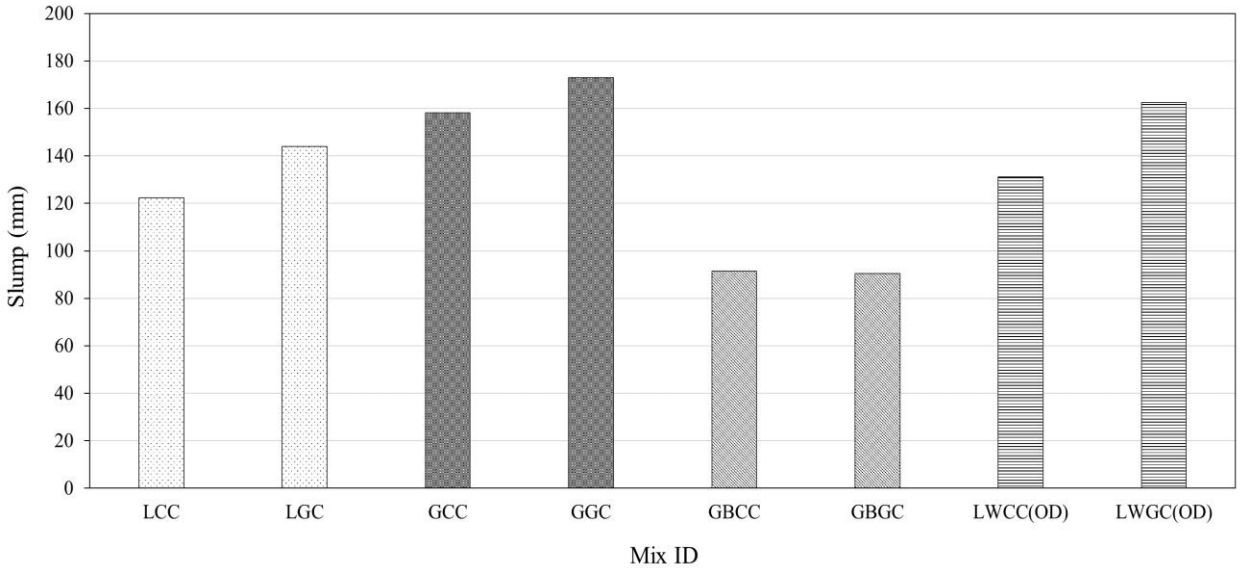

Figure 5-6. Average values of variation of the slump repeatability tests for concrete mixed with different types of aggregate.

Concrete mixes with aggregates that have absorption capacity have improvements in workability through slump increase when EOGO was added. However, the workability of concrete made with glass balls, which have zero absorption capacity, was slightly decreased after incorporation of EOGO. Fresh concrete with LWA (23.68% absorption) causes higher slump to increase than limestone (3.96% absorption) and granite (0.62% absorption). Fresh concrete with glass balls (0% absorption) and EOGO has negative slump effect because EOGO are dispersed in cement matrix and reduce the workability. The EOGO may interacted with the surface of aggregate. The aggregates absorption controls the level of the interaction between EOGO and aggregate. Therefore, the amount of water absorbed by dry aggregates is reduced in the mix includes EOGO. This leads to increase the effective water in the concrete mixes.

In order to investigate the effect of EOGO addition on the condition of aggregate, LWAs that have high absorption capacity and uniform shape were chosen for this purpose. LWA were mixed with concrete in two different conditions (OD and SSD) before conducting slump test. The purpose of using aggregate with different condition is to investigate the absorption effect with the same type of aggregate since aggregate with SSD condition will have very low or zero absorption. The slump measurements of concrete made with LWA in OD and SSD condition are presented in Figure 5-7.

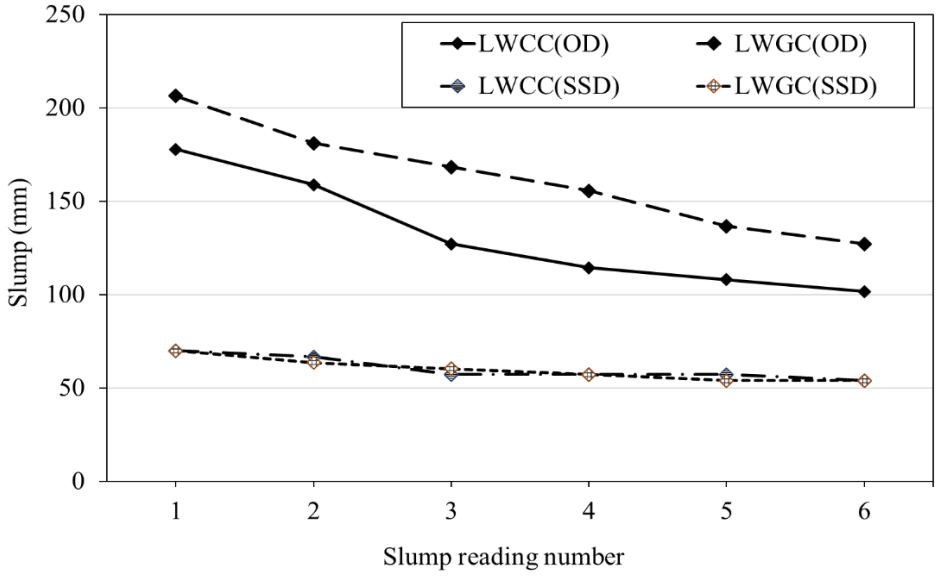

Figure 5-7. Repeatability of slump measurements of concrete made with different conditions of LWA.

The results in Figure 5-7 (a) and (b) show that the slump of concrete mixes with LWA in OD condition is higher than SSD condition. This is attributed to the fact that LWAs do not fully absorb the total water added for absorption. As a result, there is more effective water in the concrete mixes with OD aggregates, leading to more workable mixes than those with SSD aggregates. In addition, slump loss with time is greater with dry aggregates due to the water absorption by dry

aggregate compared to SSD aggregates. The average of the six reading as shown in Figure 5-8 demonstrates that the addition of 0.05% of EOGO into concrete mixes with LWAs in OD condition (LWGC (OD)) increased the slump by around 23% compared to LWCC (OD). The results also illustrate that the incorporation of 0.05% of EOGOs into concrete mixed with LWAs with SSD condition has lower or no effect on the slump of concrete. This phenomenon supports the indication that EOGO in cement matrix reduces the water absorbed by dry aggregates, resulting in increased the effective water in concrete mixes.

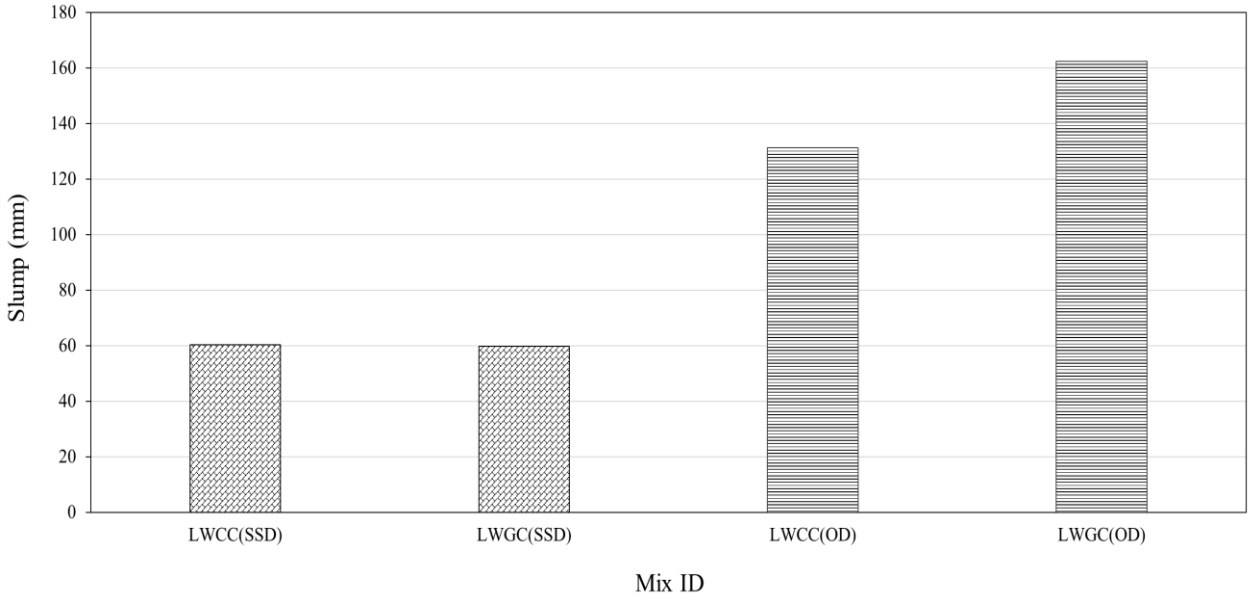

Figure 5-8. Average values of variation of slump measurements of concrete with different conditions of LWA

5.5.2 Aggregate Absorption

The water absorbed by aggregates in cement paste was investigated to represent the actual water absorption during the mixing of concrete. The water absorption in cement paste is slower than that in pure water. This is due to the small particles in cement matrix blocking the surface aggregate pores. Also, the cement consumes some water for hydration process. In addition, the

viscosity of pure water is lower than cement paste. This effect depends on whether cement paste can be absorbed by aggregates or not. A study by Zhang and Gjorv showed that aggregates did not absorb any cement paste [99]. Therefore, it appears that aggregates only absorb water even in the presence of cement paste. The water absorption of limestones, granite, and lightweight aggregates in pure water was measured over the time. It is based on weighing the aggregates in SSD condition after submerging the known weight of oven-dried aggregates in pure water at specific intervals. Figure 5-9 shows the results of water absorption in pure water of different types of aggregate over time. The results illustrate that LWAs have a higher water absorption rate compared to limestone and granite. In addition, granite aggregates show no difference in the water absorption with time.

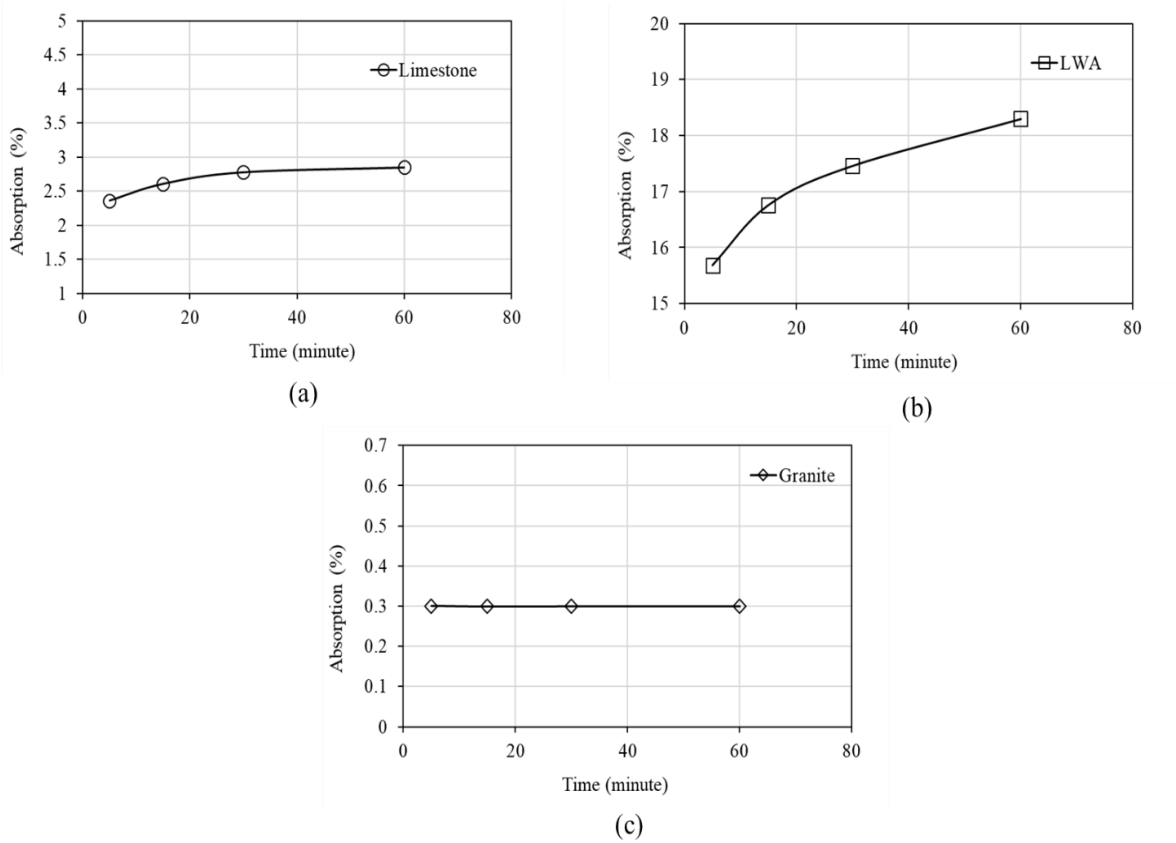

Figure 5-9. Water absorption rate of (a): limestone aggregate, (b) Lightweight aggregate, and (c): granite aggregate.

A test method proposed by Bello et. al [98] was adopted for estimating the water absorption of different types of aggregates in the presence of control and EOGO-cement paste. The test was performed with dry limestone, granite and lightweight aggregates in cement paste of w/c ratio of 0.5. The test was repeated five times and the time interval 15 minutes was chosen for all mixes. Table 5-4 shows the results of water absorption of all types of aggregates in plain and EOGO-cement paste. Generally, the water absorption values of aggregates in cement paste are lower than those in pure water. The water absorption at 15 minutes of limestone aggregates was reduced from 2.61% in pure water to 1.6% in control cement paste. For granite aggregates, the water absorption in cement paste was decreased from 0.3% in pure water to 2.1% in control cement paste. In addition, the water absorption of LWA at 15 minutes in cement paste was decreased from 16.76% in pure water to be 15% in control cement paste. These differences were expected due to the reasons mentioned previously in this section.

Figure 5-10 illustrates the average values of water absorption tests in cement paste. The results demonstrate that the addition of EOGO into cement paste reduced the water absorbed by coarse aggregates compared by plain cement paste. The water absorption of limestone aggregates in aggregates-cement paste mixture decreased from 1.63% to 0.38% when EOGOs were added. The absorption percentage of granite aggregates decreased from 0.21% in control cement paste mixture to 0.12% in EOGO-cement paste. For LWA, the incorporation of EOGOs into cement paste decreased the water absorption from 15% to 4.2%. The reason for this is that when coarse aggregate particles coated by EOGO-cement paste, the water penetration into the pores of aggregates seems limited in comparison with control cement paste. The results prove that the water absorbed by aggregates is reduced in the presence of EOGO in cement paste, leading to having

more effective water in mixtures. This ultimately results in more workable concrete. In addition, these results can also explain the higher slump of concrete mixes when EOGO was added.

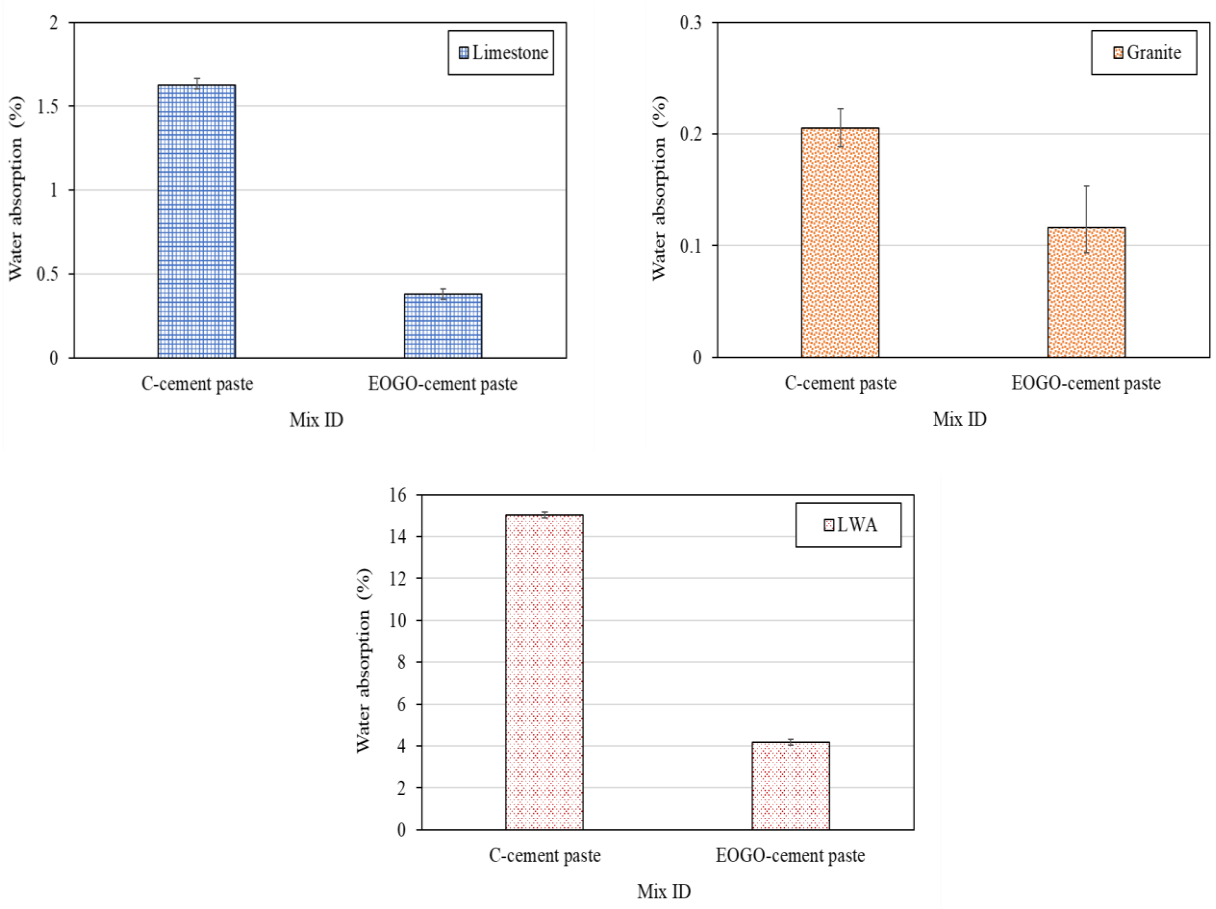

Figure 5-10. Average water absorption values of different types of aggregate in cement paste.

Table 5-4. Water absorption of different types of aggregates in cement paste.

Aggregate Type	Mixture ID	Series	C (g)	W (g)	A_0 (g)	A_1 (g)	A_2 (g)	W (%)	Average W (%)
Limestone	C-concrete	1	264.0	132.0	528.6	575.7	554.9	1.61	
		2	264.0	132.0	528.5	578.8	556.8	1.66	
		3	264.0	132.0	528.8	582.5	559.5	1.64	1.63
		4	264.0	132.0	528.5	581.4	558.7	1.62	
		5	264.0	132.0	528.6	579.8	557.7	1.61	
Limestone	EOGO-concrete	1	264.0	132.0	528.6	570.2	555.1	0.39	
		2	264.0	132.0	528.5	571.4	555.9	0.38	
		3	264.0	132.0	528.5	573.8	557.6	0.35	0.38
		4	264.0	132.0	528.7	573.4	557.2	0.41	
		5	264.0	132.0	528.6	572.8	556.9	0.37	
Granite	C-concrete	1	264.0	132.0	629.7	658.2	555.1	0.39	
		2	264.0	132.0	629.6	659.8	555.9	0.38	
		3	264.0	132.0	629.6	658.7	557.6	0.35	0.21
		4	264.0	132.0	629.8	661.0	557.2	0.41	
		5	264.0	132.0	629.7	660.1	556.9	0.37	
Granite	EOGO-concrete	1	264.0	132.0	629.6	657.3	647.6	0.12	
		2	264.0	132.0	629.5	656.6	647.2	0.09	
		3	264.0	132.0	629.7	657.2	647.6	0.11	0.12
		4	264.0	132.0	629.7	657.6	647.9	0.10	
		5	264.0	132.0	629.5	658.3	648.1	0.15	
LWA	C-concrete	1	264.0	132.0	154.9	212.6	179.3	15.0	
		2	264.0	132.0	155.0	213.1	179.8	14.9	
		3	264.0	132.0	155.0	214.0	180.3	15.0	15.0
		4	264.0	132.0	154.9	212.5	179.1	15.1	
		5	264.0	132.0	155.0	212.8	179.3	15.2	
LWA	EOGO-concrete	1	264.0	132.0	155.0	207.9	186.4	4.2	
		2	264.0	132.0	155.0	207.0	186.0	4.0	
		3	264.0	132.0	155.0	206.8	185.6	4.3	4.2
		4	264.0	132.0	155.1	202.7	183.0	4.1	
		5	264.0	132.0	155.0	203.9	183.8	4.1	

5.6 Summary and Conclusions

In this chapter, two experimental tests were evaluated to investigate the mechanism of the workability of EOGO-concrete improvement. Different types of coarse aggregates were used for this investigation. Concrete mixes for each type of aggregate were made to conduct slump and aggregate absorption tests. EOGO content was kept 0.05% for all mixes based on the results found in section 4.4.3. Based on the current experimental results and discussion in Chapter 5, the following conclusions may be drawn:

- The slump of concrete mixed with dry limestone, granite and lightweight aggregates increases when EOGO is added compared to control concrete, leading to workability improvement. Nevertheless, there is negative slump of EOGO-concrete mixed with glass balls aggregates because EOGO is dispersed in cement matrix and reduces the workability. This indicates that the inclusion of EOGO into concrete reduces the water absorbed by dry coarse aggregates in mixes, leading to an increase in effective water in the mixes and as well as the workability.
- Concrete mixed with dry LWAs, which has high absorption capacity, causes higher increase in the slump when EOGO is added compared to the concrete mixed with limestone or granite aggregates. This finding demonstrates that the effect of EOGO is correlated with the absorption capacity of coarse aggregate.
- The slump of EOGO-concrete mixes with LWAs in SSD condition, which has no absorption capacity, has low or no change compared with the control samples. This result strongly supports the hypothesis that EOGO reduces the water absorbed by coarse

aggregate in OD condition when mixed with concrete.

- The results of aggregate absorption test indicate that the water absorption of coarse aggregate in cement paste is different than that in pure water. This is due to different reasons including the fact that the viscosity of cement paste is higher than of pure water. Hydration process consumes water, and some pores on the surface of the aggregates are blocked by small particles.
- The addition of EOGO in cement paste/coarse aggregate mixes reduces the water absorbed by dry coarse aggregates. Mixes with dry LWAs has a higher reduction in water absorption when EOGO is added, compared to the mixes with limestone or granite aggregates. This finding is consistent with the slump test results and supports the suggested hypothesis.

CHAPTER 6: CONCLUSIONS AND RECOMMENDATION[6]

6.1 Conclusions

Finally, an overview of the major conclusions drawn from this study is summarized below:

- The mechanical properties of all EOGO-cement pastes and mortars were improved over the control cement composite specimens for both dry and wet-mix designs. In addition, it was observed that 0.05% by cement weight of EOGO is the optimum concentration for the improvement of strength of cement paste and mortar for both mix designs.
- For both dry and wet-mix designs, the addition of EOGO has a slight positive effect on the total porosity of cement composites. For water sorptivity test, most of EOGO-cement composites showed significant improvement, indicating a reduction of a continuity of capillary pores and the total amount of pores due to the promoted nucleation of hydration products and filling effect. This ultimately leads to an improvement in the durability of the cement composites.
- The petrographic Quantitative analysis of XRD data indicates that EOGO may act as Nano-seeding material in cement pore solution to promote CSH and other hydration products. Petrographic analyses (SEM/EDS) are in agreement with the XRD analysis. EOGOs are mostly found in the presence of CSH, confirming EOGO having a potential

[6] The partial content of this chapter appeared and will be appeared in:
Alharbi, Y., An, J., Cho, B.H., Khawaji, M., and Nam, B.H.* "Mechanical and Pore Structure Characteristics of Edge-Oxidized Graphene Oxide (EOGO)-Cement Composites: Dry and Wet-Mix Design Methods", Nanomaterials 2018, 8(9), 718.
An J., Nam B.H.*, Alharbi Y., Khawaji M., and Cho B.H. "Edge-oxidized graphene oxide (EOGO) in Cement Composites: Cement Hydration and Microstructure", Peer-reviewed journal paper.

role as nano-seeding material in cement composite.

- For both dry and wet-mix designs, the use of EOGO reduces the fluidity and workability of cement paste and mortar, while the viscosity increases as amount of EOGO increases. This may be due to large surface area of EOGO leading to high absorption of the free water in the mixes. It may also be due to fast re-agglomeration of cement particles because of the oxygen-containing functional groups in EOGO.
- The rheological properties of cement paste, and the workability of mortars are more affected by the mixes containing well-dispersed EOGO (wet-mix design) than those containing dry powder EOGO (dry-mix design). The reason is that wet-mix design increases the water requirement of the mixes.
- The comparison of dry and wet-mix designs showed that the mechanical properties of EOGO-cement composites using the wet-mix design method was slightly improved compared to dry-mix design. This difference is likely due to wet-mix design exhibiting a higher reduction in the workability of cement composites compared to dry-mix design. Wet-mix design has better exfoliation and dispersion of EOGO in cement matrix.
- The results reveal that the dry-mix design method also has a significant influence on the workability and the mechanical properties of cement composites. This indicates that dry-mix design is feasible and might be an economical and practical alternative method for EOGO-cement composites for large-scale production.
- The slump of concrete mixed with dry limestone, granite, and lightweight aggregates increases when EOGO is added compared to control concrete, leading to workability

improvement. Nevertheless, there is negative slump of EOGO-concrete mixed with glass balls aggregates because EOGO is dispersed in cement matrix and reduces the workability. This indicates that the inclusion of EOGO into concrete reduces the water absorbed by dry coarse aggregates in mixes, leading to an increase of the effective water in the mixes as well as the workability.

- Concrete mixed with dry LWA, which has high absorption capacity, causes higher increase in the slump when EOGO is added compared to the concrete mixed with limestone or granite aggregates. This finding demonstrates that the effect of EOGO is correlated with the absorption capacity of coarse aggregate.
- The slump of EOGO-concrete mixed with LWA in SSD condition (which has no absorption capacity) has low or no change compared to the control samples. This result strongly supports the hypothesis of that EOGO reduces the water absorbed by coarse aggregate in OD condition when mixed with concrete.
- The results of aggregate absorption test indicate that water absorption of coarse aggregates in cement paste is different for water absorption of aggregates in pure water. This is due to different reasons including the viscosity of cement paste being higher than that of pure water, hydration process consuming water, and some pores on the surface of the aggregates being blocked by small particles.
- The addition of EOGO in cement paste/coarse aggregate mixes reduces the water absorbed by dry coarse aggregates. Mixes with dry LWAs has a higher reduction in water absorption when EOGO is added compared to the mixes with limestone or granite aggregates. This

finding is consistent with the slump test results and supports the suggested hypothesis.

6.2 Recommendations

From the results, the improvement in the strength of cement composites is mainly because of the number of oxygen-containing functional groups on the edge of EOGO, bridging, and filling effects. Functional groups play an important role in acting as a nano-seed to promote nucleation of cement hydration product. It is recommended to increase the number of oxygen-functional groups in EOGO by changing the ball-milling time and oxidation process. This can increase its effect on the cement composites properties including strength, durability and microstructure.

The dispersion of EOGO as additive nanomaterial in cement matrix is extremely important. Using high shear mixer is recommended to better disperse dry EOGO in cement matrix. The well-dispersion of EOGO in cement matrix can help to improve the strength, porosity, and durability of cement composites.

6.3 Future Work

There are two interesting research tasks that are worth investigation further:

- The effect of EOGO on the interfacial transitional zone (ITZ), which has directly influence on the strength of concrete, can be investigated. This will provide better understanding of the improvement in the strength and workability of EOGO-concrete.
- The results from the current study indicate that the addition of EOGOs improve the workability of concrete. The EOGOs interact with the surface of the aggregate, and the absorption of aggregate controls the level of the interaction between EOGOs and aggregate. Therefore, four types of aggregate with different absorption capacities are used based on

these criteria. Further research can be done on the effect of EOGOs on the workability of concrete using aggregate with different surface area and gradation.

APPENDIX: PERMISSION FOR COPYRIGHTED MATERIAL

Permission from Nanomaterials MDPI to reuse the content in the author's published paper:

Alharbi, Y., An, J., Cho, B.H., Khawaji, M., and Nam, B.H.* "Mechanical and Pore Structure Characteristics of Edge- Oxidized Graphene Oxide (EOGO)-Cement Composites: Dry and Wet-Mix Design Methods", Nanomaterials 2018, 8(9), 718.

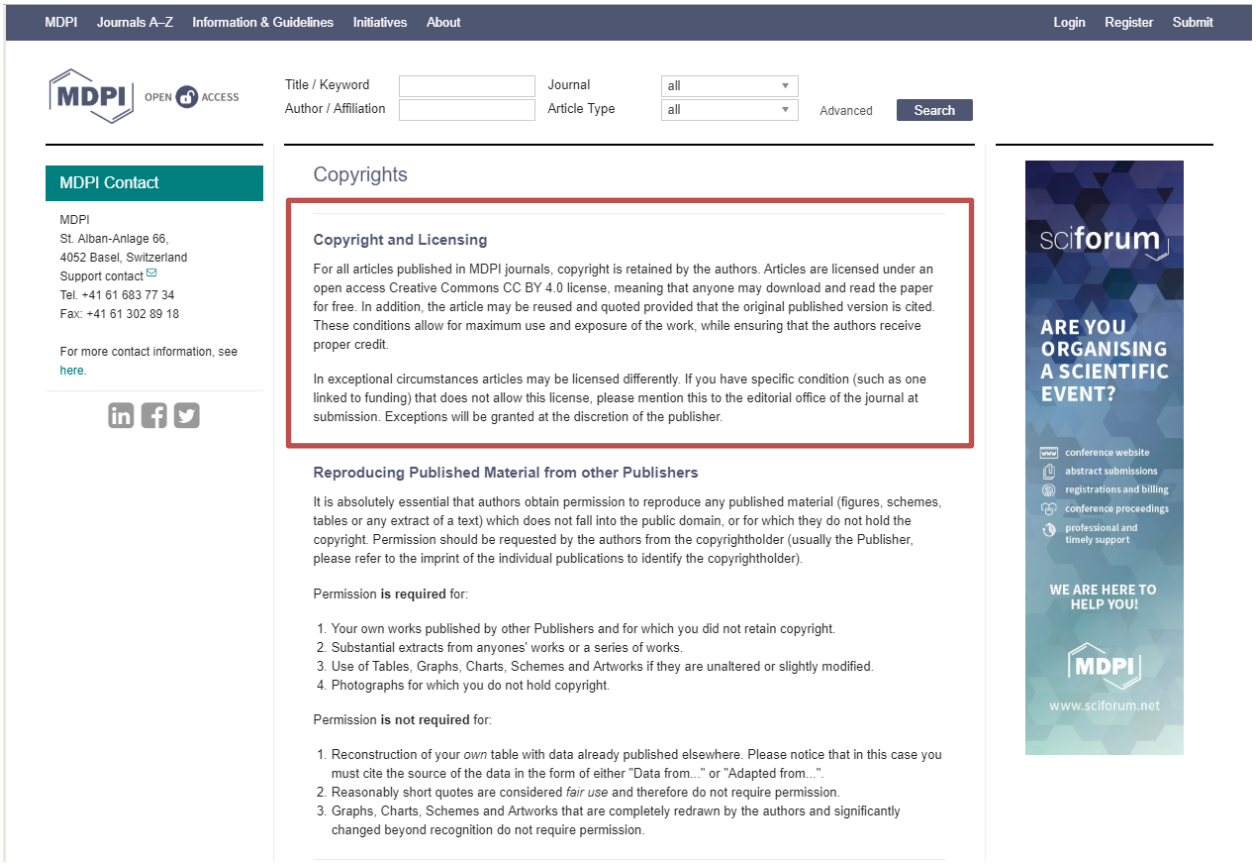

Figure 2-2 used with permission from Nature Materials Publishing Group

4/15/2019 RightsLink Printable License

SPRINGER NATURE LICENSE TERMS AND CONDITIONS

This Agreement between University of Central Florida -- Yousef Alharbi ("You") and Springer Nature ("Springer Nature") consists of your license details and the terms and and Copyright Clearance Center.

License Number	4565490598183
License date	Apr 10, 2019
Licensed Content Publisher	Springer Nature
Licensed Content Publication	Nature Materials
Licensed Content Title	The rise of graphene
Licensed Content Author	A. K. Geim, K. S. Novoselov
Licensed Content Date	Mar 1, 2007
Licensed Content Volume	6
Licensed Content Issue	3
Type of Use	Thesis/Dissertation
Requestor type	academic/university or research institute
Format	print and electronic
Portion	figures/tables/illustrations
Number of figures/tables/illustrations	1
High-res required	no
Will you be translating?	no
Circulation/distribution	>50,000
Author of this Springer Nature content	no
Title	Investigation on effect of edge-oxidized graphene oxide (EOGO) on properties of cement composites
Institution name	University of Central Florida
Expected presentation date	Apr 2020
Portions	Figure 1: Mother of all graphitic forms. Graphene is a 2D building materials of all other dimensionalities. It can be wrapped up into 0D buckyballs, rolled int
Requestor Location	University of Central Florida 4000 Central Florida Blvd. Building 91, Suite 211 Orlando, FL 32816 United States Attn: University of Central Florida

Figure 2-4 used with permission from Elsevier Publishing Group.

ELSEVIER LICENSE
TERMS AND CONDITIONS

Apr 11, 2019

This Agreement between University of Central Florida -- Yousef Alharbi ("You") and Elsevier ("Elsevier") consists of your license details and the terms and conditions provided by Elsevier and Copyright Clearance Center.

License Number	4565971149357
License date	Apr 11, 2019
Licensed Content Publisher	Elsevier
Licensed Content Publication	Carbon
Licensed Content Title	Synthesis of graphene-based nanosheets via chemical reduction of exfoliated graphite oxide
Licensed Content Author	Sasha Stankovich,Dmitriy A. Dikin,Richard D. Piner,Kevin A. Kohlhaas,Alfred Kleinhammes,Yuanyuan Jia,Yue Wu,SonBinh T. Nguyen,Rodney S. Ruoff
Licensed Content Date	Jun 1, 2007
Licensed Content Volume	45
Licensed Content Issue	7
Licensed Content Pages	8
Start Page	1558
End Page	1565
Type of Use	reuse in a thesis/dissertation
Portion	figures/tables/illustrations
Number of figures/tables/illustrations	1
Format	both print and electronic
Are you the author of this Elsevier article?	No
Will you be translating?	No
Original figure numbers	Fig. 1. A non-contact mode AFM image of exfoliated GO sheets with three height profiles acquired in different locations
Title of your thesis/dissertation	Investigation on effect of edge-oxidized graphene oxide (EOGO) on properties of cement composites
Publisher of new work	University of Central Florida
Expected completion date	Apr 2020
Estimated size (number of pages)	1
Requestor Location	University of Central Florida 4000 Central Florida Blvd. Building 91, Suite 211 Orlando, FL 32816 United States Attn: University of Central Florida

Figure 3-3 (a) and 3-4 (a) used with permission from Elsevier Publishing Group.

ELSEVIER LICENSE
TERMS AND CONDITIONS

Apr 11, 2019

This Agreement between University of Central Florida -- Yousef Alharbi ("You") and Elsevier ("Elsevier") consists of your license details and the terms and conditions provided by Elsevier and Copyright Clearance Center.

License Number	4565990057528
License date	Apr 11, 2019
Licensed Content Publisher	Elsevier
Licensed Content Publication	Construction and Building Materials
Licensed Content Title	Effect of graphene oxide on the rheological properties of cement pastes
Licensed Content Author	Yu Shang,Dong Zhang,Chao Yang,Yanyun Liu,Yong Liu
Licensed Content Date	Oct 15, 2015
Licensed Content Volume	96
Licensed Content Issue	n/a
Licensed Content Pages	9
Start Page	20
End Page	28
Type of Use	reuse in a thesis/dissertation
Intended publisher of new work	other
Portion	figures/tables/illustrations
Number of figures/tables/illustrations	2
Format	both print and electronic
Are you the author of this Elsevier article?	No
Will you be translating?	No
Original figure numbers	Fig. 2.The characterization of GO (a) AFM image and height profile of GO. Fig. 3.(a) TEM image of GO.
Title of your thesis/dissertation	Investigation on effect of edge-oxidized graphene oxide (EOGO) on properties of cement composites
Publisher of new work	University of Central Florida
Expected completion date	Apr 2020
Estimated size (number of pages)	1
Requestor Location	University of Central Florida 4000 Central Florida Blvd. Building 91, Suite 211 Orlando, FL 32816 United States Attn: University of Central Florida

REFERENCES

[1] R.E.R.-H. Reza Abbaschian, Lara Abbaschian, Physical Metallurgy Principles, USA, 2008.

[2] S. Parveen, S. Rana, R. Fangueiro, M.C. Paiva, Microstructure and mechanical properties of carbon nanotube reinforced cementitious composites developed using a novel dispersion technique, Cem. Concr. Res. 73 (2015) 215–227. doi:10.1016/j.cemconres.2015.03.006.

[3] Y. Gao, X. Ren, X. Tan, T. Hayat, A. Alsaedi, C. Chen, Insights into key factors controlling GO stability in natural surface waters, J. Hazard. Mater. 335 (2017) 56–65. doi:10.1016/j.jhazmat.2017.04.027.

[4] T. Zhang, P. Gao, P. Gao, J. Wei, Q. Yu, Effectiveness of novel and traditional methods to incorporate industrial wastes in cementitious materials - An overview, Resour. Conserv. Recycl. 74 (2013) 134–143. doi:10.1016/j.resconrec.2013.03.003.

[5] N. AM, B. JJ, Concrete technology, Prentice Hall/Pearson, 2010.

[6] S. Hanehara, K. Yamada, Interaction between cement and chemical admixture from the point of cement hydration, absorption behaviour of admixture, and paste rheology, Cem. Concr. Res. 29 (1999) 1159–1165. doi:10.1016/S0008-8846(99)00004-6.

[7] P. Pereira, L. Evangelista, J. De Brito, The effect of superplasticisers on the workability and compressive strength of concrete made with fine recycled concrete aggregates, Constr. Build. Mater. 28 (2012) 722–729. doi:10.1016/j.conbuildmat.2011.10.050.

[8] J. Cheung, A. Jeknavorian, L. Roberts, D. Silva, Impact of admixtures on the hydration kinetics of Portland cement, Cem. Concr. Res. 41 (2011) 1289–1309. doi:10.1016/j.cemconres.2011.03.005.

[9] K. Sobolev, Mechano-chemical modification of cement with high volumes of blast furnace slag, Cem. Concr. Compos. 27 (2005) 848–853. doi:10.1016/j.cemconcomp.2005.03.010.

[10] C. Shi, J. Qian, High performance cementing materials from industrial slags - A review, Resour. Conserv. Recycl. 29 (2000) 195–207. doi:10.1016/S0921-3449(99)00060-9.

[11] M. Şahmaran, H.A. Christianto, I.O. Yaman, The effect of chemical admixtures and mineral

additives on the properties of self-compacting mortars, Cem. Concr. Compos. 28 (2006) 432–440. doi:10.1016/j.cemconcomp.2005.12.003.

[12] T. Tong, Z. Fan, Q. Liu, S. Wang, S. Tan, Q. Yu, Investigation of the effects of graphene and graphene oxide nanoplatelets on the micro- and macro-properties of cementitious materials, Constr. Build. Mater. 106 (2016) 102–114. doi:10.1016/j.conbuildmat.2015.12.092.

[13] J.Y. Wang, N. Banthia, M.H. Zhang, Effect of shrinkage reducing admixture on flexural behaviors of fiber reinforced cementitious composites, Cem. Concr. Compos. 34 (2012) 443–450. doi:10.1016/j.cemconcomp.2011.12.004.

[14] C. Juárez, P. Valdez, A. Durán, K. Sobolev, The diagonal tension behavior of fiber reinforced concrete beams, Cem. Concr. Compos. 29 (2007) 402–408. doi:10.1016/j.cemconcomp.2006.12.009.

[15] I.B. Topçu, M. Canbaz, Effect of different fibers on the mechanical properties of concrete containing fly ash, Constr. Build. Mater. 21 (2007) 1486–1491. doi:10.1016/j.conbuildmat.2006.06.026.

[16] D. Galpaya, Synthesis, Characterization and Applications of Graphene Oxide-Polymer Nanocomposities, (2015).

[17] T. Kuila, S. Bose, A. Kumar, P. Khanra, Progress in Materials Science Chemical functionalization of graphene and its applications, Prog. Mater. Sci. 57 (2012) 1061–1105. doi:10.1016/j.pmatsci.2012.03.002.

[18] K.S. Geim, K.A. and Novoselov, THE RISE OF GRAPHENE, Nat. Mater. 6 (2007).

[19] A.A.F. K. S. Novoselov, A. K. Geim,S. V. Morozov, D. Jiang,1 Y. Zhang, S. V. Dubonos, I. V. Grigorieva, Electric Field Effect in Atomically Thin Carbon Films, Science (80-.). 306 (2004) 666–669. doi:10.1126/science.1102896.

[20] D.R. Dreyer, S. Park, C.W. Bielawski, R.S. Ruoff, The chemistry of graphene oxide, Chem. Soc. Rev. 39 (2010) 228–240. doi:10.1039/b917103g.

[21] A.M. Dimiev, L.B. Alemany, J.M. Tour, Graphene Oxide. Origin of Acidity, Its Instability in Water, and a New Dynamic Structural Model, ACS Nano. 7 (2012) 576–588.

doi:10.1021/nn3047378.

[22] R. Nakajima, T Mabuchi, A Hagiwara, A new structure model of graphite oxide, Carbon N. Y. 26 (1988) 357–361.

[23] T. Nakajima, Y. Matsuo, Formation process and structure of graphite oxide, Carbon N. Y. 32 (1994) 469–475. doi:https://doi.org/10.1016/0008-6223(94)90168-6.

[24] H. He, T. Riedl, A. Lerf, J. Klinowski, Solid-State NMR Studies of the Structure of Graphite Oxide, J. Phys. Chem. 100 (1996) 19954–19958. doi:10.1021/jp961563t.

[25] B.C. Brodie, On the atomic weight of graphite, Science (80-.). 2 (1859) 249–259. doi:10.1525/tph.2001.23.2.29.

[26] W.S. Hummers, R.E. Offeman, Preparation of Graphitic Oxide, J. Am. Chem. Soc. 80 (1958) 1339. doi:10.1021/ja01539a017.

[27] J. Chen, An improved Hummers method for eco- friendly synthesis of graphene oxide synthesis of graphene oxide, Carbon N. Y. 64 (2013) 225–229. doi:10.1016/j.carbon.2013.07.055.

[28] A.M. Dimiev, J.M. Tour, M. Science, C. Science, N. Science, M. Street, U. States, a Z.E. Materials, M. Avenue, Mechanism of Graphene Oxide, ACS Nano. (2014) 3060–3068. doi:10.1021/nn500606a.

[29] S. Stankovich, D.A. Dikin, R.D. Piner, K.A. Kohlhaas, A. Kleinhammes, Y. Jia, Y. Wu, S.B.T. Nguyen, R.S. Ruoff, Synthesis of graphene-based nanosheets via chemical reduction of exfoliated graphite oxide, Carbon N. Y. 45 (2007) 1558–1565. doi:10.1016/j.carbon.2007.02.034.

[30] Y. Shang, D. Zhang, C. Yang, Y. Liu, Y. Liu, Effect of graphene oxide on the rheological properties of cement pastes, Constr. Build. Mater. 96 (2015) 20–28. doi:10.1016/j.conbuildmat.2015.07.181.

[31] Q. Wang, X. Cui, J. Wang, S. Li, C. Lv, Y. Dong, Effect of fly ash on rheological properties of graphene oxide cement paste, Constr. Build. Mater. 138 (2017) 35–44. doi:10.1016/j.conbuildmat.2017.01.126.

[32] L. Shahriary, A. a. Athawale, Graphene Oxide Synthesized by using Modified Hummers Approach, Int. J. Renew. Energy Environ. Eng. 2 (2014) 58–63. doi:10.1016/j.aca.2014.02.025.

[33] S. Mindess, J.F. Young, D. Darwin, Concrete, 2nd ed., Prentic-Hall, 2003.

[34] P.K. Mehta, P.J.M. Monteiro, Concrete: Microstructure , Properties and Materials, (2001).

[35] S. Chuah, Z. Pan, J.G. Sanjayan, C.M. Wang, W.H. Duan, Nano reinforced cement and concrete composites and new perspective from graphene oxide, Constr. Build. Mater. 73 (2014) 113–124. doi:10.1016/j.conbuildmat.2014.09.040.

[36] J. Vera-Agullo, V. Chozas-Ligero, D. Portillo-Rico, M.J. García-Casas, A. Gutiérrez-Martínez, J.M. Mieres-Royo, J. Grávalos-Moreno, Mortar and Concrete Reinforced with Nanomaterials, Nanotechnol. Constr. 3 Proc. NICOM3. (2009) 383–388. doi:10.1007/978-3-642-00980-8_52.

[37] K. Gong, S.M. Asce, Z. Pan, A.H. Korayem, D. Ph, L. Qiu, D. Li, F. Collins, C.M. Wang, W.H. Duan, a M. Asce, Reinforcing Effects of Graphene Oxide on Portland Cement Paste, J. Mater. Civ. Eng. vol 27 (2014) 1–6. doi:10.1061/(ASCE)MT.1943-5533.0001125.

[38] S. Lv, Y. Ma, C. Qiu, T. Sun, J. Liu, Q. Zhou, Effect of graphene oxide nanosheets of microstructure and mechanical properties of cement composites, Constr. Build. Mater. 49 (2013) 121–127. doi:10.1016/j.conbuildmat.2013.08.022.

[39] X. Li, Y.M. Liu, W.G. Li, C.Y. Li, J.G. Sanjayan, W.H. Duan, Z. Li, Effects of graphene oxide agglomerates on workability, hydration, microstructure and compressive strength of cement paste, Constr. Build. Mater. 145 (2017) 402–410. doi:10.1016/j.conbuildmat.2017.04.058.

[40] H.F. Taylor, Cement Chemistry, Thomas Telford, 1997.

[41] S. Lv, J. Liu, T. Sun, Y. Ma, Q. Zhou, Effect of GO nanosheets on shapes of cement hydration crystals and their formation process, Constr. Build. Mater. 64 (2014) 231–239. doi:10.1016/j.conbuildmat.2014.04.061.

[42] Q. Wang, J. Wang, C. Lu, B. Liu, K. Zhang, C. Li, Influence of graphene oxide additions on

the microstructure and mechanical strength of cement, New Carbon Mater. 30 (2015) 349–356. doi:10.1016/S1872-5805(15)60194-9.

[43] Z. Pan, L. He, L. Qiu, A.H. Korayem, G. Li, J.W. Zhu, F. Collins, D. Li, W.H. Duan, M.C. Wang, Mechanical properties and microstructure of a graphene oxide-cement composite, Cem. Concr. Compos. 58 (2015) 140–147. doi:10.1016/j.cemconcomp.2015.02.001.

[44] F. Babak, H. Abolfazl, R. Alimorad, G. Parviz, Preparation and mechanical properties of graphene oxide: cement nanocomposites., ScientificWorldJournal. 2014 (2014) 276323. doi:10.1155/2014/276323.

[45] E. Horszczaruk, E. Mijowska, R.J. Kalenczuk, M. Aleksandrzak, S. Mijowska, Nanocomposite of cement/graphene oxide - Impact on hydration kinetics and Young's modulus, Constr. Build. Mater. 78 (2015) 234–242. doi:10.1016/j.conbuildmat.2014.12.009.

[46] Z. Pan, W. Duan, D. Li, F. Collins, Graphene oxide reinforced cement and concrete, WO Patent App. PCT/AU2012/001, 582, 2012., 2012.

[47] A. Mohammed, J.G. Sanjayan, W.H. Duan, A. Nazari, Incorporating graphene oxide in cement composites: A study of transport properties, Constr. Build. Mater. 84 (2015) 341–347. doi:10.1016/j.conbuildmat.2015.01.083.

[48] A.M. Neville, Properties of Concrete, 2011. doi:10.4135/9781412975704.n88.

[49] J.P.L. Brunet, L. Li, Z.T. Karpyn, B.G. Kutchko, B. Strazisar, G. Bromhal, Dynamic evolution of cement composition and transport properties under conditions relevant to geological carbon sequestration, Energy and Fuels. 27 (2013) 4208–4220. doi:10.1021/ef302023v.

[50] I. De La Varga, R.P. Spragg, C. Di Bella, J. Castro, D.P. Bentz, J. Weiss, Fluid transport in high volume fly ash mixtures with and without internal curing, Cem. Concr. Compos. 45 (2014) 102–110. doi:10.1016/j.cemconcomp.2013.09.017.

[51] C.B. Cheah, M. Ramli, The fluid transport properties of HCWA-DSF hybrid supplementary binder mortar, Compos. Part B Eng. 56 (2014) 681–690. doi:10.1016/j.compositesb.2013.09.021.

[52] S.P. Zhang, L. Zong, Evaluation of Relationship between Water Absorption and Durability of Concrete Materials, 2014 (2014). doi:10.1155/2014/650373.

[53] T. Ji, Preliminary study on the water permeability and microstructure of concrete incorporating nano-SiO2, Cem. Concr. Res. 35 (2005) 1943–1947. doi:10.1016/j.cemconres.2005.07.004.

[54] Q. Wang, J. Wang, C.X. Lu, X.Y. Cui, S.Y. Li, X. Wang, Rheological behavior of fresh cement pastes with a graphene oxide additive, Xinxing Tan Cailiao/New Carbon Mater. 31 (2016) 574–584. doi:10.1016/S1872-5805(16)60033-1.

[55] W.D. Kai Gong, Tuo Tan, Martin Dowman, Ling Qiu, Dan Li, Francis Gerard Collins, Rheological behaviours of graphene oxide reinforced cement composite, in: Int. Compos. Conf. - Melb. Vic Aust. Melb. Vic Aust., Monash University Publishing, Melbourne Vic Australia, 2012: pp. 95–99.

[56] ASTM C125-15b, Standard Terminology Relating to Concrete and Concrete Aggregates, in: Annu. B. ASTM Stand. Sect. 4-Construction, Vol.04.02-Concrete Aggregates, ASTM Int., 2015.

[57] M. Kosmatka, S., and Wilson, Design and control of mixtures, 15th ed., Portland Cement Association, Stokie, IL., 2011.

[58] T.C. Powers, The properties of fresh concrete, Wiley, New York, 1968.

[59] J. Punkki, Effect of water absorption by agregate on properties of high strength lightweight aggregate concrete, CEB/FIP Int. Symp. Struct. Light. Aggreg. Concr. Hol. Al (Ed.), Sandefjord, Norway, pp.604-616. (1995).

[60] H. Asgeirsson, Hekla pumice in Lightweight Concrete, Icelandic Build. Res. Inst. (1994).

[61] S. Hammer, T.A., Narum, T., Materialutvikling høyfast betong, delrapport 2.6. Bestemmelse av riktig materialsammensetning I lettbetong., Trondheim, Norway., 1992.

[62] P. Weigler, H., Karl, S., and Lieser, The bending load capacity of reinforced lightweight concrete, Betonw. Und Fert. (1972) 324-334-449.

[63] R.G. Blair, K. Chagoya, S. Biltek, S. Jackson, A. Sinclair, A. Taraboletti, D.T. Restrepo, The scalability in the mechanochemical syntheses of edge functionalized graphene materials and biomass-derived chemicals, Faraday Discuss. 170 (2014) 223–233. doi:10.1039/C4FD00007B.

[64] Garmor, 2015. http://garmortech.com/technology.htm., (n.d.).

[65] ASTM C150, Standard Specification for Portland Cement, Annu. B. ASTM Stand. (2007) 1–8. doi:10.1520/C0150.

[66] ASTM C305-14, Standard Practice for Mechanical Mixing of Hydraulic Cement Pastes and Mortars of Plastic Consistency, Astm. (2015) 1–3. doi:10.1520/C0305-14.2.

[67] ASTM C192, Standard Practice for Making and Curing Concrete Test Specimens in the Laboratory, (2002) 1–8. doi:10.1520/C0192.

[68] ASTM C109 / C109M-16a, Standard Test Method for Compressive Strength of Hydraulic Cement Mortars (Using 2-in. or [50-mm] Cube Specimens), ASTM International, West Conshohocken, PA, 2016, www.astm.org, (n.d.).

[69] ASTM C348, Standard Test Method for Flexural Strength of Hydraulic-Cement Mortars, Annu. B. ASTM Stand. 4 (1998) 2–7. doi:10.1520/C0348-14.2.

[70] ASTM C1754 / C1754M-12, Standard Test Method for Density and Void Content of Hardened Pervious Concrete, ASTM International, West Conshohocken, PA, 2012, www.astm.org, (n.d.).

[71] ASTM C1585-13, Standard Test Method for Measurement of Rate of Absorption of Water by Hydraulic-Cement Concretes, ASTM International, West Conshohocken, PA, 2013, www.astm.org, (n.d.).

[72] ASTM C39, Standard Test Method for Compressive Strength of Cylindrical Concrete Specimens, Am. Soc. Test. Mater. (2016) 1–7. doi:10.1520/C0039.

[73] ASTM C 293, Standard Test Method for Flexural Strength of Concrete (Using Simple Beam with Third-Point Loading), (2010) 1–3. doi:10.1520/C0293.

[74] I.G. Richardson, The calcium silicate hydrates, 38 (2008) 137–158. doi:10.1016/j.cemconres.2007.11.005.

[75] P.E. Stutzman, P. Feng, J.W. Bullard, Phase Analysis of Portland Cement by Diffraction and Scanning Electron Microscopy, 121 (2016) 47–107.

[76] P.M. Suherman, A. van Riessen, B. O'Connor, D. Li, D. Bolton, H. Fairhurst, Determination of amorphous phase levels in Portland cement clinker, Powder Diffratcion. 17 (2002) 178–185.

[77] A. Mohammed, J.G. Sanjayan, W.H. Duan, A. Nazari, Graphene Oxide Impact on Hardened Cement Expressed in Enhanced Freeze – Thaw Resistance, J. Mater. Civ. Eng. 28 (2016) 4016072-1-4016072–6. doi:10.1061/(ASCE)MT.1943-5533.0001586.

[78] K. Gong, Z. Pan, A.H. Korayem, L. Qiu, D. Li, F. Collins, C.M. Wang, W.H. Duan, Reinforcing Effects of Graphene Oxide on Portland Cement Paste, J. Mater. Civ. Eng. 27 (2015) A4014010. doi:10.1061/(ASCE)MT.1943-5533.0001125.

[79] S. Lv, S. Ting, J. Liu, Q. Zhou, Use of graphene oxide nanosheets to regulate the microstructure of hardened cement paste to increase its strength and toughness, CrystEngComm. 16 (2014) 8508. doi:10.1039/C4CE00684D.

[80] R.A. e Silva, P. de Castro Guetti, M.S. da Luz, F. Rouxinol, R.V. Gelamo, Enhanced properties of cement mortars with multilayer graphene nanoparticles, Constr. Build. Mater. 149 (2017) 378–385. doi:10.1016/j.conbuildmat.2017.05.146.

[81] B.A. Al-Muhit, B. Nam, L. Zhai, J. Zuyus, Investigation on the mechanical, microstructural and electrical properties of graphene oxide-cement composite, in: Transp. Res. Board 97th Annu. Meet., 2015.

[82] J. An, M. McInnis, W. Chung, B. Nam, Feasibility of Using Graphene Oxide Nanoflake (GONF) as Additive of Cement Composite, Appl. Sci. 8 (2018) 419. doi:10.3390/app8030419.

[83] W. Long, H. Li, C. Fang, F. Xing, Uniformly Dispersed and Re-Agglomerated Graphene Oxide-Based Cement Pastes: A Comparison of Rheological Properties, Mechanical

Properties and Microstructure, Nanomaterials. 8 (2018) 31. doi:10.3390/nano8010031.

[84] C. Zhou, F. Li, J. Hu, M. Ren, J. Wei, Q. Yu, Enhanced mechanical properties of cement paste by hybrid graphene oxide/carbon nanotubes, Constr. Build. Mater. 134 (2017) 336–345. doi:10.1016/j.conbuildmat.2016.12.147.

[85] G. Bastos, F. Patiï¿½o-Barbeito, F. Patiï¿½o-Cambeiro, J. Armesto, Nano-inclusions applied in cement-matrix composites: A review, Materials (Basel). 9 (2016) 1–30. doi:10.3390/ma9121015.

[86] B. Wang, R. Jiang, Z. Wu, Investigation of the Mechanical Properties and Microstructure of Graphene Nanoplatelet-Cement Composite, Nanomaterials. 6 (2016) 200. doi:10.3390/nano6110200.

[87] J. An, B.H. Cho, Y. Alharbi, M. Khawaji, M. Mclnnis, B.H. Nam, Optimized Mix Design for Graphene Oxide Nano ake (GONF)– Cement Composite, in: Transp. Res. Board 97th Annu. Meet., 2018: pp. 1–2.

[88] X. Li, W. Wei, H. Qin, Y. Hang, Co-effects of graphene oxide sheets and single wall carbon nanotubes on mechanical properties of cement, J. Phys. Chem. Solids. 85 (2015) 39–43. doi:10.1016/j.jpcs.2015.04.018.

[89] G. Sant, D. Bentz, J. Weiss, Capillary porosity depercolation in cement-based materials: Measurement techniques and factors which influence their interpretation, Cem. Concr. Res. 41 (2011) 854–864. doi:10.1016/j.cemconres.2011.04.006.

[90] R. Henkensiefken, T. Nantung, J. Weiss, Saturated lightweight aggregate for internal curing in low w/c mixtures: Monitoring water movement using x-ray absorption, Strain. 47 (2011) 432–441. doi:10.1111/j.1475-1305.2009.00626.x.

[91] G.Y. Li, P.M. Wang, X. Zhao, Pressure-sensitive properties and microstructure of carbon nanotube reinforced cement composites, Cem. Concr. Compos. 29 (2007) 377–382. doi:10.1016/j.cemconcomp.2006.12.011.

[92] A. Sobolkina, V. Mechtcherine, V. Khavrus, D. Maier, M. Mende, M. Ritschel, A. Leonhardt, Dispersion of carbon nanotubes and its influence on the mechanical properties of the cement

matrix, Cem. Concr. Compos. 34 (2012) 1104–1113. doi:10.1016/j.cemconcomp.2012.07.008.

[93] ASTM C230, Standard Specification for Flow Table for Use in Tests of Hydraulic Cement 1, Annu. B. ASTM Stand. (2010) 4–9. doi:10.1520/C0230.

[94] Russ, J. The Image Processing Handbook, 3rd Ed.; CRC Press & IEEE Press: Boca Raton, FL, 1999., n.d.

[95] ASTM C1437, Standard Test Method for Flow of Hydraulic Cement Mortar, Am. Soc. Test. Mater. (2016) 1–2. doi:10.1520/C1437-15.2.

[96] C.F. Ferraris, K.H. Obla, R. Hill, The influence of mineral admixtures on the rheology of cement paste and concrete, Cem. Concr. Res. 31 (2001) 245–255. doi:10.1016/S0008-8846(00)00454-3.

[97] ASTM C 143, Standard Test Method for Slump of Hydraulic-Cement Concrete, (2011) 1–9. doi:10.1520/C0917-05R11.2.

[98] L. Bello, E. Garcia-diaz, P. Rougeau, An original test method to assess water absorption / desorption of lightweight aggregates in presence of cement paste, 154 (2017) 752–762.

[99] M.-H. and Zhang, O.E. Gjorv, Penetration of Cement Paste into Lightweight Aggregate, Bestem. Av Virkelig Mater. Mater. Heyfast Betong, Rapp. Nr 2.6. Trondheim. SINTEF, STF65 F91037.10 P. (1990).